OPPORTUNITIES AND CHALLENGES OF INTEGRATED LARGE SCALE PFAS MODELING

By

Anna Raschke

A THESIS

Submitted to
Michigan State University
in partial fulfillment of the requirements
for the degree of

Biosystems Engineering – Master of Science

ABSTRACT

OPPORTUNITIES AND CHALLENGES OF INTEGRATED LARGE SCALE PFAS MODELING

By

Anna Raschke

Perfluoroalkyl substances (PFAS) have been observed around the world in air, water, and soil. Recent research and monitoring studies have alluded to the widespread presence of PFAS, but most observe the impact of PFAS as a snapshot in time and space. In an effort to better understand PFAS fate and transport in the environment, computational models have been developed. For this study, we synthesized the model applications of PFAS fate and transport via water medium through surface water, vadose zone, groundwater, streamflow, as well as their uptake and accumulation in plants and aquatic organisms. In addition, the system under this study is permeable to incoming (sources) and outgoing (sinks) PFAS compounds. Ultimately, knowledge gaps in modeling PFAS for each subsystem (e.g., surface water) area were identified. From there, a case study was performed to highlight the shortcomings of widely used models for PFAS fate and transport within a large and complex watershed. With a large number of PFAS using industries, Michigan is at the forefront of PFAS sampling. Therefore, the study area chosen was the Huron River watershed, a highly PFAS impacted watershed in Southeastern Michigan. The results showed the importance of organized monitoring studies and model improvements to better understand PFAS fate and transport in a large watershed.

Copyright by ANNA RASCHKE 2022

ACKNOWLEDGEMENTS

There are so many people who were imperative to this thesis. First and foremost, though, thank you Dr. Pouyan for your friendship and mentorship. In a short year and a half, I learned and accomplished more than I could have ever dreamed of within a master's program, all thanks to you. This work would also not have been possible without the help of Nicolas and Vahid, who have an unmatched understanding of computational modeling of the natural environment. Thank you also to my committee members, Dr. Harrigan and Dr. Li, for your guidance on the project and for teaching me the ins and outs of groundwater contamination.

I would like to thank all of my friends and co-workers, Hannah, Sebastian, Ian, Kieron, Shashank, Josue, Enid, and Mervis, who were always up for a quick or long chat and great lunchtime discussions! Thank you also, Christian Loveall, for helping me process data and develop beautiful tables and figures. Thank you, BAE graduate friends and faculty, for always saying hi in the hallways and sharing great stories at social hours.

This work would also not have been possible without the support of my family, especially my parents, Alex, and Faisal, for always being there for me and making me laugh even after the hardest days.

Finally, I would like to thank the Center for PFAS Research, MPART, Huron River watershed council, and the Michigan Department of Natural Resources for providing data and funding for this project!

TABLE OF CONTENTS

LIST OF TABLES	vii
LIST OF FIGURES	. viii
1 Introduction	1
2 Literature Review	4
2.1 Water contamination overview	4
2.1.1 Agricultural pollutants	4
2.1.2 Industrial pollutants	7
2.2 Biological versus chemical contaminants	8
2.2.1 Biological Contaminants	9
2.2.2 Chemical Contaminants	11
2.3 General PFAS	15
2.3.1 Dominant PFAS	16
2.3.2 Sources of PFAS	17
2.3.3 Fate of PFAS	19
2.3.4 Transportation of PFAS	21
2.4 Fate of PFAS in an aquatic environment	
2.5 Mathematical representations of PFAS fate and transport	
2.5.1 Overland flow	25
2.5.2 Groundwater flow	28
2.5.3 Streamflow	32
2.5.4 Conceptual system models	35
2.6 Limitations and goals of research	
2.6.1 Limitations and recommendations.	
2.6.2 Goals	
3 Introduction to the Methodology	39
4 Opportunities and Challenges of Integrated Large Scale PFAS Modeling Part I: Overview	v of
Modeling, Applications, and Knowledge Gaps	40
4.1 Introduction	
4.2 Overview of PFAS transport	
4.3 Environmental factors affecting PFAS transport	
4.4 Sources of PFAS	
4.5 Overland flow and streamflow models	
4.5.1 Governing equations of overland flow and streamflow	
4.5.2 Applications of PFAS in overland and streamflow models	
4.6 Vadose Zone	
4.6.1 Governing equations for the vadose zone	
4.6.2 Applications of PFAS transport in vadose zone models	56

4.7 Groundwater models	58
4.7.1 Governing equations for groundwater flow	58
4.7.2 Applications of groundwater models for PFAS transport	61
4.8 Sinks of PFAS	63
4.9 Plant uptake models	63
4.9.1 Governing equations for plant uptake	64
4.9.2 Applications of plant uptake models	65
4.10 Aquatic Ecosystems Models	66
4.10.1 Governing equations for PFAS fate and transport in aquatic organisms	67
4.10.2 Applications of aquatic ecosystem models	69
4.11 Knowledge gaps of PFAS fate and transport modeling	71
5 Opportunities and Challenges of Integrated Large Scale PFAS Modeling Part 2: A C	
for PFAS Modeling at a Watershed Scale	
5.1 Introduction	
5.2 Methodology	
5.2.1 Study area	
5.2.2 Introduction to integrated PFAS model	
5.2.3 PFAS sources within the Huron River watershed	
5.2.4 Modeling the Huron River watershed	
5.2.5 Surface water model	
5.2.6 Groundwater model	
5.2.7 Linking surface water and groundwater	
5.2.8 Stream water quality model	
5.2.9 PFAS monitoring within the Huron River watershed	
5.2.10 The integrated model calibration	95
5.3 Evaluation of the integrated model for PFAS fate and transport	
5.4 Technical gaps in simulating PFAS	
5.5 Conclusion	108
6 Overall Conclusion	111
7 Future Research Recommendations	114
APPENDIX	116
RIBI IOGRAPHY	128

LIST OF TABLES

Table 1. Models applied to PFAS fate and transport to date
Table 2. Summarized knowledge gaps of PFAS application environmental models
Table 3. List of processes available in SWAT, MODFLOW-RT3D, SWAT-MODFLOW-RT3D and WASP for simulating PFAS. – means that the model cannot simulate the process. √ means that the model can potentially simulate the process but need further model development
Table A1. Groundwater sampling locations and frequency of PFAS within the Huron River Watershed
Table A2. Surface water sampling locations and frequency of PFAS within the Huron River watershed

LIST OF FIGURES

Figure 1. Schematic presentation of PFAS sources, sinks, and transport elements within the environment
Figure 2. Huron River watershed with USGS gaging stations and main dams
Figure 3. The groundwater model domain of the Huron River Watershed
Figure 4. Flowchart describing WASP river network building. 90
Figure 5. Stream network for WASP simulation, wastewater treatment plants, and PFAS observation sites
Figure 6. Daily baseflow rate simulated vs. observed
Figure 7. Daily streamflow calibrated vs. observed
Figure 8. Comparison of hydrographs in SWAT and WASP: a) Headwaters (subbasin 8); b) Middle river (subbasin 69); c) Lower river (subbasin 132)
Figure 9. Comparison between the results from the integrated model and observed values at the Strawberry Lake monitoring site: a) PFOS; b) PFOA
Figure A1. Groundwater, fish, and surface water PFAS sampling sites in the Huron River watershed
Figure A2. Soil sampling locations of PFAS within the Huron River watershed
Figure A3. Stormwater PFAS sampling locations within the Huron River watershed
Figure A4. Parameters value vs. objective function. The parameter value with index r shows relative change to the original value. The values in the horizontal axes for HK, VK, SS, and SY are the exponent of 10. Co stands for confined aquifer in the first layer; Un stands for the unconfined aquifer. Par1, Par2, Par3 stand for the layers of the groundwater
Figure A5. Monthly simulated vs. observed baseflow
Figure A6. Monthly streamflow simulated vs. observed
Figure A7. Simulated a) annual cell-by-cell groundwater water table and b) annual cell-by-cell recharge
Figure A8. Model samples in relation to observations from groundwater wells within the study area.

Figure A9. Huron River observations and model results for PFOS and PFOA at a) Wixom Rd,	, b
Burns Rd, c) Strawberry Lake, d) Base Line and Portage Lakes, and e) Regan Drain Downstrea	am
	127

KEY TO ABBREVIATIONS

AFFF Aqueous Film-Forming Foam

BMP Best Management Practices

BPA Bisphenol A

CAFO Concentrated Animal Feeding Operation

CDC Centers for Disease Control and Prevention

CN Curve Number

CNOEF Curve Number Coefficient

CYP Cytochrome P450

DDT Dichlorodiphenyltrichloroethane

DEM Digital Elevation Model

DHRU Disaggregated Hydrological Response Unit

DW Dry Weight

EDC Endocrine-Disrupting Chemicals

EU European Union

FBSA Perfluorobutane Sulfonamide (FBSA)

FTOH Fluorotelomer Alcohol

HAN Horizontal Anisotropy Ratio

HCA Hierarchical Cluster Analysis

HK Horizontal Hydraulic Conductivity

HPA Hypothalamic Pituitary Adrenal

HPI Hypothalamic Pituitary Interrenal

HRU Hydrological Response Unit

n Manning's Roughness

NSE Nash-Sutcliffe Model Efficiency Coefficient

Oat Organic Anion-Transporting Peptide

PBIAS Percent Bias

PCA Principal Component Analysis

PCA-MLR Principal Component Analysis – Multiple Linear Regression

PCDD Polychlorinated dibenzo-p-dioxins

PCDF Polychlorinated dibenzofurans

PFA Perfluoroalkoxy

PFAA Perfluoroalkyl Acids

PFAS Polyfluoroalkyl Substances

PFBA Perfluorobutyrate

PFCA Polyfluoroalkyl Carboxylic Acids

PFOA Perfluorooctanoic Acid

PFOS Perfluorooctane Sulfonate

PFOSA Perfluoroctansulfonamid

PFPeA Perfluoro-n-Pentanoic Acid

pKa Acid Dissociation Constant

POP Persistent Organic Pollutant

RB Riverbed

RC River Conductance

RES_BOTE Reservoir Bottom Percolation

RES_CON Reservoir Groundwater Conductance

RES_PVOL Reservoir Volume at the Normal Pool

ResMaxVolume Reservoir Volume at the Emergency Pool

RSR Ratio of the Root Mean Square Error to the Standard Deviation of Measured Data

SCS Soil Conservation Service

SS Specific Storage

SURLAG Surface Lag Time

SY Specific Yield

SWAT Soil Water Assessment Tool

TIMP Snow Melting Coefficient

USDA ARS United States Department of Agriculture Agricultural Research Service

USEPA United States Environmental Protection Agency

USGS United States Geological Survey

VK Vertical Hydraulic Conductivity

WASP Water Quality Analysis Simulation Program

weirk Reservoir Weir Discharge Coefficient

WHO World Health Organization

WWTP Wastewater Treatment Plant

1 Introduction

The staggering quantity of chemicals and nutrients found in the aqueous environment has been of increasing concern (Moody et al., 2003; Templeton et al., 2009). Pollution has a widespread adverse effect on human health (Kolpin et al., 2002a; Simon et al., 2019), aquatic organism fitness (Cui et al., 2017; Liu & Gin, 2018), and ecosystem makeup (Rodriguez-Moza & Weinberg, 2010a; Zhu & Kannan, 2019). There are many persistent organic pollutants of concern; however, one of the largest groups of emerging contaminants is poly- and perfluoroalkyl substances (PFAS), which have been produced in the U.S. since the 1940s (US EPA, 2018b). All PFAS are artificial and are characterized by a chain of fluorinated carbons (perFAS) or partially fluorinated carbons (polyFAS) connected to a functional group, giving them persistent, hydrophobic, and hydrophilic properties. Currently, the most commonly detected substances in the PFAS family are perfluorooctanoic acid (PFOA) and perfluorooctane sulfonate (PFOS) (US EPA, 2018b), but over 9000 different chemicals have been identified and categorized as PFAS to date (EPA, 2021).

PFAS provide the functioning of many goods regularly used, such as non-stick coating for cookware, rain repelling outerwear treatment, grease-free food packaging, aqueous film-forming foam, and chrome plating treatment suppressants (USEPA, 2017). PFAS have been found in organisms, soil, surface water, and groundwater all around the world (Boisvert et al., 2019). Observations from large scale blood sampling surveys, such as the C8 Health Project, suggest that all people on earth have some level of PFAS in their blood (Frisbee et al., 2009; Steenland et al., 2010), but some geographical areas have higher exposure than others (Evans et al., 2020). Pockets of elevated PFAS soil and water contamination have been found to be especially common around the current and former industrial and military sites (Hu et al., 2016).

The number of PFAS and their sources, fates, and avenues of transport is vast. With every new discovery, a new question arises on the impact it is having on the environment. Researchers are still unraveling the possibilities of how polar bears carry such high doses of PFAS in their liver (Boisvert et al., 2019). It is clear that these observations cannot be simply answered by in vivo samples and analytical tests. Computational models have been shown to be a powerful tool for identifying the pollution source, fate, and transport (Simon et al., 2019). Exposure pathways have been modeled to show how contaminations affect the organisms within an ecosystem over long periods of time (Ankley et al., 2010). Groundwater models have been used to show contamination transport and identify likely sources and fates (Metheny, 2004). The vadose zone has been modeled to show how contaminants can move through the soil into different exposure routes (Schaefer et al., 2019). The modeling of surface water has been used to show the transport of sediment and nutrients from agricultural fields to vulnerable areas (Arnold et al., 1998). Air deposition models have been used to show how particulates are transported and deposed or inhaled to contaminate people and the environment miles away (Tysklind et al., 1993). All of these types of models have been applied to PFAS, showing the movement within different environmental areas (Boisvert et al., 2019; Brusseau, 2020; Dauchy et al., 2019; Schaefer et al., 2019), but the small scale and incomprehensive nature of the models leave much of the PFAS story untold.

Currently, many research limitations prevent us from painting the bigger PFAS picture. This study aims to summarize the current applications of computational models for PFAS and assess the potential opportunities and challenges of large-scale and integrated PFAS modeling. Through this study, an effective modeling procedure is developed, which can help with the development of large-scale mitigation strategies to address the PFAS problem.

The specific objectives of this study are to:

- Review current literature on fate and transport of persistent organic pollutants.
- Synthesize the current applications of PFAS transport models and their governing equations.
- Summarize knowledge gaps and future work necessary to model PFAS on a large scale.

2 Literature Review

2.1 Water contamination overview

Anthropic practices have been adversely impacting ecosystems and human health for centuries, with many effects just now being linked and observed (Myers et al., 2013; Santos et al., 2010). Chemical, biological, and physical introductions and changes have been heavily linked to both agricultural (Centner & Feitshans, 2006; Kasorndorkbua et al., 2005; Nygård et al., 2019; H. Zhang & J., 2014) and industrial (Ivleva et al., 2017; Jantzen et al., 2016; Kolpin et al., 2002b; Rodriguez-Moza & Weinberg, 2010a) sources. Contaminants are everywhere – on the food we eat, in the water we drink, and the air we breathe. Many of the long- and short-term effects of contaminants are unknown, such as pesticides and chemicals in the waterways, but technological and research advancements are discovering that our actions are causing greater human and ecological health problems than foreseen (Santos et al., 2010).

2.1.1 Agricultural pollutants

The world wars spiked US agricultural production in the early 1900s leading to the discovery and widespread use of chemical insecticides, such as dichlorodiphenyltrichloroethane (DDT) (Henderson et al., 2011), and synthetic nitrogen and phosphorus fertilizers (Brand, 1945; Lassaletta et al., 2014; J. Liu et al., 2010). Thinning eggshells were observed to be related to dichlorodiphenyldichloroethylene (DDE), one of DDT's degrading products, and eventually led to the ban of DDT in the US and other countries around 1970 (Nygård et al., 2019; Ratcliffe, 1967). The observed effects of DDT on bird population were just one of a handful of human-related environmental effects that led to the formation of the United States Environmental Protection Agency (USEPA) in 1970 to drive and enforce environmental protection on a federal level (EPA History | US EPA, n.d.).

Other soil amendments, such as fertilizer, have also adversely impacted the ecosystem by polluting waterbodies and causing eutrophication (J. Liu et al., 2010). Over the past 20 years, research that focuses on developing best management practices (BMPs) and limitations for fertilizer applications has increased to reduce nutrient loading in waterways (Centner & Feitshans, 2006; Jayasundara et al., 2007). There are many factors that go into farmer's decisions about implementing different practices, but many are just starting to be addressed to help increase acceptance and implementation of BMPs (Erisman et al., 2008; Liu et al., 2018). Notoriously low fertilizer costs and low profits are two economic factors that have played a role in preventing the implementation of BMPs (Erisman et al., 2008) in addition to risk adversity (Liu et al., 2018). As a result, soil amendments continue to be applied in greater quantities than usable for the crops. It is estimated that global nitrogen use efficiency has dropped from about 68% in the 1960s to around 47% in 2014 (Lassaletta et al., 2014).

Excess nutrients, especially nitrogen and phosphorus, may be retained by the soil until used, but tilling, irrigation, and precipitation all degrade soil structure increases the chances of the nutrients leaching into runoff and groundwater (Liu et al., 2010). Synthetic fertilizers deliver nitrogen mostly in the form of ammonia generated through the Haber-Bosch process from dinitrogen, which is often overapplied, especially in countries without a lot of regulation, such as China (Glibert et al., 2014). The current staggering world population can be directly attributed to the implementation of the Haber-Bosch process and the use of synthetic fertilizers, but as with DDT, it has also had negative environmental impacts (Glibert et al., 2014). Increased nitrogen applications have been attributed to increased cases of methemoglobinemia, eutrophication, nitrous oxide emissions, and toxic algae blooms along coastal shores (Erisman et al., 2008).

Not only are we increasing the volume of fixed nitrogen on the Earth's surface, but we are also changing topsoil structure and conditions through machinery induced compaction, crop rotations, and tillage (Sainju et al., 2012). Human impact on soil escalates changes in nitrogen forms by promoting aeration through tilling, which provides conditions for denitrification of fixed nitrogen into nitrous oxide, and anaerobic conditions through compact or water-logged soils to nitrogenate into nitrate and nitrite ions, which leach easily into groundwater since they have an affinity for water's polar heads (Kanter et al., 2016; Mitch et al., 2003). With a global warming potential 298 times as potent as carbon dioxide and a long atmospheric lifetime, nitrous oxide has already had a significant impact on the environment and is predicted to increase with rising temperatures (Kanter et al., 2016; Skiba & Rees, 2014). Between 1979 and 1996, there were six methemoglobinemia attributed infant deaths reported in the national death certificate database maintained by the Centers for Disease Control and Prevention (CDC) in the US (Knobeloch et al., 2000). Additional fatal and non-fatal cases in the US and around the world have been linked to nitrate contamination through drinking water from private wells in rural areas, all with concentrations between 22.9 and 27.4 mg/L. Not only does nitrate affect infants, but according to the World Health Organization (WHO), chronic exposure may pose significant health threats such as thyroid disease, birth effects, and type I diabetes (WHO/SDE/WSH, 2016). Standards for nitrate levels in drinking water have been limited to 10 mg/L or below by the (USEPA) to prevent inducing human health problems (Boards, 2006).

Eutrophication of waterbodies due to increased levels of nitrogen and phosphorus promote algae blooms through increased aquatic primary productivity, reducing dissolved oxygen levels in the water to dangerously low levels, a condition known as hypoxia (Diaz & Rosenberg, 2008). Hypoxia has already increased in the last 20 years, posing a great economic threat due to impacts

on water quality altering ecosystems and contaminating drinking water, but will only become more common with global climate change (Rabalais et al., 2009).

2.1.2 Industrial pollutants

Nutrients are not the only accumulating pollutant in water; plastics are also posing a major threat to aquatic environments throughout the world (Sigler, 2014). Plastics have exponentially grown in population over the past half a century, with production exceeding 300 million metric tons annually (Law, 2017). Unfortunately, the increasing rates in production have not been paired with increasing recycling or reuse rates, leading to an accumulation of plastic litter. It is predicted that plastic materials make up approximately 60-80% of marine waste (Derraik, 2002; Law, 2017). The generally lightweight and durable properties of plastic make it easily transportable and non-biodegradable: ideal for accumulation in a marine environment (Thiel et al., 2013).

Long-chained hydrocarbons, which plastics are composed of, are most commonly derived from fossil fuels. Additives are integrated into the chemical compounds during plastic formation, depending on the final plastic properties desired (Law, 2017). As a result, there are many different makeups and sizes of plastics, some extremely large and dense others microscopic, with a variety of fates and environmental impacts when not recycled or disposed of properly (Thiel et al., 2013). One of the major problems with plastic accumulation in aquatic environments is ingestion and entanglement of marine wildlife leading to death through starvation or choking (Gregory, 1991). More recently, microplastics have been of great concern due to their increasing abundance and wide geographical impact (Green & Johnson, 2019). Shorelines of all continents and all oceans on the Earth have reported microplastic observations with many reports in freshwater systems as well, but they are not yet widely researched (Ivleva et al., 2017). Accumulation has been shown to be directly correlated with spatial distance to human sewage, with most of the microplastic

contamination coming from textile degradation (Browne et al., 2011). Not only does the accumulation pose a threat as a disturbance in sensitive habitats, microplastics also have the potential of carrying and distributing toxic chemicals, such as organotins, tributyltin, and triphenyltin (Fent, 1996).

As society progresses, water quality is impacted by our actions. There are millions of environmental contaminants of biological, chemical, and physical nature, which are carried by water to every place on this Earth. Through time we have polluted the environment with concentrations of different microorganisms and chemicals and are now paying the consequences with continued pollution (Myers et al., 2013). Environmental contaminants do not have borders and their adversity is correlated with other aquatic stressors making their 'safe dosage' and long-term impact difficult to predict. In order to accurately predict adverse outcomes of chemical contaminants, biological and physical stressors have to be taken into account as well. The following sections describe current knowledge of biological and chemical stressors and how they are impacting ecosystems and their movement is being modeled for effective remediation.

2.2 Biological versus chemical contaminants

The anthropogenic world revolves around water – humans bathe in it, drink it, eat animals and plants that have consumed it, use it for cooling and heating as well as producing goods, but often it is taken for granted and disposed of after use without much thought into makeup and fate. Contaminants can impact an ecosystem in different ways, as previously discussed, but they all increase stress on the systems and organisms from both external and internal exposure. Biological contaminants have the potential to decrease the dissolved oxygen levels within the water (Glibert, 2017; Weinke & Biddanda, 2018) and cause illness (Kasorndorkbua et al., 2005). Chemical contaminants also have the ability to deplete dissolved oxygen levels through chemical reactions

(Wei et al., 2019), change pH levels (Doney et al., 2009), bioaccumulate (Pajević et al., 2008), and disrupt pathways and functions within organisms (Keiter et al., 2012; Willi & Fent, 2018). Both biological and chemical contaminants come from anthropic sources and are a product of modern society.

2.2.1 Biological Contaminants

Biological contaminants come in many forms and are the cause of many acute human waterborne illnesses. Microbial contamination in water causes diarrheal diseases, which are a great threat to human health (Hasan et al., 2020). Even with modern technological advancements and increased knowledge on hygiene, a 2016 WHO report approximated a yearly death rate of 2 million attributed to waterborne illness (World Health Organization, 2016). There are trillions of different microorganisms on this Earth, but not all pose a risk to human health. According to (Dufour et al., 2012), the most common human illness-causing zoonic pathogens include *Cryptosporidium*, *Giardia*, *Campylobacter*, *Salmonella*, and *E. coli O157*, which have been directly linked to animal waste. In addition to zoonic pathogens, viruses can be transmitted through animal waste (Kasorndorkbua et al., 2005).

Daily animal-based protein consumption increased worldwide by 130% from 1961-2011 with increased wealth and urbanization (Sans & Combris, 2015). As a result, there are over 1 million animal farms in the US, producing over 1 billion tons of animal manure annually (Entertainment Close-up, 2011; H. Zhang & J., 2014). Many of these farms fall under the concentrated animal feeding operation (CAFO) category, which produce the most manure per unit area and are under strict regulation for disposal (Centner & Feitshans, 2006). Storage in lagoons or concrete holding tanks is a common solution for holding pathogen infested manure before it is land applied. Kasorndorkbua et al. (2005) performed a study on hepatitis E virus (HEV) in swine

manure in the US Midwest and found that fifteen of 22 tested farms had HEV-positive manure slurry. Heavy rainfall, cracks in storage tanks, and runoff from land-applied fields can all contribute to contamination of nearby waterways by pathogens found in fecal matter.

In the US, most modern drinking water treatment technologies are capable of eliminating microbial contaminants before consumption, but contaminated drinking water is not the only method of exposure to biological pollutants. Reservoirs, bays, estuaries, and lakes are commonly used for recreational activities and have high chances of contamination, exposing bathers to pathogens (Fleisher et al., 2010). It is suggested that certain algae growth, such as *Cladophora*, which is commonly found along the shorelines of the great lakes, provides optimal conditions for a variety of multicellular organisms, including E. Coli (Vanden Heuvel et al., 2010). Cladophora thrives in phosphorus-rich shallow areas of the great lakes and has been a nuisance for decades (Auer et al., 2010). The green algae grow in mats, which have been observed to provide a suitable habitat for growth and reproduction of E. Coli bacteria, concentrating levels of pathogens at beaches and in bathing areas. USEPA uses E. Coli concentration as an indicator of fecal contamination in freshwater (Mclellan & Salmore, 2003). E. Coli is found in a healthy gut of most living mammals and aviators and it is commonly associated with other pathogens. Its ease of identification makes it a standard indicator for water quality with concentrations over 35 cfu/100 mL deemed unsafe (Mclellan & Salmore, 2003; US EPA, 2012). Exposure through bathing in contaminated water has also been linked to skin sensitization, eye and ear irritation, and gastrointestinal irritation (Fleisher et al., 2010Heuvel et al., 2010).

Additionally, the consumption of raw or improperly cooked contaminated aquaculture and animals can also lead to illness (Chanpiwat et al., 2016; Kasorndorkbua et al., 2005). Research is currently being conducted on the reduction and transport of these pathogens from excreta to

exposure sites as well as how the pathogens affect all wildlife in addition to humans (Al-Fifi et al., 2019; Fleisher et al., 2010; Rodriguez-Moza & Weinberg, 2010b; Heuvel et al., 2010). The number of illness cases is slowly decreasing with increased knowledge, regulation, and the implementation of modern infrastructure. However, there is still a long way to go as many areas of the world still do not practice safe waste management or water treatment (United Nations Children Fund & World health Organisation, 2017).

2.2.2 Chemical Contaminants

Over the past few decades, the amount of known chemical contaminants in water and aquatic ecosystems has dramatically increased (Kolpin et al., 2002a). New analyzing equipment and research has given light to many anthropogenic chemicals never seen before in the environment (Santos et al., 2010; Templeton et al., 2009). Recent research has suggested that even the most minute contamination can have adverse environmental health effects (Caldwell et al., 2010; Rodriguez-Moza & Weinberg, 2010c). Sublethal health effects are being realized in both humans and wildlife, which are impacting chemical production and regulations (Rodriguez-Moza & Weinberg, 2010c). Chemical regulation is not global, instead by country/political region. In the US regulation is at the industry level, unlike the European Union, where regulation is led by the government (Report to Congressional Requesters, 2007). Consequently, many chemicals have been produced and released or leached in large doses without communication or a firm knowledge of short- and long-term environmental effects (Santos et al., 2010). Unlike regulating bodies, chemicals do not stay within geographical boundaries and can be carried and affect every ecosystem on the Earth. Antibiotics, pharmaceuticals, chemical additives, dioxins, polyfluoroalkyl substances (PFAS), and additional chemicals have all been detected in water and organisms all

around the world with linked environmental and drinking water impacts (Aminov, 2010a; Rodriguez-Moza & Weinberg, 2010c; Santos et al., 2010).

Since ancient times antibiotics, such as tetracycline found in the bones of ancient Sudanese Nubia, are believed to have protected populations from detrimental diseases and infection (Aminov, 2010b). Jordanian red soil, among other natural sources of antibiotics, has led to the discovery of particular antibiotics, but the beginning of mass production and widespread use is known as the "antibiotic era" that has been attributed to Paul Ehrlich and Alexander Fleming (Aminov, 2010b). For the past century, antibiotics have not only been used as a treatment, but also as preventative measures in both human and animal medicine. Widespread use of antibiotics has led to increased concentrations in natural waterways and sensitive ecosystems (Kim et al., 2008). CAFOs use large volumes of antibiotics in low doses to control diseases within production facilities and ensure a safe food supply (Awad et al., 2014; Lathers, 2001). Antibiotic water contamination generates a plethora of concerns, including antibacterial resistance in the environment and biological wastewater treatment (Larcher & Yargeau, 2012). Research on shortand long-term effects of antibiotics is still in beginning phases, but the urgency for immediate action is being felt around the world as a result of the increasing number of antibiotic-resistant strains and accumulation potential (Kim & Carlson, 2006; Maclean & Millan, 2019).

In addition to antibiotics, other pharmaceuticals are problematic for waterways. The human or animal body is not able to metabolize every ounce of active ingredients within a drug; what is not absorbed ends up in wastewater streams post excretion (Ternes, 1998). The fate of pharmaceuticals is dependent on many variables, such as prescription dosage, mineral or steroid makeup, use frequency, and wastewater treatment technology (Caldwell et al., 2010). Over the counter drugs tend to be found in greater concentrations than prescribed drugs, but exposure to even small

concentrations in aquatic environments can detrimentally impact organisms (Runnalls et al., 2010; Ternes, 1998). Wastewater treatment systems generally have the ability to partially remove pharmaceuticals from the effluent, but the removal does not always degrade the pharmaceutical (Gao et al., 2012; Ternes, 1998). Many of the removed pharmaceuticals are captured in the sludge in their full form, with the potential of either being released back into the water through equilibrium changes or land application (Gao et al., 2012). Additional exposure can come from consuming aquatic organisms; many pharmaceuticals have been readily detected in waterbed sediment and fish liver (Koba et al., 2018).

The true dangers of pharmaceuticals in the greater environment are their long-term effects, often unforeseen and irreversible (Santos et al., 2010). Pharmaceuticals are readily discharged into the environment in very low quantities (Kümmer, 2010). Many have high bioaccumulation potentials, such as 17α -ethynylestradiol, which is an endocrine-disrupting chemical (EDC) and the main ingredient in birth control pills (Al-Ansari et al., 2010). EDCs mimic reproductive hormones disrupting the organisms' natural regulation and production of reproductive cells (Labadie & Budzinski, 2006).

Not all EDCs are pharmaceuticals, though; there are many chemicals that have chemical structure and properties that mimic hormones. These chemicals then bind to proteins and affect hormone signaling and movement (Gore et al., 2015). Labadie and Budzinski observed high disruption potential of *p*-nonylphenol and bisphenol A (BPA), two xenoestrogens, on testicular steroid biosynthesis in male juvenile turbot. Rehan et al. (2015) observed a high affinity of BPA for the androgen and progesterone receptors, suggesting high potential for disrupting natural androgen and progesterone signaling and, therefore, reproductive function in humans. BPA is a chemical commonly added for polymer synthesis and is mainly used in products that are intended

for contact with food such as reusable bottles, baby bottles, plastic cutlery, and internal can coatings as well as building material and consumer plastic goods (Scippo, 2011). Elevated temperatures, pH differences, environmental impacts, and simple contact with food can lead to leaching of chemical substances from plastic. In 2008, Canada and some US states placed a ban on the use of BPA in baby bottle plastic followed by the EU three years later in response to a multitude of studies suggesting BPA adversely impacting endocrine functioning, having the potential to impact puberty, ovulation, and infertility (Huo et al., 2015; Keiter et al., 2012; Labadie & Budzinski, 2006; Matuszczak et al., 2019; Popovic et al., 2014; Scippo, 2011; Ullah et al., 2018).

Reproduction is not the only organism function impacted by chemical exposure. Dioxins are a class of chemicals with high bioaccumulation potential and depending on their chemical structure, have highly toxic effects (Kulkarni et al., 2008). Two observed dioxins with high toxicity are polychlorinated dibenzo-p-dioxins (PCDDs) and polychlorinated dibenzofurans (PCDFs), which are distributed into the environment through combustion processes (Chang et al., 2016). Emissions from industrial processes, vehicles, forest fires, and landfill fires all spew dioxins into the atmosphere where they are either volatilized and photodegraded or deposited into the soil ultimately accumulating in aquatic sediment and organisms (Kulkarni et al., 2008; Tysklind et al., 1993). Due to their structure and resistance to biodegradation, PCDDs and PCDFs are both classified as persistent organic pollutants (POPs), which have been commonly found in fatty tissues of both aquatic and terrestrial species (Kulkarni et al., 2008). A number of adverse health effects have been observed as a result of exposure to these chemicals, including chloracne, wasting syndrome, immunosuppression, reproductive function, and neuro function, among others (Mitrou et al., 2001). Due to their presence in soil and sediment, aquatic and grazing animals are directly exposed and have been observed to have elevated levels in their fat tissue (Chang et al., 2016;

Chen et al., 2003). The majority of human exposure then comes from fatty animal products such as fish, meat, milk, and vegetables, whereas air pollution is relatively minute in comparison (Beck et al., 1989; Chen et al., 2003).

There are thousands of chemicals produced and discharged into the environment; it is impossible to measure the impact of each chemical specifically through an individual in vivo study (Villeneuve et al., 2019). New methods of classifying impacts are being developed to estimate results of exposure, influence regulation, and establish treatment methods (Wetmore et al., 2015). The development of validated high-throughput testing methods can help reduce production and contamination from potentially hazardous chemicals and promote the production of less impactful alternatives.

One of the most demanding areas for high-throughput testing is PFAS chemicals (Patlewicz et al., 2019). Thousands of chemicals fall into the PFAS category, but only a few have been researched for toxicity and long-term health effects (Simon et al., 2019). The USEPA is working with the National Toxicology Program to generate high-throughput screening assays for PFAS chemicals to increase knowledge on PFAS influence on the environment and develop less toxic compounds (Patlewicz et al., 2019). High-throughput screening is one step in ensuring a healthy environment in the future, but first, PFAS makeup, sources, and fates have to be fully understood (Simon, 2019).

2.3 General PFAS

PFAS chemicals are used in a wide variety of products and have been manufactured for decades due to their unique oil and water repelling properties (Kotthoff et al., 2015). There are thousands of PFAS chemicals, but only a few have been thoroughly researched up to this point and shown to be highly toxic and ecologically diminishing (Simon et al., 2019). 3M and DuPont

were the largest PFAS manufacturers in the US and were the first to detect the adverse impacts of the chemicals on mammals (McCrystal, 2019). Through lenient manufacturing processes (Matheny, 2019) and consumer use (Kotthoff et al., 2015), PFAS chemicals have infected the Earth traveling through air (Armitage et al., 2009), soil (Washington et al., 2019), organisms (Bhavsar et al., 2014), and water (Moody et al., 2003) and continue to impact individuals and communities (USEPA, 2017).

2.3.1 Dominant PFAS

There are thousands of manmade molecules that fall into the PFAS group, which are highly fluorinated aliphatic molecules (USEPA, 2017). PFAS can be further broken down into two subgroups: per- and polyfluoroalkyl substances. Perfluoroalkyl substances include carbon compounds completely saturated with fluorine besides a functional group, whereas polyfluoroalkyl substances include compounds with a mixture of hydrogens and fluorine attached to the carbon molecules (Lindstrom et al., 2011). The carbon-fluorine bond is one of the strongest bonds found in nature, making PFAS chemicals very chemically and thermally stable and persistent (Park et al., 2020). In addition to the stability and persistence, PFAS chemicals have a hydrophobic-lipophilic nature promoting their production and use in a wide range of products such as carpet (Chen et al., 2020), textiles (Gremmel et al., 2016), food wrapping (Kotthoff et al., 2015), and cookware (Sajid & Ilyas, 2017) among other consumer goods (Matheny, 2019). Their widespread production and use have led to global contamination of air (Simon et al., 2019), soil (Moody et al., 2003), and water (Hu et al., 2016), in addition to organisms with long-chained PFAS molecules (8 or more carbons) bioaccumulating through food chains (Lindstrom et al., 2011)

Two increasingly detected PFAS chemicals of concern are perfluorooctane sulfonate (PFOS) and perfluorooctanoic acid (PFOA), which are both 8-carbon perfluoroalkyl substances.

Both PFOA and PFOS have hydrophilic functional groups, which allow them to bind to proteins and bioaccumulate in higher protein areas such as the blood and liver (Houde et al., 2008). PFOA has a carboxylate functional group, while PFOS has a sulfonate (Lindstrom et al., 2011). Their widespread use, persistence, and affinity for protein have led to high levels of exposure, with 99% of American blood testing positive for PFAS chemicals (Matheny, 2019). PFOA is less studied in humans but has been linked to tumors and neonatal death in addition to immune, liver, and endocrine system disfunction (Lindstrom et al., 2011; Steenland et al., 2010). PFOS has been classified as a chemical toxic to mammalian species with links to developmental retardation and cancer (OECD, 2002). Most PFOA and PFOS exposure have come from soil and water contamination (Moody et al., 2003).

In addition to PFOA, other long-chain polyfluoroalkyl carboxylic acids (PFCAs) are of great concern with both direct and indirect sourcing (Wang et al., 2014). All PFCAs are hydrophilic with a carboxylate functional group (Conder et al., 2008). Some longer chained PFCA molecules have been observed to degrade (Armitage et al., 2009). Since bioaccumulation potential is directly related to chain length, only PFCAs with greater than 7 carbon molecules are considered bioaccumulative (Conder et al., 2008). Direct sources of PFCA include manufacturer emissions and discharge, but PFCAs can also be formed through precursor degradation and impurities (Wang et al., 2014). Most PFCAs have been estimated to have been emitted from industrial manufacturers into the atmosphere, which distribute them around the world and eventually into water (Zhao et al., 2012).

2.3.2 Sources of PFAS

The stability of PFAS chemicals, especially PFOS and PFCAs, have allowed them to be identified from a multitude of both point and nonpoint sources (US Environmental Protection

Agency, 2019). PFAS manufacturing sites have been identified as point sources, such as perfluorobutane sulfonamide (FBSA) from the 3M plant in Decatur, Alabama into the Tennessee River (Hogue, 2019), PFOA from a fluorochemical facility in Washington, WV into the surrounding drinking water source (Hu et al., 2016), PFCA emissions from plants around the world (Wang et al., 2014), and underground PFAS contamination from footwear company Wolverine World Wide in Michigan ("Michigan Briefs," 2018). In some cases, manufacturers waste was sent to a wastewater treatment plant instead of direct discharge, but most wastewater treatment plants do not have adequate technology for destroying PFAS chemicals fating them to either the main waterways through discharge, soil through land application of sludge, or the landfill (Mortensen et al., 2011). Manufacturers are not the only source of direct discharge, ground and surface water surrounding civilian airports and military sites have PFAS levels 3 to 4-fold higher than USEPA health advisory levels (Hu et al., 2016).

Before 2001, PFOS was used as a main component in aqueous film-forming foam (AFFF) (USEPA, 2017). AFFF is heavily used at civilian airports and on military sites for firefighting training, which travels directly into the nearby waterways as runoff (Dauchy et al., 2019; Hu et al., 2016). Even though AFFF is no longer manufactured using PFOS, the PFOS concentrations around these areas are still very high due to its bioaccumulation and persistent nature (Houde et al., 2008; Moody et al., 2003) and continued use of previously manufactured AFFF.

There are also many nonpoint sources of PFAS chemicals leaching low amounts into the environment every day, such as outdoor consumer products (Gremmel et al., 2016), aerosols (Kotthoff et al., 2015), and food wrappers (Rosenmai et al., 2016). Perfluoroalkoxy (PFA) chemicals are used to make outdoor wear and other outdoor products waterproof, which are exposed to friction during use, making them susceptible to breaking apart and being carried into

water (Sidebottom et al., 2018). Aerosols contain fluorotelomer alcohol (FTOH) molecules, which can biotransform into PFOA, putting those who work heavily with aerosols at increased risk (Nilsson et al., 2013). Finally, PFAS chemicals are widely used in food contact paper and their affinity for proteins and fats leads them to contaminate protein- and fat-rich foods (OECD, 2002). Continued research and awareness of chemical properties and sources can help to reduce exposure for both individuals and ecosystems (Simon et al., 2019).

2.3.3 Fate of PFAS

Bioaccumulation has been of increasing concern for PFAS chemicals around the world, even in remote areas (Haukås et al., 2007). As previously discussed, exposure to PFAS chemicals can occur in many different ways PFOS and PFCAs, specifically PFOA, have been detected across the northern hemisphere (Haukås et al., 2007). Due to the stability and longevity of PFAS chemicals, they have the ability to accumulate within organisms and even biomagnify through food webs (Conder et al., 2008). PFOS and PFOA have been shown to preferentially bind to proteins and bioaccumulate in the bloodstream, liver, and kidney of both aquatic organisms and mammals (Jones et al., 2003; Mortensen et al., 2011). An affinity for protein differentiates PFAS from other persistent organic pollutants (POPs), which are generally lipophilic and bioaccumulate in adipose tissue (Baynes et al., 2012).

Adverse effects of PFAS chemicals have been observed in both aquatic organisms and mammals (Lindstrom et al., 2011). The unique properties of PFOS and PFOA have been observed to adversely alter vital proteins within organisms altering pathways and disrupting normal hormonal responses (Jantzen et al., 2016). The presence of PFAS chemicals in the bloodstream and protein affinity allow them to bioaccumulate and affect proteins in many organs within the organism, especially the pancreas (Cui et al., 2017), kidney (Keiter et al., 2012), and liver (Das et

al., 2017). Proteins and pathways can be unique to individual species (Nigam et al., 2015); therefore, PFAS chemicals can impact species in different ways leading to a diverse range of adverse outcomes (Behr et al., 2020; Cui et al., 2017). PFOA has been observed to proliferate peroxisome through activating the peroxisome proliferator-activated receptor α in marsupials, which is suggested to induce tumors and administer immune and hormonal alterations (Steenland et al., 2010). Cui et al. (2017) observed adverse alterations in lipid metabolism due to low level of chronic PFOS exposure within zebrafish.

Since PFAS chemicals are persistent and species agnostic, it is important to analyze their impact on cross-species pathways. There are few pathways and proteins that are similar amongst species. Still, the hypothalamus-pituitary-adrenal (HPA) in mammals and hypothalamus-pituitary-interrenal (HPI) axis in fish is observed as one of the most ubiquitous pathways as it is similar amongst many living organisms (Hawkley et al., 2012). The HPA/I-axis plays a major role in mediating stress responses (Lee et al., 2018) and is regulated by corticosteroid receptors (Norris & Hobbs, 2006). Both PFOS and PFOA have been observed to alter CR by causing an undesirable activation or deactivation of the HPA axis (Salgado-Freiría et al., 2018), leading to either upregulation or downregulation of a SR in an organism and eventually an adverse outcome (Ord et al., 2017).

Chronic PFAS exposure is being observed across all species worldwide (Haukås et al., 2007). Even though a great amount of research has already been conducted on the adverse effects of PFAS within organisms (Ge et al., 2016; Jantzen et al., 2016; Keiter et al., 2012; Mortensen et al., 2011), there is still a large data gap on the impact of PFAS with other chemicals (Keiter et al., 2012), bioaccumulation (Wang et al., 2014), and biomagnification (Conder et al., 2008). With increasing knowledge of PFAS movement, receptor binding, and dose-responses across species,

proper regulation and mitigation techniques can be developed and implemented (Lindstrom et al., 2011).

2.3.4 Transportation of PFAS

The unique properties of PFAS chemicals allow them to be transported via air (Nilsson et al., 2013), soil (Zhu & Kannan, 2019), and water (Hu et al., 2016). The physical-chemical properties of PFAS chemicals are not optimal for long-range atmospheric transport (Haukås et al., 2007), but many can be transported short-range with the help of dust and high temperatures (Nilsson et al., 2013). Fluoropolymer manufacturing emits PFCAs as a byproduct and has historically been viewed as the single largest emitter of PFCA (Prevedouros et al., 2006). Recent research by Nilsson et al. (2013) has observed high levels of PFOA exposure for professional ski waxers when using aerosols and applying wax. PFAS chemicals are a component of the petroleum base of ski wax, which is heated to 130-220 °C when being applied, releasing gaseous forms of PFOA, among other organofluorine compounds, and fluorotelomer alcohols (FTOHs) (Hameri et al., 1996). FTOHs have been observed to degrade into PFCA products through a reaction with HO_x in the atmosphere in the absence of NO_x and biotransform within animals (Nilsson et al., 2013; Prevedouros et al., 2006).

As aforementioned, military sites have been observed as a major source of PFAS exposure (Hu et al., 2016). Runoff from these military and firefighting training grounds is a main method of transportation for soil and water contamination in the surrounding area (Dauchy et al., 2019). Dauchy et al. (2019) suggest that the PFOS and PFCA remanence from AFFF can remain on military sites and be transported into nearby soil and water via runoff around a month or more after use. Moody et al. (2003) observed elevated PFOS and PFOA levels in the groundwater surrounding a retired firefighting training ground five years after use.

It is suggested that the affinity for soil versus water for particular PFAS chemicals is dependent on both the chain length and functional group (Zhu & Kannan, 2019). Zhu & Kannan (2019) detected both PFOS and PFOA in soil samples from a good field, with an average PFOA concentration 40 times higher than the average PFOS, suggesting that PFOS has a greater affinity for water and PFOA have a greater affinity for solids. Not only do PFOA molecules tend to accumulate in the soil, but research suggested that PFCAs, in general, have a higher solid affinity than PFOS (Dauchy et al., 2019; Plassmann & Berger, 2013; Zhu & Kannan, 2019). Particularly long-chained PFCA molecules have been observed to have a higher solid affinity, whereas shortchained have a higher affinity for water (Plassmann & Berger, 2013).

PFAS water contamination is of increasing concern (US EPA, 2016a). PFAS chemicals have been observed in both groundwater and surface waters with primarily long-chained molecules detected in groundwater, and primarily short-chained molecules detected in surface water (Hu et al., 2016), which follows the observations made by Plassmann & Berger (2013) showing that long-chained PFAS molecules are more likely to move through the soil to reach the groundwater aquifer than short-chained molecules. Once in the water, PFAS molecules are suggested to be taken up by both plants and animals (Bhavsar et al., 2014; Lindstrom et al., 2011). A recent analysis of PFAS molecules in polar bears has suggested bioaccumulation and biomagnification as a major route of exposure to all animals in addition to contaminated water (Boisvert et al., 2019).

2.4 Fate of PFAS in an aquatic environment

High levels of PFAS concentrations in water and sediment is not only of concern for humans but has the potential to adversely affect the populations of aquatic organisms (Jantzen et al., 2016; Martin et al., 2003) and entire food webs (Haukås et al., 2007). As previously discussed, many PFAS chemicals are bioaccumulative (Zhu & Kannan, 2019) and even toxic (Kotthoff et al.,

2015). Both PFOS and PFCAs have been detected in water and sediment, inevitably fating aquatic organisms to contamination (Mussabek et al., 2019a).

A great amount of research has been conducted on PFAS in fish as a concentrated exposure route to humans (Bhavsar et al., 2014; Simon, 2019). Many POPs readily found in the aquatic environment tend to bioaccumulate in the lipid sections of organisms (Crane, 1996), which are either removed or cooked off during preparation (Bhavsar et al., 2014). Since PFAS chemicals have been shown to preferentially bind to proteins rather than fats, they are not as easily removed during the preparation process (Berger et al., 2009). PFAS concentrations, especially PFOS, have been observed to stay the same or increase through the cooking process (Bhavsar et al., 2014). Fish consumption has thought to be one of the greatest influences on individual human PFAS levels, especially PFOS and PFOA (Berger et al., 2009), but humans are not the only predatory species being affected (Haukås et al., 2007).

A recent study by Boisvert et al. (2019) observed a relationship between PFAS concentrations in ringed-seals and polar bears. They observed significant levels of both PFCAs and PFOS in the adipose tissue and liver of polar bears and seals, with increased concentration related to trophic level (Boisvert et al., 2019). High PFOS concentration in the liver is of growing concern, due to the potential for hepatocellular damage, amongst other organ damage (Gallo et al., 2012; USEPA, 2017). Cui et al. (2017) observed liver damage in relation to high PFOS concentrations as well as alterations in lipid metabolism and transport within zebrafish. Keiter et al. (2012) also observed hepatotoxicity in PFOS and BPA exposed zebrafish in addition to alterations in vitellogenin, suggesting that PFOS could have a whole-body impact within aquatic species.

PFOA has also been observed in high concentrations within aquatic species with negative impacts (Mortensen et al., 2011; Popovic et al., 2014). In the kidney and liver, both PFOS and PFOA have been observed to disrupt the cytochrome P450 (CYP) levels, which play a vital role in the oxidative metabolism of steroid hormones and other compounds within the body (Mortensen et al., 2011). Interestingly, PFOS and PFOA were observed to have significantly different influences on CYP expression within both the kidney and the liver of juvenile Atlantic Salmon, showing a need for species-specific and organ-specific research to fully understand the impact of PFOS and PFOA bioaccumulation (Mortensen et al., 2011). Popovic et al. (2014) also observed differences between the impact of PFOS and PFOA in relation to the organic anion transporting peptide (Oatp) expression, which regulates compound uptake into target tissues, within zebrafish. PFOS was observed to have a high affinity for the Oatp1d1 substrate, while PFOA was observed to be an uncompetitive inhibitor (Popovic et al., 2013).

Current findings are giving light to the potential impacts of PFAS compounds within aquatic species with adverse outcomes from the individual up to ecosystem level (Haukås et al., 2007; Jantzen et al., 2016; Kotthoff et al., 2015; Martin et al., 2003; Zhu & Kannan, 2019). In order to best mitigate ecosystem level adverse outcomes, PFAS sources, transportation, and fate have to be analyzed together with the potential impact of PFAS molecules on individual pathways within organisms (Ankley et al., 2010). Modeling the movement of PFAS through watersheds is a vital component in developing knowledge and remediation techniques to ensure a healthy environment for all. The following section goes into detail on the different types of models used to simulate the PFAS movement.

2.5 Mathematical representations of PFAS fate and transport

The following section reviews different models developed to better understand the implications of PFAS sources, transportation, and fate in the environment. Even though some PFAS chemicals have been phased out of production, they are continually detected in soil and water, posing a threat to ecosystem health. Overland, stream, groundwater, and conceptual models are being developed to assess PFAS contamination and formulate effective remediation techniques.

2.5.1 Overland flow

A modified Saint-Venant equation (1) can be used as the governing equation to model overland flow over a uniform impervious slope (Heng et al., 2009). Equation (1) describes the relationship between rainfall intensity (P); water depth (h); and unit discharge (q):

$$\frac{\partial h}{\partial t} + \frac{\partial q}{\partial x} = P \tag{1}$$

where q is calculated using the Manning's equation $q = \frac{\sqrt{s_0}}{n} h^{5/3}$ with (s_0) accounting for the slope (s_0) and Manning's roughness coefficient (s_0) . As previously discussed, PFAS can be transported via water flowing overland into the soil (Nguyen et al., 2016; Xu et al., 2013) or directly into a waterbody (Ghiold, 2019; Li et al., 2017; Sharma et al., 2015). Studies have looked into the relationship between physicochemical properties of PFAS compounds and aqueous and solid compounds near contaminated areas to better understand transportation and fate (Nguyen et al., 2016; Xu et al., 2013). Sorption to solids, as well as other physicochemical properties of specific PFAS compounds, are the basis of overland models to better understand transportation and fate in the environment (Nguyen et al., 2016; Xu et al., 2013).

One of the most influential parameters for modeling PFAS overland fate and transport is the solid/liquid distribution coefficient (K_D), which is derived from the organic carbon distribution coefficient (K_{OC}). The K_D value for PFAS substances are variable in literature due to the influence of other components to adsorption (Brusseau & Van Glubt, 2019; Nguyen et al., 2016; Shin et al., 2011). Nguyen et al. (2016) derived the K_D and K_{OC} values for PFOS, PFOA, and other PFAS compounds to observe their mechanism of transport and fate in relation to sediment:

$$K_D = \frac{C_S}{C_{aq}} \tag{2}$$

$$K_{OC} = \frac{K_D}{f_{OC}} \tag{3}$$

where, C_S (ng/L) is the concentration in the solid phase; C_{aq} (ng/L) is the concentration in the aqueous phase; and f_{OC} are the organic carbon fractions within soil and sediment. Commonly found PFAS compounds, such as PFOA and PFOS, were detected in water samples and their transport and fate as related to suspended solids were evaluated using equations (2) and (3) compared to the laboratory determined K_D and K_{OC} values of suspended solids (Nguyen et al., 2016). Observations showed differences between the fate of strongly hydrophobic PFAS compounds and less hydrophobic PFAS compounds. Strongly hydrophobic PFAS compounds were observed to be sorbed to suspended solids and accumulated in the bottom sediment, whereas the transportation of less hydrophobic PFAS compounds were observed to be less influenced by suspended solids. Most of the PFAS detected in field studies were observed accumulated in the sediment at the bottom of the waterbed, but the K_D values for PFOA and PFOS sorbing to the bottom were lower than the K_D values of suspended solids (Nguyen et al., 2016). Distribution of PFOS, PFOA, and other highly accumulative PFAS compounds were consistent with previously

reported values, showing promise of determining the coefficients using equations (2) and (3). Accurate determination of K_D and K_{OC} values will be helpful for optimizing transportation and fate dynamic models.

Receptor models were used by (Xu et al., 2013) to simulate the relationship between PFC compounds and sediment detected through a two-dimensional hierarchical cluster analysis (HCA) heat map of the Dianchi Lake in China. The three receptor models used were the principal component analysis – multiple-linear regression (PCA-MLR) model, positive matrix factor (PMF) model, and Unmix model, which can all be described by equation (4):

$$x_{ik} = \sum_{i=1}^{p} g_{ip} f_{pk} + e_{ik}$$
 (4)

where x_{ik} is the concentration of *i*th species for k^{th} sample; f_{pk} is the contribution of the p^{th} source to the k^{th} sample; g_{ip} is the *i*th species concentration from the p^{th} source; and e_{ik} is the error (Xu et al., 2013). Each model was observed to be statistically accurate, with comparable results between observed data and modeled outcomes (Xu et al., 2013). Through data analyzation and modeling, primary abundant PFAS chemicals found in sediment in the Dianchi Lake, PFOS and PFOA, and their various emission sources, electroplating factories or food-packaging processes industrial facilities, were identified (Xu et al., 2013). Successful calibration of the receptor models validated with a comparison to observed field data suggest the potential for such techniques to be applied to other areas for investigation in addition to the use of simulation results for better understanding PFAS fate and movement and developing remediation plans (Xu et al., 2013).

2.5.2 Groundwater flow

Groundwater is modeled as a single-phase fluid moving through a porous medium under Darcy's law (Anderson et al., 2015). Darcy's law (6) is used to describe the specific discharge (q) in relation to head (h) and the conductivity tensor (K). The water balance equation (5) is used to model water movement in relation to the representative elementary volume describing the recharge of water storage:

$$\frac{\partial q_x}{\partial x} + \frac{\partial q_y}{\partial y} + \frac{\partial q_z}{\partial z} - W^* = -S_s \frac{\partial h}{\partial t}$$
 (5)

where, q_x , q_y , and q_z represent the specific flow rate of water in the x, y, and z direction, respectively; W^* represents the volumetric inflow rate from sources and sinks; S_s represents specific storage; and h is head. Since flow (q) is not practically measured in wells, the equation is written in terms of the head (h) from the (l) direction using Darcy's law:

$$q = -K \frac{\partial h}{\partial l} \tag{6}$$

Darcy's law is first written in terms of specific flow in the x, y, and z direction, then substituted into equation (5) to generate a three-dimensional transient groundwater flow (7):

$$\frac{\partial}{\partial x} \left(K_x \frac{\partial h}{\partial x} \right) + \frac{\partial}{\partial y} \left(K_y \frac{\partial h}{\partial y} \right) + \frac{\partial}{\partial z} \left(K_z \frac{\partial h}{\partial z} \right) = S_s \frac{\partial h}{\partial t} - W^*$$
 (7)

which can be applied to heterogeneous and anisotropic conditions (Anderson et al., 2015). Computational models have been developed using equation (7) to simulate PFAS movement to groundwater (Brusseau, 2018; Brusseau et al., 2019; Guo et al., 2020; Schaefer et al., 2019). Before contaminating the aquifer, PFAS chemicals must make their way through the vadose zone, where different saturation conditions affect the speed at which movement occurs (Brusseau, 2018; Brusseau et al., 2019; Guo et al., 2020; Schaefer et al., 2019). Mathematical equations, such as the

Szyzkowski equation (8) (Brusseau et al., 2019) and Freundlich model (9) (Schaefer et al., 2019), have been used to simulate and better understand PFAS retardation in the subsurface environment:

$$\gamma = \gamma_0 \left[1 - B \ln \left(1 + \frac{C}{A} \right) \right] \tag{8}$$

where, γ is the interfacial tension (dyn/cm or mN/m); γ_0 is the interfacial tension at [PFAS] = 0; C is the aqueous phase concentration (mol/cm³); A is the variable related to properties of the specific compound; and B is the variable related to properties of the homologous series.

$$\Gamma = k(C_T)^n \tag{9}$$

which describes the relationship between surface excess (Γ) (mol/cm²) and the square mean of ionic activity (C_T) ([mol/m³]²) using constants k and n. The air-water and decane-water interface within soil has been shown to directly influence PFOS and PFOA retardation trends (Brusseau et al., 2019).

Brusseau et al. (2019) observed PFOS and PFOA movement through quartz sand and soil in both unsaturated- and saturated-water conditions. An extended conceptual model was developed using equations (8), (10), and (11) to calculate the retardation factor for aqueous-phase transport of solute with multiple compartments divided between source zones and plumes based on a previous model developed by Brusseau, (2018). The Szyszkowski equation (8) was used to unify the surface-tension and interfacial-tension data to obtain factors for equations (10) and (11). Adsorption quantities at the fluid-fluid interface were determined using equation (10) and (11):

$$\Gamma = \frac{-1}{xRT} \frac{\partial \gamma}{\partial lnC} \tag{10}$$

where Γ is the surface excess (mol/cm²) of the compound; γ is the interfacial tension (dyn/cm or mN/m); C is the aqueous phase concentration (mol/cm³); T is the temperature (°K); R is the universal gas constant (dyne-cm/mol °K); and x is a coefficient equal to 1 for nonionic surfactants or ionic surfactants with excess electrolyte in the solution and equal to 2 for systems with ionic surfactants without excess electrolyte.

$$K_i = \frac{\Gamma}{C} \tag{11}$$

where K_i is the fluid-fluid interfacial adsorption coefficient between the fluid pair (cm); Γ is the surface excess (mol/cm²) of the compound; and C is the aqueous phase concentration (mol/cm³). Various breakthrough curves from the different conditions and PFAS chemicals were compared, with noticeable differences between saturated- and unsaturated-water conditions and the chemicals. Within both mediums, unsaturated-water conditions promoted more retardation for both PFOS and PFOA, with PFOS having the greatest level of retardation in the sand (Brusseau et al., 2019). The model developed by Brusseau et al. (2019) uses adsorption at the air-water interface to accurately estimate the retardation factor for PFAS in source zones.

Mathematical models of PFOS movement through both sand and soil with the variably saturated flow were also developed by Guo et al. (2020) using equations (12) and (13). The Richards equation (Guo et al., 2020):

$$\frac{\partial \theta}{\partial t} - \frac{\partial}{\partial z} \left[K \left(\frac{\partial h}{\partial z} - 1 \right) \right] = 0 \tag{12}$$

where, θ is the volumetric water content and is equal to ΦS_w where Φ is the porosity of the porous medium and S_w is the water saturation; K is the unsaturated hydraulic conductivity (cm/s); h represents the water pressure head (cm); h is the special coordinate (cm); and h is time (s). Equation (12) was used to simulate the flow in the vertical dimension using 10-year data (replicated three times) from Arizona, USA and New Jersey, USA to represent semiarid and humid climates, respectively. Accusand and Vinton soil were used as the porous media simulated for both climates with variable PFOS concentrations and air-water interfacial adsorption (Guo et al., 2020). PFOS movement was described using an advection-dispersion equation (13) with adsorption terms:

$$\frac{\partial(\theta C)}{\partial t} + \rho_b \frac{\partial(K_f C^N)}{\partial t} + \frac{\partial(A_{aw} K_{aw} C)}{\partial t} + \frac{\partial}{\partial z} \left(\theta D \frac{\partial C}{\partial z}\right) = 0 \tag{13}$$

where, θ is the volumetric water content; C is the aqueous concentration (μ mol/cm³); t is time (s); ρ_b is the bulk density of the porous medium (g/cm³); K_f and N are fitting parameters to experimental data; A_{aw} is the air-water interfacial area (cm²/cm³); K_{aw} is the air-water interfacial adsorption coefficient (cm³/cm²); D is the dispersion coefficient (cm²/s); and z is the special coordinate (cm). Equations (12) and (13) simulated PFOS movement using both solid-phase and air-water interfacial adsorption processes, observing that PFOS migration is greatly influenced by adsorption at the air-water interface in the vadose zone. Observations from the simulation suggested that soils with higher water concentrations, such as clay, have lower PFOS retention rates than those with lower water, such as sand, increasing the rate of PFOS contamination in the groundwater (Guo et al., 2020).

Schaefer et al. (2019) observed the best match is the Freundlich model (equation 9) for the movement of other PFAS compounds, such as PFAA, at the air-water interface when compared to results using the Langmuir model (equations(14) and (15).

$$\Gamma = \frac{\Gamma_m \alpha C_T}{1 + \alpha C_T} \tag{14}$$

$$\sigma = \sigma_0 - RT\Gamma_m ln \left[1 + \alpha C_T\right] \tag{15}$$

Where, Γ is the surface excess (mol/cm²) of the compound; Γ_m is the interfacial sorption capacity (mol/m²); α is the adsorption affinity coefficient ([m³/mol]²); square mean of ionic activity (C_T) ([mol/m³]²); σ_0 is the air-water interfacial tension without PFAS; R is the universal gas constant (dyne-cm/mol °K); and T is the temperature (°K). Predictions varied by orders of magnitude between the two models when modeling sorption trends with respect to PFOS concentration, with the Langmuir model underestimating interfacial sorption (Schaefer et al., 2019). Benchtop experiments were used to validate the model predicting the movement of PFAS with varying background NaCl concentrations. It was observed that the length of the PFAS compound was highly related to the interfacial uptake, with long-chained compounds having greater interfacial uptake than shorter-compounds (Schaefer et al., 2019). Observations from this study show that previous estimates of PFAS chemical uptake and retardation could be lower than actuality.

2.5.3 Streamflow

The movement of water allows oxygenation to occur and nutrients to be carried, but it also distributes POPs far from their source, promoting widespread contamination (Ghiold, 2019; Li et al., 2017; Sharma et al., 2015). It is important to model streamflow to understand the full impact of POPs and develop effective remediation techniques. The conservation law of water mass (16) and linear momentum (17) can be used as the governing equation for modeling streamflow in a

1D river/stream (Yeh et al., 1998). Equation (16) represents a continuity equation showing the relationship between time (t); river/stream cross sectional area (A); river/stream flow rate (Q); and various sources (S):

$$\frac{\partial A}{\partial t} + \frac{\partial Q}{\partial x} = S_S + S_R - S_I + S_1 + S_2 \tag{16}$$

where S_s is the man-induced source; S_R is the source due to rainfall; S_I is the sink due to infiltration; and S_1 and S_2 are the source terms contributed from overland flow (Yeh et al., 1998). The momentum equation (17) describes the relationship between water depth (h); river/stream velocity (u); gravity (g); bottom elevation (Z_0) ; momentum flux due to eddy viscosity (F_x) ; and shear stress (T):

$$\frac{\partial Q}{\partial t} + \frac{\partial uQ}{\partial x} = -gA\frac{\partial (Z_0 + h)}{\partial x} + \frac{\partial F_x}{\partial x} + u^r S_R - u^i S_I + u^{Y_1} S_1 + u^{Y_2} S_2 + \frac{T^s - T^b}{\rho}$$

$$\tag{17}$$

where u^r is the rainfall velocity in the direction of the river/stream; u^i is the infiltration velocity in the river/stream direction; u^{Y1} and u^{Y2} are the velocities of water from overland to the river/stream along the river/stream direction; ρ is the water density; and T^s and T^b are the surface and bottom sheer stress respectively (Yeh et al., 1998). Models have been developed using equations (16) and (17) to better understand and predict PFAS movement and contamination in flowing water (Li et al., 2017; Sharma et al., 2015).

Li et al. (2017) used the MIKE-11 model with both hydrology and advection-dispersion modules to simulate PFOS and PFOA movement through the Daling River network. Simulations were conducted using three scenarios based on measured surface water concentrations: time changing concentrations, constant max loads, and continuous constant loads required for reaching harmful concentrations (Li et al., 2017). Through data analyzation and simulation results, it was

apparent that PFOS and PFOA concentrations varied depending on the season, with PFOS having highest concentrations in the spring and PFOA with the highest concentrations in the summer, due to fluctuating flow rates and fluorinated chemical production (Li et al., 2017). Great differences between simulated and observed results were apparent, especially between PFOS and PFOA, where PFOS had less accuracy than PFOA, but the differences were not significant enough to deem the model irrelevant (Li et al., 2017). Critical loads for PFOS and PFOA were determined for the Daling River through the third simulation scenario (Li et al., 2017), but they did not take other chemicals and stressors into account. The simulation by Li et al. (2017) successfully modeled PFOS and PFOA movement through the Daling River and observed possible impacts of the chemicals in Seas further downstream.

A study performed by Sharma et al. (2015) on PFAS in the Ganges River basin observed the effects of different PFAS sources on river contamination. The Ganges River basin is an area with an emerging industrial economy, including over 400 million people, with PFAS contamination from both volatile **PFAS** compounds, such **FTOHs** and perfluoroctansulfonamida (PFOSAs), degraded at the air-water interface as well as direct PFOS and PFOA discharges (Sharma et al., 2015). The integrative INCA-Contaminants model was used to simulate the complex hydro biogeochemical processes and PFAS contamination fate in the Ganges River system (Sharma et al., 2015). Both organic carbon and suspended settlement dynamics were included in the model in addition to climate data. Specific PFAS physicochemical properties, emission scenarios, and initial PFOS and PFOA atmospheric concentration and wet deposition were all used to parametrize the model (Sharma et al., 2015). Direct PFOS and PFOA discharges were estimated by the model through running it in "reverse-mode" and using a Monte Carlo frame to derive a distribution of subbasin specific discharges to the river. Simulation results suggested strong correlation between both the urban population and total population with PFOS and PFOA emissions (Sharma et al., 2015).

2.5.4 Conceptual system models

It is apparent that PFAS compounds are mobile through air, soil, and water systems (Brusseau, 2018; Brusseau et al., 2019; Guo et al., 2020; Schaefer et al., 2019), therefore, representative system models, which include all three systems are being developed for fully understanding and predicting PFAS movement and contamination (Barr, 2017; Shin et al., 2011; Simon et al., 2019). Only a couple of conceptual models have been successfully developed for PFAS movement and published to this date, due to their complex construction and computation (Barr, 2017; Shin et al., 2011; Simon et al., 2019). Continued research on PFAS compounds has observed increased sources and transportation mechanisms than before, providing ever higher motivation for the development of conceptual models (Barr, 2017; Shin et al., 2011; Simon et al., 2019; Zhu & Kannan, 2019)

Bennington, Vermont is an area with many PFAS sources and observed elevated PFOA concentrations in soil, surface water, groundwater, and private wells (Barr, 2017). Barr (2017) identified numerous different previous sources, including PFOA emissions from two former Chemfab lab facilities, contaminate landfill leachate, contaminated land applied wastewater treatment plant sludge and other commercial discharge. Numerical models in series have been developed to simulate all modes of transportation from the various sources to best assess the groundwater contamination potential (Barr, 2017). PFOA transportation through air was modeled using AERMOD developed by the USEPA. Individual air dispersion models were created for the various sites, with some emissions data estimated due to a lack of data (Barr, 2017). The Soil-Water Balance model was used to calculate infiltration rates based on daily hydrological data with

the monthly output grids used for the groundwater flow and unsaturated zone modeling, which was simulated using the MODFLOW-NWT and unsaturated zone flow and unsaturated zone transport packages from the MT3D-USGS codes (Barr, 2017). HYDRUS-1D database was used to describe linear water movement through a varied unsaturated zone thickness (Barr, 2017). The source and fate of PFOA were simulated using the model described above to provide a conservative estimate of PFOA concentrations in the groundwater and private wells. Results from the simulations were comparable to observed data in private wells in North Bennington, but were not comparable for wells located south of the Bennington landfill (Barr, 2017). More data and calibration are necessary to better simulate and predict PFOA movement and fate in private drinking water wells in Bennington, Vermont.

Shin et al. (2011) also developed a conceptual model on PFOA movement and fate through air, surface water, groundwater, and municipal wastewater treatment systems in West Virginia around the Washington Works Plant. The model was developed using AERMOD, PRZM-3, BreZo, MODFLOW, and MT3DMS calibrated using historical emissions rates from the plant, wastewater treatment water quality data from six municipal treatment plants, physicochemical PFOA properties, and geologic and meteorological data from the area (Shin et al., 2011). Results from the model were similar to observed concentrations in public well water and showed that the groundwater around the facility might remain contaminated for another decade, depending on the public well-pumping rates, which were observed to greatly influence groundwater contamination levels (Shin et al., 2011). Accuracy in results was limited by both observed data and long simulation time, which prevented the use of a Bayesian model optimization with water concentration data (Shin et al., 2011). Additional processing power and data on private wells, landfill seepage, and PFOA particle size distributions could help reduce the output uncertainties.

2.6 Limitations and goals of research

The limitations of the current studies and the goals of this research study are described below.

2.6.1 Limitations and recommendations

Previous studies have helped develop a better understanding of the sources and transportation of PFAS through the environment, but there are still many gaps, such as:

- Environmental mobility due to little knowledge on sorption/non-sorption to soils and sediment (Nguyen et al., 2016; Schaefer et al., 2019; Shin et al., 2011; J. Xu et al., 2013)
- Aquatic ecosystems modeling as regard to PFAS are in their infancy (Gallo et al., 2012; C.
 Liu & Gin, 2018)
- Studies have focused on lethal rather than sublethal effects (SETAC, 2019; Simon et al., 2019)
- Develop models in series to simulate movement through air, soil, and water and unveil the complexity of PFAS contamination (Barr, 2017; Shin et al., 2011; Simon et al., 2019).
- Research different sources, ecosystems, and PFAS compounds to prevent long-term contamination and associated adverse outcomes (Jantzen et al., 2016; Simon et al., 2019)
- Much of the current research focuses on PFOS and PFOA, but the transport and fate of their short-chain alternatives has not yet been observed nor modeled in detail (Brusseau & Van Glubt, 2019; Li et al., 2017; Shin et al., 2011)
- Future research on the movement of other PFAS chemicals as well as the impact of PFAS in relation to other POPs within flowing water systems will be needed to better predict long-term impact of the chemicals (Brusseau & Van Glubt, 2019; O'Driscoll et al., 2013)

2.6.2 Goals

The goal of this study is to develop a conceptual hydrodynamic model to simulate the fate and transport of PFAS through the Huron River watershed. The hydrodynamic model will be used to identify potential reservoirs for more directed sampling and informed management decisions. Finally, this model will be used in conjunction with experimental data on exposure, bioaccumulation, and effects of PFAS mixtures to better inform future monitoring efforts and recommendations for next steps.

3 Introduction to the Methodology

This thesis comprises two research papers that have been submitted to scientific journals. The first paper is a comprehensive literature review of PFAS fate and transport modeling. Over 100 references from the past two decades were synthesized the model applications of PFAS via water medium through surface water, vadose zone, groundwater, streamflow as well as their uptake and accumulation in plants and aquatic organisms. Ultimately, knowledge gaps in modeling PFAS for each environmental area were identified.

The second study aims to assess the capabilities and shortcomings of widely used models to study large-scale PFAS fate and transport. A surface water model (Soil and Water Assessment Tool-SWAT), a groundwater model (modular finite difference model-MODFLOW), and a streamflow model (Water Quality Analysis Simulation Program-WASP) were set up and integrated to simulate PFAS fate and transport in a large watershed. The study area was the Huron River watershed, a highly PFAS impacted watershed in Southeastern Michigan.

4 Opportunities and Challenges of Integrated Large Scale PFAS Modeling Part I:
Overview of Modeling, Applications, and Knowledge Gaps

4.1 Introduction

Chemicals have extended the average human lifespan, increased agricultural yields, and transported goods and services on a global scale, but they have also adversely impacted our environment, health, and wellbeing (Glibert et al. 2014; Pajević et al. 2008; Runnalls et al. 2010). One of the most ubiquitous and persistent artificial chemicals apparent today is per- and polyfluoroalkyl substances (PFAS), encompassing over 9000 different fluorocarbons (US EPA 2021). PFAS are characterized by the number of carbons within the chain and their functional group, giving PFAS their unique hydrophilic and hydrophobic properties (Simon et al. 2019) and their toxicity (Frisbee et al. 2009; Simon et al. 2019). These unique properties have been applied to many convenience items such as nonstick cookware coatings, weatherproofing outerwear, and stain proofing carpet (Kotthoff et al. 2015) and safety items, such as a chemical fume suppressant for the chrome plating industry and aqueous film forming foam (AFFF) fire suppressant for oil fires (Hu et al. 2016; ITRC 2018). Due to the strong nature of the carbon-fluorine bond, PFAS have estimated half-lives of hundreds (precursors) to thousands of years (ITRC 2020a). The bond strength with historic worldwide manufacturing and usage have led to PFAS being detected worldwide (EEA 2019; US EPA 2019; IPEN 2019).

In 2005, the C8 Health Project was the first large-scale blood survey that gave light to the health implications of perfluorooctanoic acid (PFOA) exposure (Frisbee et al. 2009). The main exposure route observed by Frisbee et al. (2009) was contaminated drinking water in six water districts, which all stemmed from the DuPont Washington Works facility. Survey results observed

a strong connection between high blood PFOA concentrations and major health implications such as heart disease, cancers, neurologic disorders, inflammatory and autoimmune disorders, and pregnancy complications for all ages and demographics (Frisbee et al. 2009). Although the C8 Health Project focused primarily on PFOA, it led to additional research on other PFAS, identifying the class of perfluoroalkyl acids (PFAA), which includes perfluorooctane sulfonate (PFOS), as a toxic group of PFAS molecules with serious adverse effects for both humans and aquatic species (Tsuda 2016; USEPA 2017). Thus, the C8 health project highlighted the implications of drinking water contamination and water and aquatic species' ability to create an extensive breadth of exposure (Ahrens & Bundschuh 2014; Borthakur et al. 2021; Nguyen et al. 2016).

From 2013-2015, the USEPA led a drinking water sampling study to prevent PFAS contamination around the country (US EPA 2019). Additional large-scale studies were performed in other parts of the world, such as Italy (Mastrantonio et al. 2018), China (Liu et al. 2021), and Australia (Toms et al. 2019). These sampling efforts have identified high-risk areas and have led to more in-depth health studies. Through the sampling studies, PFAS compounds have been observed in surface water (Borthakur et al. 2021; Li et al. 2017), groundwater (Guelfo & Adamson 2018; Mahinroosta et al. 2021), aquatic ecosystems (Aherne & Briggs 1989), air (Nilsson et al. 2013), plants (Gassmann et al. 2020; Ghisi et al. 2019), and soil (Høisæter et al. 2019; Schaefer et al. 2019). Among these PFAS exposure routes, the highest concentrations have been recorded in drinking water and aquatic organisms (ATSDR 2020), given the bioaccumulation and biomagnification patterns of PFAS in aquatic species (Ahrens & Bundschuh 2014).

Multiple computational models have been developed from experimental studies to improve the understanding of PFAS fate and their spatiotemporal transport within an environment (Ahrens & Bundschuh 2014; Gomis et al. 2015; Lyu et al. 2018). Although these studies have provided

greater insight into the environmental factors driving PFAS transport, they focus on isolated components of the system rather than illustrating the connectivity of PFAS fate and transport across the entire system of exposures. Therefore, the overall goal of this study is to synthesize the potential opportunities and challenges of large-scale and integrated PFAS modeling. This will allow policymakers to better develop mitigation strategies to holistically address the environmental and social difficulties caused by the introduction of PFAS and the widespread usage of this compound. In order to achieve this goal, two objectives were sought including, 1) synthesizing the literature and identifying the governing equations that describe the fate and transport of PFAS compounds within different mediums and 2) identifying the knowledge gaps and future experimental and modeling research needs as related to the PFAS fate and transport.

4.2 Overview of PFAS transport

To describe the fate and transport of PFAS compounds within different mediums, published manuscripts were summoned via Google Scholar and Web of Science using over 50 different search terms. The top ten terms used were "PFAS", "perfluoroalkyl substances", "mechanistic", "model", "uptake", "transport", "contaminant", "PFOS", "PFOA", and "organic pollutant". Under each major search term, sub terms were also considered for a more comprehensive search. We also limited the period of search to literature published in the last two decades. The literature suggested a strong connection between PFAS chemistry and environmental fate and transport. Therefore, the literature summarization begins with an overview of the environmental drivers influencing PFAS within the soil and water mediums. With the environmental factors established, the paper traces PFAS transport through the surface water, vadose zone, and groundwater. Governing equations for each environmental media with corresponding limitations were identified and described.

A boundary condition was established to describe the modeling processes (Figure 1). The boundary condition encompasses the vadose zone, groundwater, and surface water (overland flow and streamflow) environment for this study. Meanwhile, the control volume is permeable to incoming (sources) and outgoing (sinks) PFAS compounds.

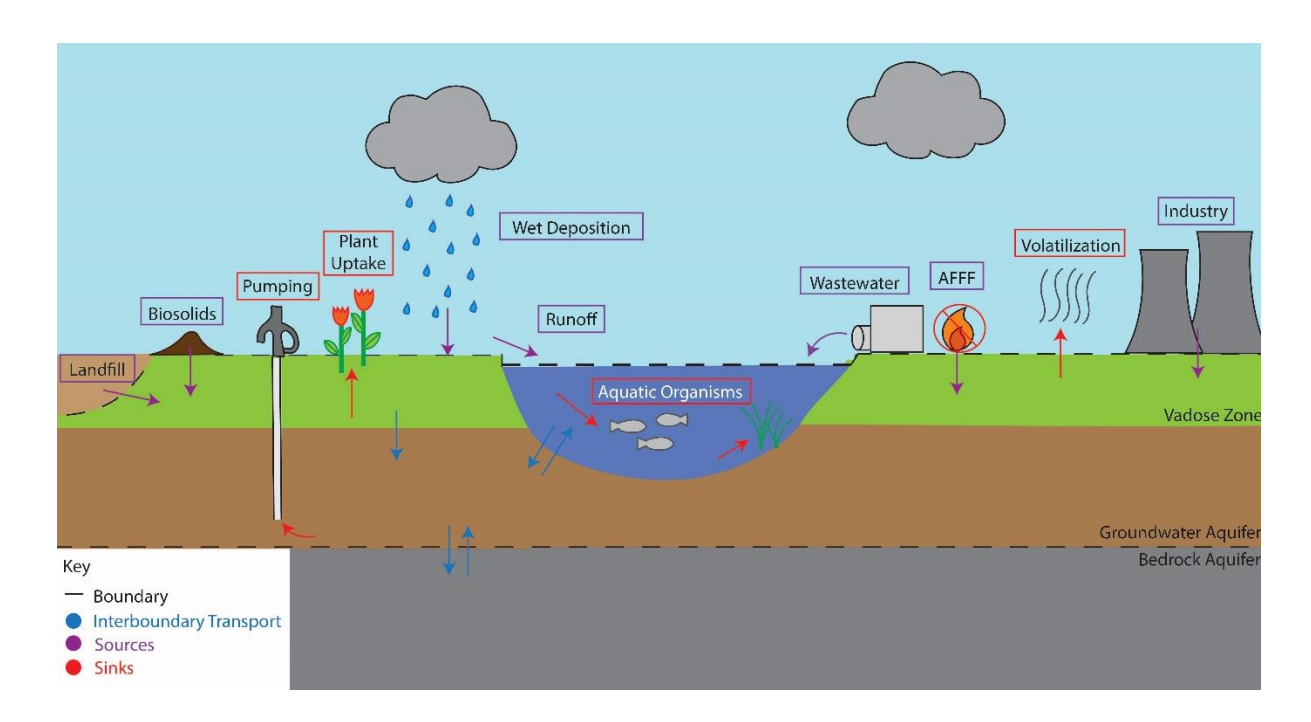


Figure 1. Schematic presentation of PFAS sources, sinks, and transport elements within the environment.

Following the connections observed in Figure 1, PFAS is introduced to the overland portion of the system boundary via nonpoint sources (e.g., biosolids, wet, and air depositions) and point sources (e.g., landfill and wastewater). From there, PFAS percolate through the soil layers, disperses in the vadose zone, and finally leaches into the groundwater. PFAS can also be attenuated within the vadose zone and saturated zone via chemical and geochemical retention processes. PFAS can be taken up and removed from the control volume by natural (e.g., plant) or artificial (e.g., pumping) actions herein called sinks, or be transported within the control volume (e.g., from

lateral groundwater flow to streams and lakes). After discussing PFAS fate and transport mechanism through the subsurface and surface environment, the needs for additional experimental and modeling research were identified and summarized.

4.3 Environmental factors affecting PFAS transport

PFAS characteristics, such as functional group and chain length, influence PFAS transport through soil and water. The PFAS functional group often has an ionic charge, which influences the PFAS' affinity for charged substances. One of the main ionic subsurface components is organic matter, which has both neutral and charges sites. Organic matter is comprised of anionic compounds, such as phenolic hydroxyl groups and carboxyl groups, which provide cationic binding sites for positively charged species (Wei et al. 2017). Other soil constituents can provide anionic binding sites, which become stronger with a decrease in soil pH (Bolt 1976). Through contact with water, PFAS can become anionic via deprotonation, which depends on the acidity of the functional group represented by the acid dissociation constant (pKa) (Vierke et al. 2013). Two common deprotonating functional groups are sulfonic acid and carboxylic acid, which have different anionic strengths given their negative charge distributions; the sulfonic acid can distribute the negative charge across three oxygens as opposed to two oxygen in carboxylic acid (Bedford 2003). In the example of PFOS and PFOA, the PFOS would be more readily available to bind in acidic soil than PFOA due to the sulfonic acid's low pKa or strong acidity (ITRC 2020c). Additionally, chain length has been directly correlated with the sorption coefficient of PFAS, with the longer chained PFAS having a stronger sorption affinity than the shorter chained (Higgins & Luthy 2006). This is due to the longer-chained PFAS having larger hydrophobic tails available for interactions with organic carbon, a neutrally charged constituent of organic matter (Borthakur et al. 2021).

The PFAS not adsorbed onto the soil is available for either dissolving in the percolating water (Brusseau & Chorover 2019) or migrating through plant roots (Mei et al. 2021), depending on their structure and charge. Plant roots are composed of a phospholipid bilayer, allowing other hydrophobic molecules to pass through (Mei et al. 2021). Therefore, the chain length phenomenon also holds true for root uptake, with longer chains having a higher chance of making it into the plant than shorter chains. In unsaturated soil, the hydrophobic compounds compete between the soil particles and the root phospholipid bilayer, whereas in saturated environments, there are fewer soil binding sites for the PFAS to attach to, so they are more likely to make it into the plant (Wang et al. 2020b). Cationic PFAS can also make their way into plants via anionic soil minerals, which travel through anion channels in the phospholipid bilayer via cation exchange (Wang et al., 2020b). Finally, the dissolved PFAS are available for root uptake of plants or gravitational mobility to the groundwater.

4.4 Sources of PFAS

Without a source, PFAS would not be found on Earth; this summary aims to outline the major sources of PFAS in both the soil and water environments. One of the major nonpoint sources of PFAS in the soil environment is the use of AFFF for aviation and vehicle firefighting (Brusseau et al., 2020; Guelfo et al., 2020; Moody et al., 2003). Because AFFF is the most effective method of containing oil and gas fires, it has been widely used on military installations (ITRC, 2018). Additionally, the application of biosolids, a solid byproduct of wastewater treatment, is another nonpoint source of contamination in the soil environment. Due to the rich-nutrient content of biosolids, they have been used as a fertilizer on agricultural fields for decades (US EPA, 2021). Recently, high concentrations of PFAS have been detected inbiosolids (Arcadis, 2020; Brusseau et al., 2020; Winchell & Propato, 2019). Biosolids tend to be landfilled when they cannot be land

applied. The landfill then receives PFAS contamination from biosolids as well as consumer contamination which can potentially leach into groundwater aquifers (ITRC, 2020). Moreover, the air emissions from PFAS manufacturing sites deposit onto the surrounding region, serving as an additional source of PFAS in the soil environment. (Nilsson et al., 2013; Shin et al., 2011).

Wind can transport PFAS attached to particulates to the most remote locations and deposit on soil and on surface water (Åkerblom et al., 2017). Also, industries discharge their PFAS contaminated effluent either directly into surface water bodies or to a wastewater treatment plant (WWTP), which finally reach the surface water (EGLE, 2019a; Möller et al., 2010). Runoff can transport dissolved and particulate PFAS in the soil to downstream waterbodies (Borthakur et al., 2021; Codling et al., 2020). Further on, PFAS leaching from the vadose zone can contaminate groundwater aquifers and consequently diffuse within the system and become another source of PFAS for the surface waterbodies (Hu et al., 2021; Shin et al., 2011). These sources are not all alike though, WWTP and industry effluent are point sources of PFAS to water bodies, AFFF, biosolids, and landfills are nonpoint sources to the vadose zone and wind, air, and runoff are nonpoint sources to the physical environment.

4.5 Overland flow and streamflow models

Given the plentiful above-ground production and uses of PFAS, it is predicted that almost all surface water has been contaminated (Åkerblom et al., 2017). Many software platforms have been developed to simulate the transport of chemicals within surface water, but only a few have been applied to PFAS to date. The Delft3D model suite calculates non-steady flow and transport via hydrodynamics in both 2D and 3D (Deltares, 2021). The spatially and temporally resolved exposure assessment model for European basins (STREAM-EU) applies a fugacity approach to estimate organic contaminant transport via water and sediment (Lindim et al., 2016). The

multimedia, multipathway, and multireceptor risk assessments (3MRA) model performs risk assessment and uncertainty analysis using air, soil, surface water, groundwater, and plant fate and transport pathways (Marin et al., 2010). In addition, the BreZo model is a finite-volume 2D transport model for simulating wet and dry periods in shallow-water flow (Begnudelli & Sanders, 2006). Surface water transport of PFAS has been simulated using the Delft3D, STREAM-EU, 3MRA, and BreZo models based on different applications of the following governing equations.

4.5.1 Governing equations of overland flow and streamflow

During and after a storm event, water runs across the Earth's surface towards a stream or waterbody, otherwise known as overland flow, or percolates into the subsurface. Runoff has been notorious for carrying nutrients, sediment, and other pollutants into nearby streams and waterbodies (Diaz & Rosenberg, 2008). Recently, PFAS has been observed to be adsorbed onto suspended particles carried by runoff, especially in urban areas (Borthakur et al., 2021; Codling et al., 2020). To estimate the amount of runoff from a rainstorm, the overland flow has been modeled using two different methods. The first is through the soil conservation service (SCS) curve number (CN) method, which estimates runoff based on the volume intercepted by the plants and soil type as seen in Equation (18):

$$Q = \frac{(P - I_a)^2}{(P - I_a) + S} \tag{18}$$

where, Q is the runoff (L), P is the precipitation (L), I_a is the initial abstraction (L), and S is the potential maximum retention after runoff begins (L) (USDA, 1986). Through the maximum retention value, runoff is correlated with the groundcover CN through the following relationship: $S = \frac{1000}{CN} - 10$. For agricultural areas with high canopy interception and variable root systems, this equation provides a good estimate of runoff flow.

Rather than estimating runoff volume via plant coverage, the second method uses soil physics to calculate the amount of water available for overland flow. Through the overland slope, flow direction and magnitude can be estimated. Soil friction then refines the speed of overland water flow. Together, a modified diffusive wave equation is developed for horizontal overland transport (Equation (19)):

$$Q = \frac{K\Delta x}{\Delta x^{1/2}} \sqrt{Z_u - Z_D} h_u^{5/3}$$
 (19)

where, K is the Strickler roughness coefficient or Manning M, Δx is the horizontal distance (L), Z_u is the higher water level from datum (L), Z_D is the lower water level from datum (L), and h_u is the depth of water free for overland flow (L) (DHI, 2017). Equation (19 was built for the finite difference method and therefore can be easily integrated into most watershed models, whereas Equation 18 is better suited for lumped solvers. Although both Equation 18 and Equation (19(18 are well established and have been used in multiple watershed scale models, neither have been modified to account for PFAS transport to date.

Once the water enters the stream via runoff, direct discharge, or baseflow, it moves around and over obstacles while carrying sediment and contaminants. Though the complexities of surface water transport have yet to be successfully modeled through the Navier Stokes Equations, the models described above have successfully applied the continuity equation (Equation(20) to simply describe water transport based on the conservation of volume:

$$\frac{\partial Q}{\partial x} + \frac{\partial A}{\partial t} = 0 \tag{20}$$

where, Q is volumetric flow (L³/T), x is the direction (L), A is the cross-sectional area (L²), and t is time (T) (Ambrose & Wool, 2017). Through modification, Equation (20 can be applied to any

water transport scenario from shallow streams to deep oceans (Aly et al., 2020; Shin et al., 2011). For simplified models, Equation (18 is applied to the entire stream or water body. In an effort to capture some of the heterogeneities of water flow, a modified version of Equation (18 can be applied to different vertical or horizontal segments of the simulated study area (Deltares, 2021).

Within rivers and streams, water flow is also impacted by frictional forces on the riverbed and walls. To encompass the complexities associated with water flowing through a channel, flow can be calculated through a relationship between surface roughness, slope, and area, such as in the Manning's equation (Equation (21):

$$Q = \frac{1}{n} \frac{A^{\frac{5}{3}}}{R^{\frac{2}{3}}} \sqrt{S_0} \tag{21}$$

where, n is the Manning friction factor, A is cross-sectional area (L²), B is the width (L), and S_0 is the bottom slope (Ambrose & Wool, 2017). Not only is the flow of water affected by moving across rough surfaces, but contaminant transport is too.

As previously discussed, contaminants have varying affinities for water and sediment depending on their chemical structure (Brusseau & Chorover, 2019). Polar chemicals have been observed to be soluble in water and are driven by a gradient in concentration, otherwise known as diffusion (Brusseau & Chorover, 2019). Non-polar molecules tend to move with sediment where contaminant transport occurs in conjunction with the sediment particle, which moves at various velocities within the water body via settling, deposition, erosion, and resuspension (Ambrose et al., 2017). Finally, advection explains the bulk transport of all contaminants via water (Ambrose & Wool, 2017). Therefore, the advection-dispersion-diffusion equation (Equation (22) can be implemented to model contaminant transport through water bodies:

$$\frac{\partial C}{\partial t} = -u_x \frac{\partial C}{\partial x} + D \frac{\partial^2 C}{\partial x^2} - k_d C - \frac{v_s}{H} F_p C + \frac{v_r}{H} C_{sed} + \frac{v_d}{H} (F_{dsed} C_{sed} - F_d C) + S$$
 (22)

where, u_x is the velocity of water in the x-direction (L/T), D is the dispersion coefficient (L²/T), k_d is the decay rate (1/T), v_s is the sediment settling velocity (L/T), H is the water depth (L), F_p is the particulate fraction, v_r is the sediment resuspension velocity (L/T), C_{sed} is the contaminant concentration on the sediment (M/L³), v_d is the diffusion velocity (L/T), F_{dsed} is the dissolved fraction of contaminants in the sediment, F_d is the dissolved fraction of contaminants in the water, S are the external contaminant sources (M/L³/T) (Wool et al., 2020). When coupled together, Equations (21 and (22 can simulate contaminant transport through many different water body scenarios. The following summarized applications show how these equations have been applied to PFAS transport.

4.5.2 Applications of PFAS in overland and streamflow models

Aly et al. (2020) applied the Delft3D model suite to the Galveston Harbor to simulate PFAS transport due to wind and waves after a major oil fire using Equations (20 and (22. The Delft3D model did not account for sediment transport or sorption, but rather estimated the movement of PFAS solely from dispersion within water (Aly et al., 2020). The model was calibrated using oceanic current observations from the same season as the firefighting spill and followed similar trends to PFAS sampling observations (Aly et al., 2020). Delft3D was also applied by Hodgkins et al. (2019) to the Halifax Harbor, simulating ocean surface PFAS contamination transport via waves using the same equations. The Delft3D model was calibrated and validated using observed wind and wave data from an offshore smart buoy and simulated tides (Hodgkins et al., 2019). Short PFAS contamination events were simulated based on known naval ship fire extinguishing events using AFFF in the top water column without accounting for reaction, sorption, or volatilization

and were not compared to observed concentrations or other similar simulations (Hodgkins et al., 2019).

Lindim et al. (2016) developed the STREAM-EU, a river catchment model for simulating the fate and transport of PFAS in eleven major European rivers. The STREAM-EU model divides each river catchment into homogeneous subbasins as the spatial unit, including air, soil, surface water, and groundwater. Lindim et al. (2015) estimated PFAS input to water and soil for the Danube River using a fugacity approach based on wealth, population, land and water areas, a constant rate of atmospheric deposition, and the coverage of wastewater treatment systems of each subbasin, and modeled PFAS streamflow transport via advection. The oversimplified structure of the STREAM-EU model includes the inability to consider environmental factors and the system's connectivity and heterogeneity. Therefore, the STREAM-EU estimations for PFOA concentration in some catchments within the Danube River were significantly higher than previously recorded levels. As a result, the model's accuracy could not be guaranteed due to the significant uncertainties.

In a risk assessment study, the 3MRA model was applied to three study areas within the Cape Fear Watershed by Redmon et al. (2019) to assess PFAS contamination in drinking water. Redmon et al. (2019) built a watershed scale model to estimate both the aquatic ecosystem and human exposure to PFAS. Model complexity varied between the study areas depending on available observed data, with the most complex system including overland flow, groundwater – surface water interaction, air deposition, and vadose zone transport (Redmon et al., 2019). An uncertainty analysis was performed on simulated outcomes and used to suggest improvements in PFAS sampling (Redmon et al., 2019).

Shin et al. (2011) developed an integrated air-groundwater-surface water model of the C8 Health Project study area. Shin et al. (2011) simulated the long-term transport of PFOA from the Washington Works Plant in West Virginia into residential drinking water through the integration of the American Meteorological Society/EPA Regulatory Model (AERMOD), MODFLOW, PRZM-3, and BreZo models. The BreZo model used a simplified approach, similar to (Aly et al., 2020), using Equations (20 and (22 only accounting for dispersion and one primary source (Shin et al., 2011). Due to the extensive computational requirements of the model (about a week per run), they calibrated the model only for the PFOA soil-water partition coefficient rather than streamflow transport (Shin et al., 2011). Therefore, even though Shin et al. (2011) accounted for air, groundwater, and surface water, the models were not linked, oversimplified, and unvalidated transport estimation. Though there have been a few applications of PFAS transport via surface water, many of them are simplistic and spotlight the knowledge gaps within this area of PFAS research.

4.6 Vadose Zone

The vadose zone functions as the pathway between the atmosphere and groundwater system Hopmans & van Genuchten (2005) and is exposed to many sources of PFAS. This review identified five widely used models capable of simulating complex biological, physical, and chemical interactions between substances within the vadose zone. HYDRUS is a finite-element model used for simulating 1D, 2D, and 3D water, heat, and solute transport through both unsaturated and saturated media (Šimůnek et al., 2016). GeoStudio is a commercial numerical modeling software developed by GEO-SLOPE International Ltd. for simulating heat and mass transfer through both unsaturated and saturated subsurface flow (GeoStudio, 2021). The US Environmental Protection Agency (USEPA) pesticide root zone model (PRZM) and European

Commission pesticide leaching model (PELMO) simulate the movement of water and solute (i.e., pesticides) through the soil via a 1D finite difference method (Carsel et al., 1985; Klein et al., 1997). Also, the MACROpore flow (MACRO) model uses a simplified capacitance-type approach to simulate water and contaminant flow through soil macropores (Jarvis & Larsson, 2001).

4.6.1 Governing equations for the vadose zone

In general, contaminant transport through the vadose zone is driven by multiple kinetics, including sorption, advection, dispersion, and diffusion (Patil & Chore, 2014; Šimůnek et al., 2011). Sorption drives contaminant transport via solids, while advection, dispersion, and diffusion drive the transport via fluids (Brusseau & Chorover, 2019). In addition, certain PFAS can volatilize, degrade, and react with other contaminants (Sima & Jaffé, 2021). Given the wide range of PFAS characteristics, contaminant transport kinetics of all three physical media should be taken into account when modeling. Therefore, in order to simulate PFAS transport through the vadose zone, solid, fluid, and contaminant transport must be integrated (Šimůnek & Bradford, 2008). The upcoming governing equations are the most common and widely applied forms of transport equations for modeling the vadose zone.

The concentration of adsorbed chemicals onto solids within the vadose zone is highly dependent upon the characteristics of the contaminant (Brusseau & Chorover, 2019). Temporal sorption curves can be linear or nonlinear and often specific to a solid and contaminant pair. PFAS can also have nonlinear adsorption isotherms (Guelfo et al., 2020; Lyu et al., 2018). The nonlinear Equation (23 describes a general adsorption isotherm that can be applied to any PFAS (Šimůnek et al., 2011):

$$s_{k} = \frac{k_{s,k}c_{k}^{\beta^{k}}}{1 + \eta_{k}c_{k}^{\beta^{k}}} k\epsilon(1,\eta_{s})$$

$$\frac{\partial s_{k}}{\partial t} = \frac{k_{s,k}\beta_{k}c_{k}^{\beta_{k-1}}}{(1 + \eta_{k}c_{k}^{\beta_{k}})^{2}} \frac{\partial c_{k}}{\partial t} + \frac{c_{k}^{\beta_{k}}}{1 + \eta_{k}c_{k}^{\beta_{k}}} \frac{\partial k_{s,k}}{\partial t} - \frac{k_{s,k}c_{k}^{\beta_{k}}}{\left(1 + \eta_{k}c_{k}^{\beta_{k}}\right)^{2}} \frac{\partial \eta_{k}}{\partial t} + \frac{k_{s,k}c_{k}^{\beta_{k}} \ln c_{k}}{\left(1 + \eta_{k}c_{k}^{\beta_{k}}\right)^{2}} \frac{\partial \beta_{k}}{\partial t}$$

$$(23)$$

where, s and c are the solute concentrations in the solid (M/M) and liquid (M/L³) phase, the empirical coefficients are $k_{s,k}$ (L³/M), β_k , and η_k (L³/M), which change with temperature but are independent of concentration (Šimůnek et al., 2011). By modifying the empirical coefficients, Equation (23 can be used to represent the Langmuir, Freundlich, or linear sorption relationship. The concentrations of chemicals not adsorbed onto the solids are available for transport via fluids through advection and dispersion mechanisms (Brusseau & Chorover, 2019).

Rather than adsorbing to solids, some chemicals dissolve completely in fluids and are transported via fluid flow. This process of dissolved solids moving with fluids is known as advection, but does not account for the mixing of concentrations, or dispersion, that also occurs in subsurface systems (Patil & Chore, 2014). Therefore, the movement of contaminants via fluids in subsurface systems is described by a combined advection-dispersion Equation (24:

$$D_x \frac{\partial^2 C}{\partial x^2} - \tilde{v}_x \frac{\partial C}{\partial x} = \frac{\partial C}{\partial t}$$
 (24)

where, D_x is the coefficient of hydrodynamic dispersion (L²/T), C is the concentration (M/L³), x is the coordinate plane along which the average linear velocity (\tilde{v}) (L/T) occurs, and t is time (T) (Patil & Chore, 2014). Equation (24 can be expanded to represent 2-dimensional flow by adding corresponding y or z terms to the left side. Given the complex air-water interface and porosity of

the vadose zone materials, estimating fluid flow velocity is dependent on available information, assumptions, and simplifications (Weill et al., 2009).

The simplest way to model flow through the vadose zone is via Darcy's law. Darcy's law (Equation 25) relates flow (q) in saturated media to the hydraulic head (h):

$$q = -K \frac{\partial h}{\partial l} \tag{25}$$

where, q is flow (L³/T), h is hydraulic head (L), l is the coordinate direction (L), and K is hydraulic conductivity (Anderson et al., 2015). Darcy's law can only be applied to steady-state saturated flow since it does not account for the air-water interface or time variability. The Richards equation, which is based on Darcy's law, represents the relationship between time variable volumetric water content and unsaturated hydraulic conductivity (Richards, 1931).

The Richards equation has been adopted around the world to simulate unsaturated water flow through porous media (Weill et al., 2009; Zha et al., 2019). A modified version of the Richards Equation (26 (Šimůnek et al., 2011), which can be applied to one-, two-, or three-dimensions, mathematically represents the water movement through the air-water interface:

$$\frac{\partial \theta}{\partial t} = \frac{\partial}{\partial x_i} \left[K \left(K_{ij}^A \frac{\partial h}{\partial x_i} + K_{iz}^A \right) \right] - S \tag{26}$$

where, θ is the volumetric water content (L³/L³); S is the sink term (L³/L³/T), K is the unsaturated hydraulic conductivity (L/T), h is the hydraulic head (L), K_{ij}^A are the components of the anisotropic tensor K^A , and t is time (T) (Richards, 1931; Šimůnek et al., 2011). Additionally, fluids can be transported out of the subsurface system via plant uptake and volatilization, which would be considered by S in Equation (26.

4.6.2 Applications of PFAS transport in vadose zone models

Vadose zone models have been applied to a variety of observed situations around the world. To date, most vadose zone models have been built to simulate PFOS, due to its solubility in water, high toxicity, and presence in a variety of contamination sources (US EPA, 2016b). Both 1D and 2D computer models have been developed to simulate the vadose zone using the Richards Equation (26 and the advection-dispersion Equation (24 simultaneously. A simple 1D model was developed in HYDRUS by Silva et al. (2020) following the column experiment performed by Lyu et al. (2018) of PFOA transport through unsaturated quartz sand. Model results followed the observations of Lyu et al. (2018) under similar conditions Silva et al. (2020). Additional conceptual models were developed in HYDRUS simulating 2D transport of both PFOS and PFOA through various media (Silva et al., 2020), but were not validated due to a lack of physical observations. Guo et al. (2020) also used HYDRUS to develop transient flow 2D simulations of PFOS under both semiarid and humid conditions. The HYDRUS model used Equations (24, 25, and 26 with an added surface tension component (Guo et al., 2020). Only one model was close enough to an experiment for validation, which had good agreement between the breakthrough curves of the simulated and observed data (Guo et al., 2020).

Mahinroosta et al. (2021) used the GeoStudio software to simulate temporal 2D advection, dispersion, adsorption, and decay transport of PFOS through a study area under 100 years of climate conditions. The 2D model simulated different scenarios of transport retardation and was validated against water quality samples within the simulated study area. Both short and long-chained PFAS were simulated by McLachlan et al. (2019) using the PELMO model, which included losses to both root uptake of crops and evapotranspiration. The simulation suggested high retention (>90%) of PFAA in the soil, whereas the lysimeter observations suggested that only a

small fraction (<5%) was retained in the soil. They attributed this to the controlled lab PFAS application (McLachlan et al., 2019). Both the experiment and simulation observed more movement of shorter chained PFAS out of the vadose zone into plants or groundwater and retardation of longer-chained PFAS molecules due to strong sorption onto organic matter (McLachlan et al., 2019).

The USEPA PRZM model was used to simulate the impacts of field applied PFOS and PFOA contaminated biosolids in Maine for a long-term period (Winchell & Propato, 2019). Even though Winchell & Propato (2019) included both sorption and plant uptake in the model, it continued to overestimate leaching when validated against comparable field observations. Shin et al. (2011) also applied the PRZM model to estimate PFOA transport through the soil. More specifically, the surface soil concentration, subsurface soil concentration, storage in soil column, and the recharge flux to groundwater were all estimated for PFOA transport by (Shin et al., 2011). Given the consistent sampling data for the study area, Shin et al. (2011) were able to optimize the soil-water partition coefficient and organic carbon partition coefficient via annually observed PFOA data in six municipal water wells. Even though the parameters were optimized, the dominant processes determining the PFAS fate and transport as well as the source of errors could not be identified through this modeling framework (Shin et al., 2011).

Gassmann et al. (2020) used the MACRO model to simulate PFAA transport and plant uptake across an active, annually cropped field. Gassmann et al. (2020) compared their modeling results with a lysimeter experiment carried out by Stahl et al. (2013) and found that the simulation overestimated PFAA leaching into the groundwater from the vadose zone. Additionally, plant uptake values were overestimated for PFOS and underestimated for PFOA (Gassmann et al., 2020). The model inaccuracies were attributed to the use of similar kinetic parameters for all PFAA

compounds rather than individual parameters in addition to a lack of understanding of the non-extractable residues formation, which Gassmann et al. (2020) observed to be an important component for PFAA fate and transport. To a certain extent, these models increased the understanding of PFAS movement in the vadose zone and provided new insight into the knowledge gaps in PFAS movement with the subsurface flow.

4.7 Groundwater models

The saturated zone beneath the vadose zone is made up of heterogeneous and stratified layers of porous materials that comprise the groundwater aquifer systems (Alley, 2009). Within the US, groundwater provides domestic water for over half of the population (US EPA, 2018a), yet is one of the main exposure routes of elevated PFAS concentration (Guelfo & Adamson, 2018; Hu et al., 2016). The following review highlights both widely used and up-and-coming methods for estimating the movement of PFAS through the groundwater network.

The US Geological Survey (USGS) MODFLOW is a fully distributed physically-based model for simulating groundwater layers (USGS, 2021). MODFLOW packages such as MT3D and MODPATH have been developed to simulate particle flow paths and solute transport, which already have been applied to simulate PFAS fate and transport in the groundwater systems (Goode & Senior, 2020; Persson & Andersson, 2016; Pettersson, 2020).

4.7.1 Governing equations for groundwater flow

Groundwater can move through both unsaturated and fully saturated conditions (Alley, 2009). Therefore, groundwater transport can be estimated through the relationship between the pore space and fluid pressure (Harbaugh, 2005). Contaminant transport is driven by advection and dispersion kinetics, with adsorbed concentrations being transported via particles (Bedekar et al.,

2016). Contamination transport through the groundwater system is similar to transport through the vadose zone, with a few key differences highlighted in the following general equations.

As forementioned, Darcy's law Equation (25 describes saturated flow through porous media and is, therefore, the basis of every groundwater transport model. In order to simulate the three-dimensional movement of groundwater, Darcy's law can be expanded (Equation (27):

$$\frac{\partial}{\partial x}(K_{xx}\frac{\partial h}{\partial x}) + \frac{\partial}{\partial y}(K_{yy}\frac{\partial h}{\partial y}) + \frac{\partial}{\partial z}(K_{zz}\frac{\partial h}{\partial z}) + W = S_s\frac{\partial h}{\partial t}$$
(27)

where, K is the hydraulic conductivity along the respective coordinate axis (L/T), h is the potentiometric head (L), W is the volumetric flux per unit volume (1/T), S_s is the porous media's specific storage (1/L), and t is time (T) (Harbaugh, 2005). Even though Equation (27 provides a concise mathematical representation of groundwater flow through three-dimensional space, it is nearly impossible to solve analytically. Therefore, numerical methods have been developed to computationally simplify Equation (27 while still holding the model integrity. The numerical methods such as finite element and finite difference are widely used, dividing the study area into a finite number of cells. The flow into and out of each cell can be represented by a relationship between storage, head, and volume in a combined Darcy's law and continuity equation (Equation (28):

$$\sum Q_i = S_s \frac{\Delta h}{\Delta t} \Delta V \tag{28}$$

where, Q is the flow rate into the given cell (i) (L^3/T), V is the cell volume (L^3), and Δh is the change in head observed over the time difference (L) (Harbaugh, 2005).

In the unsaturated conditions of the vadose zone, contaminants have been observed to either sorb onto solids (Equation (23) or dissolve into fluids (Equation (24). Under the saturated groundwater conditions, the sediment surface is covered by a layer of water, which changes the sorption mechanisms for contaminants (Brusseau & Chorover, 2019). Therefore, sorption is driven by a first-order reaction (Equation (29):

$$\sum R_n = -\rho_b \frac{\partial \bar{C}^k}{\partial t} - \lambda_1 \theta C^k - \lambda_2 \rho_b \overline{C}^k$$
(29)

where, $\sum R_n$ is the term for reaction rate (M/L³/T), ρ_b is the bulk density (M/L³), \bar{C}^k is the sorbed concentration (M/M), t is time (T), λ_1 is the dissolved phase first-order reaction rate (1/T), and θ is the porosity (Zheng & Wang, 1999). Once the concentration sorbed onto the particle surfaces is identified, the amount dissolved can also be estimated. Together, sorbed and dissolved contaminant transport is driven by advection, dispersion, and reaction. Even though a general advection-dispersion was mentioned in the previous section (Equation(24), Equation (30 highlights the movement of both adsorbed and dissolved contaminants through the saturated zone:

$$\theta \frac{\partial C^k}{\partial t} + \rho_b \frac{\partial \overline{C}^k}{\partial t} = \frac{\partial}{\partial x_i} \left(\theta D_{ij} \frac{\partial C^k}{\partial x_j} \right) - \frac{\partial}{\partial x_i} \theta v_i C^k + q_s C_s^k - q_s' C_s^k - \lambda_1 \theta C^k - \lambda_2 \rho_b \overline{C}^k$$
(30)

where, θ is the porosity, C^k is the dissolved contaminant concentration (M/L³), ρ_b is the bulk density (M/L³), \overline{C} is the sorbed contaminant concentration (M/M), x_i and x_j are distances along their respective Cartesian coordinate axes (L), D_{ij} is the dispersion coefficient (L²/T), v_i linear velocity of water through pores (L/T), q_s source or sink volumetric flow rate per unit volume (T), C_s^k source or sink contaminant concentration, q_s' water storage change per unit volume (1/T), λ_1 first order reaction rate dissolved phase (1/T), and λ_2 is the first-order reaction rate for the sorbed

phase (1/T) (Bedekar et al., 2016). Through the parallel application of the finite difference method (Equation (28) and the saturated condition specific advection-dispersion-reaction equation (30), contaminant transport through the groundwater aquifer network can be estimated.

4.7.2 Applications of groundwater models for PFAS transport

The application of groundwater transport models on the movement of PFAS is a very recent endeavor. Persson & Andersson (2016) applied the MODPATH and MT3DMS modules to simulate PFOS transport from a former fire drill site (Equation (28). Groundwater movement was calibrated against observed groundwater heads (Persson & Andersson, 2016). Even though PFOS contamination sites were integrated with observed initial concentrations, transient PFOS transport data were not available for calibration or validation of PFOS movement through the study area (Persson & Andersson, 2016). Concerning PFOS retention, the observed data was too limited to support the validation exercise within the study area. Pettersson (2020) also used MODFLOW with the MT3DMS module to develop a conceptual model of PFOS, perfluorobutyrate (PFBA), and perfluoro-n-pentanoic acid (PFPeA) transport through a contaminated esker. Similar to Persson & Andersson (2016), Pettersson (2020) calibrated the groundwater simulations against the observed concentrations of the three PFAS molecules. The observed concentrations were used to establish initial conditions in the MT3DMS model, while transport kinetics were obtained from the literature (Pettersson, 2020). The model simulation results showed the varying transport distances between the PFAS types, but no data were available to validate the observations (Pettersson, 2020). Advective PFOA transport was also modeled using the MODFLOW and MT3DMS pair in groundwater using Equation (30 without the adsorbed components that were used by (Shin et al., 2011). Shin et al. (2011) linked the PRZM model and a surface water model with MT3DM in MODFLOW to predict PFOA concentrations in municipal well water. As

forementioned, the transport coefficients related to both the vadose zone and groundwater were optimized during a model calibration even though a formal sensitivity analysis for the parameters was performed (Shin et al., 2011).

A three-dimensional steady-state model was developed for a contaminated site (retired air force base and surrounding residential areas) using Equation (30 in MODPATH (Goode & Senior, 2020). Within the model, changes in both the number and the pumping rate of public supply wells were accounted for (Goode & Senior, 2020). The model was fitted with speculated PFAS sources, then calibrated using observed PFAS concentrations in shallow wells from 2014-2017 (Goode & Senior, 2020). Even though the model was not validated formally, it was observed to follow the general trends of sampling observations to date (Goode & Senior, 2020). In addition to the traditional transport models, machine learning techniques have been applied to preliminary sampling studies, of potential sources and contaminated drinking water wells, for predicting exposure (Hu et al., 2021). The preliminary PFAS data collected by the state of New Hampshire was analyzed by Hu et al. (2021) using both linear regression and random forest classification methods. Both machine learning techniques were applied to estimate the high-risk areas of PFAS from point sources and potential sources, given New Hampshire's environmental conditions. Rather than using governing equations, statistical relationships were observed between geological properties and PFAS concentrations, which followed literature findings (Hu et al., 2021). Hu et al. (2021) suggest that the random forest technique has higher prediction accuracy than linear regression due to PFAS's nonlinear transport characteristics and there is potential for using machine learning as a prediction tool so long as sources are well known. The model applications show the importance of sufficient monitoring data for high-quality groundwater modeling of PFAS

and the potential for identifying high-risk areas using the MODFLOW packages and machine learning techniques.

4.8 Sinks of PFAS

Although we have named seven major sources and modes of transport of PFAS, there are major sinks of PFAS in each environmental media as well. Within the soil environment, plants can take up PFAS through their root systems (W. Wang et al., 2020). Macroorganisms within the subsurface environment have also been sampled with high PFAS content, suggesting that they can absorb a high amount of the contaminant in the soil (Zhu & Kannan, 2019). In addition, percolated water from the vadose zone into the groundwater aquifers can carry certain PFAS and contaminate the system (Schaefer et al., 2019; Shin et al., 2011). Pumped groundwater for drinking and irrigation reduces the amount in the groundwater system (Hu et al., 2021; W. Wang et al., 2020). Algae and riparian plants have been demonstrated to act as sinks for PFAS in the aquatic environment (Penland et al., 2020). Benthic organisms and other aquatic species have had some of the highest observed PFAS concentrations to date, reducing the PFAS concentration in the sediment and surface water (Fisk et al., 2001; Glaser et al., 2021). Contaminated sediment from runoff or erosion can settle at the bottom and remain undisturbed for centuries, sinking PFAS contamination from surface water (Clara et al., 2009; Nguyen et al., 2016). Finally, Humans are also a sink for contaminated drinking and cooking water, which our bodies filter and store (Behr et al., 2020; US EPA, 2018b).

4.9 Plant uptake models

Given the application of biosolids and contaminated irrigation water on agricultural fields, plant uptake is a prevalent sink of PFAS (Brusseau et al., 2020; Costello & Lee, 2020). Most of the research to date has focused on intraplant PFAS trends rather than mechanisms of uptake

(Costello & Lee, 2020; Mei et al., 2021; Wang et al., 2020a). In addition to overall uptake, the translocation of PFAS from the soil to different plant components has been studied (Costello & Lee, 2020; Mei et al., 2021; Wang et al., 2020a; Zhang et al., 2019). The previous studies have shown concentrations of PFOA and PFOS in plants as high as 7.52 mg/kg dry weight (DW) and 254 mg/kg DW (Ghisi et al., 2019). These findings indicate that plants have high accumulation potential (Wang et al., 2020b). In addition, numerous studies investigated the physicochemical properties of the soil on PFAS translocation. For example, Zhao et al. (2018) has shown that PFCAs in wheat root and shoot increased with increasing salinity and temperature. However, the studies on PFAS translocation are limited to a few PFAS compounds. The scope of this work is to show the impact of plants on PFAS soil contamination; therefore, only the mechanistic models were reviewed. A first-order kinetic model has been applied to show the uptake of PFOS and PFOA into plants (Wang et al., 2020b; Wen et al., 2013). On a finer scale, the Michaelis-Menten equation has shown the effect of concentration on PFAS plant uptake (Costello & Lee, 2020; Wen et al., 2013).

4.9.1 Governing equations for plant uptake

Contaminant uptake into plants depends on the water's dissolved concentration and the contaminant structure (Huang et al., 2021; Wang et al., 2020a). The roots and shoots of plants are specially designed to drive the upward movement of water towards the leaves. This direction of movement provides water for photosynthesis and nutrients to support metabolic needs. Plants within contaminated soil or water have been observed to uptake dissolved contaminants in addition to nutrients, which can be estimated via a first-order kinetic equation (Equation (31):

$$Q_t = Q_0 + \frac{\alpha}{k_e} (1 - e^{-k_e t}) \tag{31}$$

where, Q_t is the total contaminant concentration in the plant at time t (M/M), Q_0 is the initial concentration of contaminant in the plant (M/M), α is the uptake flux constant (M/M/T), and k_e is the constant rate of excretion (1/T) (Wen et al., 2013). The rate of contaminant uptake in Equation (31 has been observed to be dependent on the concentration within the solution (Wen et al., 2013). Zhan et al. (2010) observed increasing uptake with increasing concentration following the Michaelis-Menten Equation 32:

$$\alpha = \frac{\alpha_{max}C}{k_m + C} \tag{32}$$

where, α_{max} is the maximum uptake rate (MM/T) and k_m is the Michaelis-Menten rate constant. Through the integration of Equations (31 and(32, PFAS uptake of plants can be estimated with a known concentration of dissolved PFAS in the subsurface system. Estimating the overall uptake rate is useful for analyzing which plants would be best suited for phytoremediation of a contaminated area Huang et al. (2021) and estimating the amount taken up versus migrating towards the groundwater. The applications of these equations are described in the following section.

4.9.2 Applications of plant uptake models

The uptake of PFOS and PFOA by maize was assessed by Wen et al. (2013) through inverse modeling of Equations (31 and(32 using their observations. Through parameter optimization, both Equations (31 and (32 closely represented the observations ($R^2 > 0.97$), showing the importance of the soluble fraction concentration on plant uptake (Wen et al., 2013). To accomplish high accuracy, each PFAS type was fitted to its own equation since PFOS was observed to have higher uptake than PFOA (Wen et al., 2013). Similarly, (Wang et al., 2020b) fitted Equations (31 and(32 to PFOS and PFOA uptake within wetland plants with $R^2 > 0.97$.

Uptake was observed to only occur with the soluble fraction of PFOS and PFOA passing through the cell walls (Wang et al., 2020b). Effective plant modeling can help design effective phytoremediation strategies and improve groundwater contamination predictions from contaminated topsoil.

4.10 Aquatic Ecosystems Models

Around the globe, water quality standards are set to prevent adverse impacts on human health even though humans are not the only organisms affected by water pollution (World Health Organization, 2018). Aquatic ecosystems have been increasingly impacted by changes in water quality, which has motivated a more robust evaluation of water quality and stream health through aquatic ecosystems models (Abouali et al., 2016; Torres-Olvera et al., 2018). PFAS bioaccumulate and biomagnify within aquatic organisms, resulting in negative toxicological effects (Ahrens & Bundschuh, 2014; Groffen et al., 2021; Rahman et al., 2014). Models have been developed and employed in an effort to predict the potential impacts of PFAS contamination on aquatic ecosystems. Biomagnification models have been developed to observe relationships between trophic levels and pollutant concentrations (Haukås et al., 2007; Penland et al., 2020). Speciessensitivity distribution curves have been developed to estimate species highly impacted by PFAS contamination (Salice et al., 2018). Mass-balance models have been developed to estimate PFAS movement within aquatic organisms (Glaser et al., 2021). In addition, the USEPA aquatic ecosystem model (AQATOX) 3.1 has an integrated PFAS component to comprehensively model water and sediment exchanges within the aquatic environment, but has not yet been applied in a peer-reviewed publication (Park & Clough, 2014). Though these models have different applications, they all are important for improving our understanding of PFAS present and extent in the aquatic environment.

4.10.1 Governing equations for PFAS fate and transport in aquatic organisms

Given the numerous external influences on aquatic organisms and the overall health of aquatic ecosystems, it is difficult to draw a clear relationship between the organism and pollution source (Ankley et al., 2010). One of the most prevalent sources of PFAS within the aquatic ecosystem is food, which has been determined by the growth of PFAS concentration throughout the food web. The enduring properties of PFAS allow it to bioaccumulate and biomagnify in aquatic species (Boisvert et al., 2019; Conder et al., 2008; Martin et al., 2003). To estimate the PFAS fate through the aquatic ecosystem, the trophic levels of each studied species are initially determined through a linear relationship between stable nitrogen isotopes of the consumer and producer (Fisk et al., 2001). Next, a biomagnification factor can be calculated for each trophic level using Equation (33, which shows the relationship between concentration and trophic level:

$$BMF = \frac{C_{p2}/C_{p1}}{TL_{p2} - TL_{p1}} \tag{33}$$

where, C_{p2} is the concentration in the predator (M/L3), C_{p1} is the concentration in the prey (M/L3), TL_{P2} is the trophic level of the predator, TL_{P1} is the trophic level of the prey, and BMF is the biomagnification factor (Haukås et al., 2007). The biomagnification factors can then be used to estimate the amount of PFAS uptake from food versus the environment of different species.

The BMF can be used to identify species with high PFAS concentrations but does not account for the sensitivity of species to the different concentration levels. To better understand the impact of various PFAS concentrations on different fish species, a distribution curve can be developed, highlighting the 95% lower confidence limit and the 5% hazardous concentration calculated from toxicology observations. Different distribution curves will simulate various data

trends in aquatic ecosystem toxicology (Salice et al., 2018; Xu et al., 2015). One of the most common distribution curves used for PFAS is the log-normal distribution, as seen in Equation (34:

$$F(x) = \frac{1}{2} \left(1 + \operatorname{erf}\left(\frac{\log(C) - \mu}{\sigma\sqrt{2}}\right) \right)$$
 (34)

where, C is the toxicant concentration, μ is the population mean, and σ is the standard deviation (Xu et al., 2015). Through Equation (34, species with high sensitivity can be estimated for further study.

To calculate PFAS uptake from a whole organism perspective, the distribution of PFAS within the aquatic organism and the rate of discharge must be considered (Martin et al., 2003; Popovic et al., 2014). A mass balance approach can be applied to calculate the total amount of PFAS being taken up by an aquatic organism. Calculating the uptake rate gives the basis for how much PFAS is leaving the streamflow system and the amount impacting the aquatic organism's food web. The relationship between both intake and output of contaminant concentration can be modeled using Equation (35:

$$\frac{dM}{dt} = \left[k_1 C_w + k_F C_F\right] W - \left[k_2 + k_E + \sum_{i=1}^{n_T} k_{M,i}\right] M$$
 (35)

where, M is the mass of a chemical in the entire body (M), C_W is the concentration of contaminant in water (M/L³), k_1 is the contaminant uptake rate for water (L³/M), C_F is the concentration of contaminants in food (M/M), k_F is the contaminant uptake rate from food (M/M), W is the body weight (M), W is the rate constant for contaminant lost at the gills (1/T), W is the fecal elimination rate constant (1/T), W is the rate constant for the metabolic transformation of contaminant (1/T), and W is the number of metabolic transformations (Glaser et al., 2021).

Equations (33, (34, and (35 can also be applied to better understand the extent of PFAS contamination within the aquatic ecosystem and the impact of aquatic organisms on PFAS concentration within the environment. Determining organism level PFAS contamination avenues (Equation (35) can help to improve our understanding of species sensitivity (Equation 34), which can, in turn give more context to the biomagnification factors (Equation (33)). These equations have been applied to PFAS transport in various aquatic ecosystems, summarized in the following section.

4.10.2 Applications of aquatic ecosystem models

The biomagnification factor of eight different PFAS compounds and other organic contaminants were observed by (Haukås et al., 2007) in four aquatic species across an arctic food web using Equation (33. Not all PFAS were quantifiable in each of the four species; therefore, BMFs were only calculated for PFOS (Haukås et al., 2007). Both trophic levels of the various species and calculated BMFs for PFOS were validated against another comparable study in the Canadian Arctic food web (Haukås et al., 2007). Additional statistical analysis was performed against other persistent organic pollutants, where PFAS were not observed to behave similarly between the proteins, but were observed to bioaccumulate and biomagnify through an arctic food web in statistically comparable quantities (Haukås et al., 2007). Penland et al. (2020) also applied biomagnification factors to assess the transport of ten different PFAS compounds through aquatic ecosystem in a river. Unlike Haukås et al. (2007), Penland et al. (2020) analyzed PFAS concentrations in plants, water, sediment, and biofilm within the aquatic ecosystem as the base food for the lowest trophic level. The observed BMFs calculated by Penland et al. (2020) were compared to recent literature (Kidd et al., 2019; Simmonet-Laprade et al., 2019) and were stated to be 'relatively similar', but were not directly validated. Within the study, the highest PFAS

concentrations were observed in insects, which are suggested to be a major food source and transporter of PFAS throughout the food web (Penland et al., 2020), but more research is necessary to validate this observation.

Rather than presenting a food web analysis, Salice et al. (2018) performed a risk assessment of PFOS in aquatic species within a contaminated bayou using Equation (34. The confidence intervals calculated for PFOS concentrations in sampled species were in agreement with previous studies (Salice et al., 2018). Each location within the study area was categorized by quantitative habitat quality and species abundance values (Salice et al., 2018). Finally, a risk assessment was performed for each location based on the number of species, surface water PFOS concentration, and toxicity levels established for aquatic ecosystems (Salice et al., 2018). Salice et al. (2018) noted that there was high uncertainty with both the surface water concentrations and the toxicity data due to the short sampling period for the surface water and small sample size for determining toxicity levels. To help better understand PFOS accumulation in aquatic species, Glaser et al. (2021) used Equation (33 to model PFOS precursor biotransformation and accumulation in different fish tissues. The model was calibrated using observations of three similar experiments, then validated using other concentration data reported in the literature (Glaser et al., 2021). Better predictability was observed for studies with large amounts of data and specifics on sampling conditions rather than studies with less sampling specifics, showing the importance of comprehensive data availability on PFOS bioaccumulation predictability (Glaser et al., 2021). Further analysis was performed by Glaser et al. (2021) using Equation (33 to calculate BMFs of PFOS and its precursors. By accounting for various avenues of PFOS exposure and the impacts of different environmental conditions on bioaccumulation and biomagnification of PFAS through

aquatic species, the mass balance approach by Glaser et al. (2021) has the potential to be a robust model for predicting PFOS accumulation in aquatic organisms.

4.11 Knowledge gaps of PFAS fate and transport modeling

To explore PFAS within the environment, a boundary condition was set for the surface and subsurface system with sources and sinks putting PFAS into and out of the system (Figure 1). Our literature review revealed many fate and transport models had been established for legacy contamination, whereas others have tried to predict the sources or fate given a monitored application rate. Table 1 summarizes the models applied to PFAS fate and transport to date which were evaluated in the literature review.

Table 1. Models applied to PFAS fate and transport to date.

Area	Model	Overall purpose	Туре	Scale	Spatial unit	Reference
Overland flow and streamflow	Delft3D	Flow and solute transport	Physically based	River, Ocean, Estuarine	3D	Aly et al. (2020) Hodgkins et al. (2019)
5 01 Cum	STREAM-EU	Surface hydrology	Process-based	Catchment	2D	Lindim et al. (2015)
	3MRA	Indicator and risk assessment	Process-based	Field & Catchment	N/A	Redmon et al. (2019)
Vadose Zone	BreZo	Surface flow/runoff	Physically based	Field & Catchment	2D	Shin et al. (2011)
	PELMO	Pesticide fate and tranport	Physically based	Field	1D	McLachlan et al. (2019)
	MACRO	Pesticide fate and tranport	Physically based	Field	1D	Gassmann et al. (2020)
Groundwater	MODFLOW	Groundwater flow	Physically based	Field & Catchment	3D	Shin et al. (2011)
	MT3DMS	Solute transport and fate	Physically based	Field & Catchment	3D	Persson & Andersson (2016) Pettersson (2020)
	MODPATH	Particle tracking	Physically based	Field & Catchment	3D	Goode & Senior (2020)
	Machine Learning	Risk Assessment	Statistical	Field & Catchment	N/A	Hu et al. (2021)
Plant uptake	First order kinetic model	Contaminant uptake rate	Process-based	Plant specific	N/A	Wen et al. (2013) Wang et al. (2020a)
	Michaelis- Menten equation	Contaminant uptake rate	Process-based	Plant specific	N/A	Wen et al. (2013) Wang et al. (2020a)

Table 1 (cont'd)

Aquatic ecosystems	Mass Balance	Accumulation potential	Process-based	Organism specific	N/A	Glaser et al. (2021)
	AQUATOX	Indicator/risk assessment/biomas s model	Process-based	Stream, small rivers, ponds, lakes, reservoirs and estuaries	N/A	Park et al. (2007)

As PFAS fate and transport changes in different mediums, the subsurface system was categorized further into the vadose zone and groundwater and the surface system covered both overland flow and streamflow models. Major PFAS sinks were also discussed, but specifically within the vadose zone, plant uptake influences the amount of PFAS retained and transported downwards. Water withdrawal for irrigation or human consumption in the groundwater system is the major sink, while within surface water, bioaccumulation of PFAS in aquatic organisms has been considered. Table 2 summarizes the knowledge gaps of modeling PFAS within each environmental medium and sink and suggests future work to overcome each shortcoming.

Table 2. Summarized knowledge gaps of PFAS application environmental models.

Subsection	Knowledge gap	References	Suggestions
Vadose zone	• PFAS have been modeled individually with focus on PFOS and PFOA.	Guo et al. (2020), Mahinroosta et al. (2021), Shin et al. (2011), Silva et al. (2020)	• Model multiple PFAS including short and long chain to show differences in transport.
	 The chemical interactions between PFAS and the competition among PFAS for adsorption and dissolving have not been considered. 	Guo et al. (2020), Mahinroosta et al. (2021), McKenzie et al. (2016), Silva et al. (2020)	• Research the impact of variable PFAS concentrations as well as different types of PFAS on sorption and dissolving within the subsurface environment.
	• The only validated vadose zone models to date are 1D.	Mahinroosta et al. (2021), Silva et al. (2020)	• Monitoring studies should be organized to capture the transport of PFAS in both the horizontal and vertical direction of the subsurface environment to provide parameterization and calibration data for 2D models.
	 Most observations and experiments are performed on a short- term basis (last 5 years), whereas PFAS contamination has been occurring since 1940s. 	Sander et al. (2017), Shin et al. (2021)	 Organized long-term PFAS studies which account for seasonality are needed for model calibration and validation.
	 Plant uptake and volatilization are known PFAS sinks yet have not been widely adopted in subsurface models. 	Guo et al. (2020), Mahinroosta et al. (2021), Silva et al. (2020)	 More research on the conditions required for plant uptake and PFAS volatilization should be conducted to provide model calibration and validation data.
Groundwater	• Organized monitoring data from PFAS sources and public exposure sites are not sufficient for developing a reliable transport model.	Goode & Senior (2020), Hu et al. (2021), Shin et al. (2011), Engers et al. (2021)	• Improve monitoring data protocols to match model calibration and validation requirements.

Table 2 (cont'd)

- PFAS physical interactions within the saturated system are widely unknown.
- Major PFAS sources, including nonpoint sources and contamination sites, are still being identified.

Surface water

- Runoff transport of PFAS has not yet been incorporated into surface water models.
- Simulations of PFAS transport within surface water often lack relevant transport mechanisms, such as sediment transport.
- Surface water models tend to be oversimplified and ignore flow diversions, such as weirs and dams.
- A lack of consistent observed data prevents adequate model calibration and validation.
- PFAS transport and deposition via air onto the surface of the water is still vastly unknown.

Brusseau et al. (2019),Pettersson (2020), Sima & Jaffé (2021), Goode & Senior (2020),Guelfo & Adamson (2018).Engers et al. (2021), Hu et al. (2021) Borthakur et al. (2021),Charbonnet et al. (2021),Codling et al. (2020),Dauchy et al. (2019), Wood et al. (2020) Hodgkins et al. (2019),Nguyen et al. (2016),Shin et al. (2011)

Redmon et al. (2019),Shin et al. (2011)

Aly et al. (2020), Hodgkins et al. (2019)

Shin et al. (2011), Simon et al. (2019), Tysklind et al. (1993)

- Research conditions and rates of PFAS sorption, adsorption, and leaching in saturated systems.
- Model groundwater systems with forwarding and backwarding tracking capabilities, malleable to integrate new findings.
- Modify existing runoff models to include PFAS transport. Additionally, organize monitoring regimes to correlate PFAS concentrations with landuse over time.
- Monitor PFAS sediment transport in different flows for parameter estimation in existing sediment transport models and calibration and validation.
- Lindim et al. (2016), Research the impact of hydraulic structures on sediment transport and deposition.
 - Organized long-term PFAS studies from both streamflow and sedimentation.
 - Monitoring studies on PFAS emissions and deposition are needed.

Table 2 (cont'd)

- Plant uptake The mechanisms of PFAS uptake into plants are not yet well understood.
- Mei et al. (2021), Wang et al. (2020a)
- More research focusing on the mechanisms and conditions driving plant uptake are required for accurate modeling.

- Most plant uptake research to date has focused on the difference between PFAS molecules accumulation areas within various plant species rather than uptake rates.
- Lan et al. (2018), Navarro et al. (2017).Wang et al. (2020a)
- Plant uptake integration and rate of removal should be considered in vadose zone models.

- Plant uptake research has relied on speciesspecific models, which can only be applied to one PFAS compound.
- Wang et al. (2020a), Wen et al. (2013)
- Models which can be applied to a subset of plants rather than individual species should be developed for prediction modeling.

Aquatic ecosystems

- Sampling studies are often performed on a short-term scale with individual PFAS, which can hide the uptake variability of long-term exposure to a mixture of emerging contaminants as experienced in the environment.
- Ahrens & Bundschuh (2014), Glaser et al. (2021), Houde et al. (2008), Li et al. (2020)
- Long-term uptake studies accounting for multiple emerging contaminants are necessary for determining variations in uptake rate and improving uptake modeling.

- Methodology for determining biomagnification factors is based on trophic relationships where many of the predators are assumed to prey on only one species, which is rarely the case.
- Haukås et al. (2007), The fraction of PFAS Mazzoni et al. (2020)
 - uptake from food versus the environment should be estimated for each level in the aquatic food chain in effort to better model PFAS uptake rates within these systems.

Table 2 (cont'd)

- Risk assessments for PFAS in aquatic ecosystems are often based on toxic rather than chronic impacts.
- Ahrens & Bundschuh (2014), Ankley et al. (2021), Glaser et al. (2021), Sardiña et al. (2019)
- Data and models should be built for long-term PFAS uptake rates and exposure effects, including toxic and chronic effects.

Although we are familiar with many PFAS sources in the environment, new sources are being discovered with increased monitoring and technology. As a result, not all types of PFAS have been incorporated into models. In the subsurface environment, PFAS characteristics are influenced by specific constituents within the heterogeneous system. In addition, the lack of organized monitoring data makes modeling PFAS fate and transport a daunting task. Similarly, within the surface environment, PFAS are known to be attached to sediment and be influenced by temperature within the water, yet many monitoring studies have not observed sediment concentration or seasonal variability impacts on PFAS. Table 2 explains the importance of carefully organizing PFAS monitoring studies to capture PFAS concentrations in different media, seasonal variation, and the influence of chemical interactions for effective PFAS modeling. Additionally, PFAS uptake mechanics are still not well understood, and further research is necessary to comprehend characteristics driving and inhibiting PFAS movement into plants. Aquatic organisms are similar as many studies have been focused on differences in concentration between organism and water or food rather than the mechanics of PFAS uptake and bioaccumulation within the organisms (Table 2). In summary, accurate modeling of PFAS fate and transport requires a better understanding of PFAS uptake in the environment. This can only be accomplished through long-term monitoring of different and integrated media.

5 Opportunities and Challenges of Integrated Large Scale PFAS Modeling Part 2: A Case Study for PFAS Modeling at a Watershed Scale

5.1 Introduction

The staggering quantity of chemicals and nutrients found in the aqueous environment has been of increasing concern (Moody et al., 2003; Templeton et al., 2009). Pollution has a widespread adverse effect on human health (Kolpin et al., 2002; Simon et al., 2019), aquatic organism fitness (Cui et al., 2017; Liu and Gin, 2018), and ecosystem makeup (Rodriguez-Moza and Weinberg, 2010; Zhu and Kannan, 2019). There are many persistent organic pollutants of concern; however, one of the largest groups of emerging contaminants is poly- and perfluoroalkyl substances (PFAS), which have been produced in the U.S. since the 1940s (US EPA, 2018). All PFAS are artificial and are characterized by a chain of fluorinated carbons (perFAS) or partially fluorinated carbons (polyFAS) connected to a functional group, giving them persistent, hydrophobic, and hydrophilic properties. Currently, the most commonly detected substances in the PFAS family are perfluorooctanoic acid (PFOA) and perfluorooctane sulfonate (PFOS) (US EPA, 2018), but over 9000 different chemicals have been identified and categorized as PFAS to date (US EPA, 2021).

In order to better understand the PFAS fate and transport, monitoring and modeling should be conducted at different scales. Hundreds of lab and field experiments have been performed in the past 20 years to examine the PFAS fate such as conversion (Mei et al., 2021), degradation (Washington et al., 2019), uptake (Krippner et al., 2015), and bioaccumulation (Ahrens & Bundschuh, 2014; Wang et al., 2020a). Other studies have focused on the PFAS transport mechanisms in the air (Shin et al., 2011), water (Mahinroosta et al., 2021), and soil (Costello &

Lee, 2020) environments. These include advection (Mahinroosta et al., 2021), dispersion (Armitage, 2009), volatilization (Sima & Jaffé, 2021), sorption (Brusseau et al., 2020; Schaefer et al., 2019), and leaching (Borthakur et al., 2021; Høisæter et al., 2019). These experimental observations have improved our understanding of PFAS in the environment, but they only represent special case scenarios on a small scale. To gain a full picture, computational models with sufficient realism are needed to simulate contaminant transport – identifying high-risk areas and helping improve monitoring strategies (Anderson et al., 2020; Ekdal et al., 2011; Love & Nejadhashemi, 2011).

After an exhaustive literature search (Raschke et al., 2022), only a few studies were found which tried to study PFAS transport through more than one environment (BARR, 2017; Shin et al., 2011; Winchell & Propato, 2019). In these studies, the transport of PFAS through multiple abiotic components were modeled. However, the linked modeling platform of air, water, and soil suffered from oversimplification, limitation in scale, and the lack of interactions among abiotic components. Meanwhile, due to the non-destructive nature of PFAS and their reversible sorption and interactions, PFAS contamination plumes exhibit unique characteristics and behaviors within different mediums. This means that the existing models require further developments to accurately evaluate PFAS fate and transport. Therefore, the next logical step is to identify knowledge gaps for developing the widely used surface water, groundwater, and water quality models. These models also need to be integrated to ensure consistency in evaluating the performances of mitigation strategies. The reason behind selecting the widely used models is that there is a higher probability of adaption and use for policymaking. In fact, many water managers are familiar with these models and probably have at least one set up for their region of interest. The goal of this paper was to develop a real-world scenario to identify the difficulties of model integration, the

shortcoming of existing models in handling PFAS fate and transport, and the next steps in the development of sub algorithms for these models to address the existing issues. In order to achieve this goal, two objectives were performed, 1) surface water, groundwater, and water quality models were parameterized and integrated and 2) evaluate the model for PFAS transport and suggest areas for technical improvement. The model integration was performed for the Huron River watershed in Michigan, US. This watershed was selected as high concentrations of PFAS were observed in surface water, groundwater, and aquatic organisms (EGLE, 2019a). In addition, due to the risk associated with elevated PFAS levels, it was selected as one of the first watersheds by the state water authorities for large-scale PFAS monitoring.

5.2 Methodology

5.2.1 Study area

The Huron River watershed encompasses over 2300 square kilometers within the Southeastern corner of Michigan, US (Wittersheim, 1993). The hydrodynamics of the Huron River is characterized by a strongly connected surface water and groundwater system. Along the main stretch of the river are 16 major reservoirs (Figure 2), while over one hundred dams and impoundments regulate the surface water flow of the entire Huron River network, providing drinking water, irrigation, and hydropower for urban areas, agriculture and industries (HRWC, 2021a).

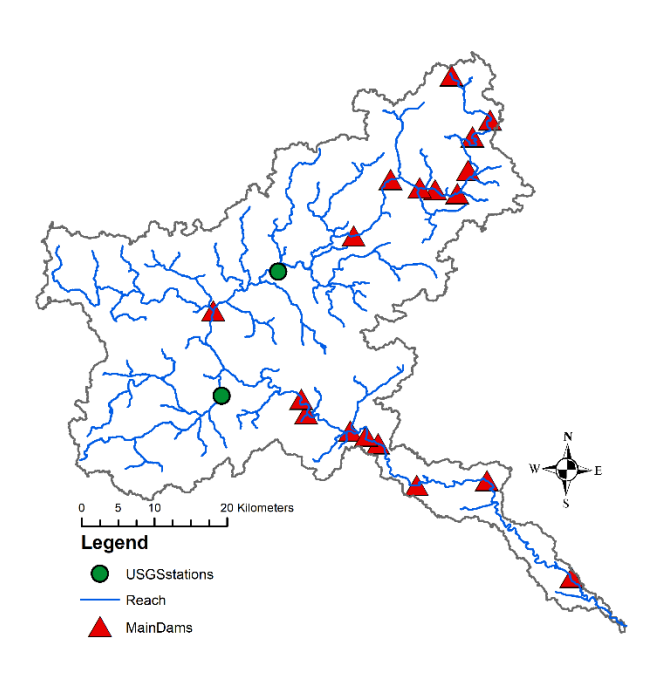


Figure 2. Huron River watershed with USGS gaging stations and main dams.

The manufacturing plants discharge pollutants both directly into the Huron River and into its connected groundwater aquifers (HRWC, 2021b). Nutrient-rich, contaminated biosolids from wastewater treatment plants within the watershed have also been spread on agricultural fields as fertilizer, acting as a nonpoint source of pollution for the watershed (EGLE, 2020). The Huron River watershed was one of Michigan's first watersheds chosen for PFAS investigation as a result of high concentrations of PFAS being detected in the city of Ann Arbor's drinking water (EGLE, 2019a).

5.2.2 Introduction to integrated PFAS model

In the following sections, we describe the three major components of model development, including 1) synthesizing PFAS source data; 2) capturing relevant transport avenues in model development and parameterization; and 3) model calibration and validation using observation data, which are described in detail in the following sections. Together, this conceptual model provides

the basis for identifying simulation and monitoring data shortcomings for estimating large-scale PFAS fate and transport.

5.2.3 PFAS sources within the Huron River watershed

The Huron River watershed is home to seven WWTPs, industrial sites, an airport, landfills, and many unknown PFAS sources. Most of the sampling has been performed on PFOS and PFOA, which are simplified to PFAS for the remainder of the section unless otherwise stated. The cities of Ann Arbor, Brighton, Dexter, and Wixom all discharge their wastewater directly into the Huron River through its tributaries (EGLE, 2019b). All WWTPs have been observed to have detectable levels of PFAS, which have been under investigation since 2018. In Wixom, it was found that a chrome plating plant and another industrial plant outside of the watershed were discharging their effluent to the Wixom WWTP. In addition to the direct discharge from Wixom WWTP, contaminated biosolids were being applied annually on the surrounding farms, but farm application of biosolids ended in 2018 (EGLE, 2020). It can be assumed that the biosolids from Ann Arbor, Brighton, and Dexter WWTPs have been applied on agricultural fields as a soil amendment as well. Meanwhile, recent testing has indicated low levels of PFOS and PFOA within Ann Arbor and Dexter biosolids (MPART, 2021). Besides WWTP sourced contamination, the former Daimler Chrysler Scio Facility was found to have contaminated groundwater and stormwater, though the stormwater was within the drinking water standards (MPART, 2021). The Willow Run Airport and surrounding area were also found to have elevated PFAS concentrations within the groundwater and stormwater, which discharges partially into a tributary of the Huron River and the Rouge River watershed (MPART, 2021). Elevated PFAS levels have also been observed at other industrial sites, in the groundwater, stormwater, discharge, and retention ponds.

The source data available was not sufficient for generating the model initial conditions. To get over this obstacle, an example estimate was calculated based on the methods developed by (Lindim et al., 2015) for the Danube River. (Lindim et al., 2015) suggest that PFAS pollution is related to the population living within each area of the watershed, the economy, and the level of wastewater treatment available for both water (Equation (36) and soil (Equation (37):

$$E_{water_SC} = \frac{GDP_{Sb}}{\overline{GDP}_{HR}} P_{Sb} \times E_i + E_{ATM} \times A_{water_Sb}$$
(36)

$$E_{soil_SC} = \frac{GDP_{Sb}}{\overline{GDP}_{HR}} (Sl \times P_{Sb} \times E_i + \frac{DS}{1 - DS} P_{SC} \times E_3) + E_{ATM} \times A_{soil_Sb}$$
(37)

where, GDP_{Sb} is the average gross domestic product of the subbasin (USD); \overline{GDP}_{HR} is the average gross domestic product of the Huron River watershed (USD); P_{Sb} is the population of the subbasin; E_i is the discharge per capita to the water for the i-th level of wastewater treatment (g/capita/d); E_{ATM} is the atmospheric deposition rate (g/m²/day); A_{water_Sb} is the subbasin surface water area (m²); Sl is the fraction of WWTP total PFAS inflow retained in sludge; DS fraction of the discharge that goes onto land; and A_{soil_Sb} is the subbasin soil area (m²). Although these equations estimate discharges into both water and soil, there are a few assumptions that differ from practices within the Huron River watershed. First, Equation (36(37 do not account for PFAS using industry, but rather have them solely based off of population use. Within the Huron River watershed however, it is apparent that these industries play a big role in contaminating the river (EGLE, 2019b). Additionally, the biosolids produced by the wastewater treatment plants are assumed to be spread within the same subbasin that the wastewater treatment plant is located in. This is often not the case since most of the wastewater treatment plants are located on the outskirts of urban areas and

provide biosolids for the neighboring agricultural lands. Even given these assumptions, this approach provides sufficient initial data for model initiation.

5.2.4 Modeling the Huron River watershed

In an effort to account for all the different transport avenues, a surface water, a groundwater model, and a streamflow water quality model were coupled together. The conceptual hydrodynamic model was produced through interconnecting the soil and water assessment tool (SWAT) (Arnold et al., 2012), modular finite difference model (MODFLOW) (Harbaugh, 2005), and the water quality simulation program (WASP) (EPA, 2019). The Soil and Water Assessment Tool (SWAT) model was developed by the United States Department of Agriculture Agricultural Research Service (USDA ARS) and has been used to simulate water quality and quantity for catchment systems around the world (Arnold et al., 1998; Einheuser et al., 2013; Gassman et al., 2014; Zhang et al., 2008). MODFLOW was developed by the United States Geological Survey (USGS) and is considered an international standard for simulating groundwater aquifers (USGS, 2021d). The WASP model was developed by the US EPA and has been widely used in the US and internationally for modeling pollutant transport (EPA, 2019).

As discussed in section Part I of this study (Raschke et al., 2022), pesticide models can be applied to simulate PFAS fate and transport. SWAT has been frequently applied to investigate the fate and transport of pesticides in surface hydrology. The model can simulate 32 pesticide fate and transport processes in soil, river, and plants. According to the review by Payraudeau and Gregoire (2012), SWAT is the most comprehensive catchment simulation model for pesticide transport available in comparison to MIKE SHE ADM, LEACHM-runoff, GR5-pesticides, SACADEAU, STREAM-pesticide, FLOWT, VESPP, I-Phy-Bvci, and PHYLOU. Additionally, SWAT has been coupled with MODFLOW-RT3D to provide a comprehensive hydrogeochemical process for

simulating particle fate and transport in groundwater and surface water. The SWAT model's pesticide fate and transport processes are similar to those required to simulate PFAS fate and transport; however, due to the unique characteristics of PFAS, simulating their fate and transport in SWAT requires additional model development. WASP was used to simulate the fate and transport of PFAS via streamflow. The WASP model was selected due to its ability to simulate multiple transport processes and its wide range of applications to date for successfully modeling water quality in streams. Additionally, it has the ability to simulate numerous constituents at the same time, for which specific reaction and transport mechanisms can be individually assigned (Camacho et al., 2018; Chueh et al., 2021; Han et al., 2019; Knightes et al., 2019; Lin et al., 2011; Shabani et al., 2021; Wool et al., 2020).

5.2.5 Surface water model

The SWAT model is a globally recognized soil and water transport model, which has been used to model watersheds in a variety of different regions around the globe (Arnold et al., 1998; Einheuser et al., 2013; Gassman et al., 2014; Zhang et al., 2008). SWAT is a computational model which uses user inputted geologic, climate, and land use data to estimate water and soil movement through a watershed via fundamental transport theories (Arnold et al., 2012). SWAT first delineates the watershed into many different subbasins with each river segment or reservoir having a unique subbasin. The subbasins are then further divided into individual hydrological response units (HRUs) identified by their unique combination of land use, soil, and slope class.

For the Huron River watershed, a 10-meter resolution Digital Elevation Model (DEM) from the United States Geological Service National Hydrography Database (USGS NHD) determined the topography of the study area (USGS 2021a). The river reach file was burned into the DEM for higher accuracy (EPA 2007) and 16 of the reservoirs on the main stem of the Huron

River were modelled according to average volume and height (Hay-Chmielewski et al., 1995). These data were used to delineate 189 subbasins within the watershed. The 2019 Cropland Data Layer provided land use data at a 30-meter resolution for overland flow simulation (USDA, 2020), the STATSGO2 soil database provided soil data at a scale of 1:250,000 for subsurface flow estimation (NRCS, 2021), and 3 slope classes were identified based on the Jenks Natural Breaks classification method (Smith et al., 2020). Using these data, the subbasins were further delineated into 9452 HRUs. Finally, maximum and minimum temperature and precipitation data from 1999-2020 from 3 national weather stations were used to establish the water coming into the system on a daily time step (NCDC, 2020). Daily river flow was simulated between 2002-2020, even though the model was run for the entire 1999-2020 time period, since the first 3 years were disregarded as the simulation warmup.

5.2.6 Groundwater model

We established the groundwater model for the Huron River catchment using the MODFLOW-NWT v.1.2.0 (Niswonger et al., 2011). First, the model domain was discretized into 23,688 grid cells (141 rows and 168 columns) with a 500×500 m grid cell size. A 10 m Digital Elevation Model (DEM) was used to represent the surface elevation. Next, we interpolated the bottom depth of 78,000 water bores across the catchment to estimate groundwater bedrock elevation. The total estimated depth was equally discretized into three convertible hydrostratigraphic layers. The first layer of groundwater is divided into two zones to account for different hydraulic properties: 1) the groundwater aquifer zone with low transmissivity and 2) the groundwater zone with relatively higher transmissivity (Figure 3). No zonation was considered for the second and third layers. Unique hydraulic parameters, including vertical hydraulic conductivity, horizontal conductivity, specific yield, specific storage, and horizontal anisotropy

ratio, were considered for the first layer's two zones and the second and third layers. Lakes and water bodies with considerable size within the catchment were also included in the MODFLOW model and modeled with Drainage Package.

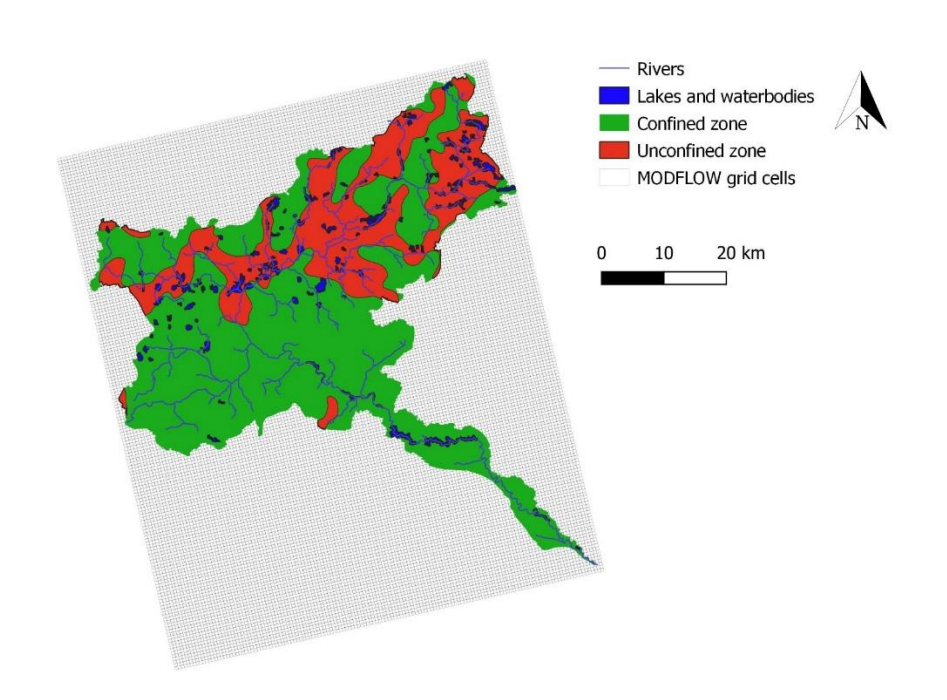


Figure 3. The groundwater model domain of the Huron River Watershed.

5.2.7 Linking surface water and groundwater

SWAT and MODFLOW have different spatial scales. Therefore, an internal mapping is required to accurately pass SWAT variables to MODFLOW grid cells and vice versa. This internal mapping and further coding for exchanging SWAT and MODFLOW output have been developed with excellent accuracy by Bailey et al. (2016). The procedure for linking SWAT and MODFLOW includes intersecting SWAT hydrologic response units (HRUs) and river networks with MODFLOW grid cells to generate Disaggregated HRUs (DHRUs). Then, the integrated SWAT-MODFLOW uses the generated DHRUs to pass SWAT recharge and river stage to MODFLOW

grid cells and groundwater return flow from MODFLOW to SWAT river network. The entire procedure for generating DHRUs and linking SWAT and MODFLOW models is described by Bailey and Park (2019). However, to simulate chemical particle mass and exchange including dispersion, diffusion, and advection in the groundwater layers, Wei et al. (2019) coupled the SWAT-MODFLOW model with Reactive Transport in 3 Dimensions (RT3D) model. They also developed SWAT-MODFLOW-RT3D to simulate the exchange of nitrate and phosphorous between groundwater and surface water.

5.2.8 Stream water quality model

After calibrating and validating the SWAT-MODFLOW-RT3D model for regional hydrology in the Huron River catchment, the features of the surface water network were imported into the WASP model. These features include streamflow, length, width, slope, elevation, and Manning's roughness coefficient for every river segment in each subbasin. In addition, storage characteristics such as volume and surface area at normal and emergency levels, as well as shape coefficients, were also used to represent all reservoirs in WASP. The flowchart in Figure 4 summarizes the decision-making algorithm followed for building the entire stream network in this model.

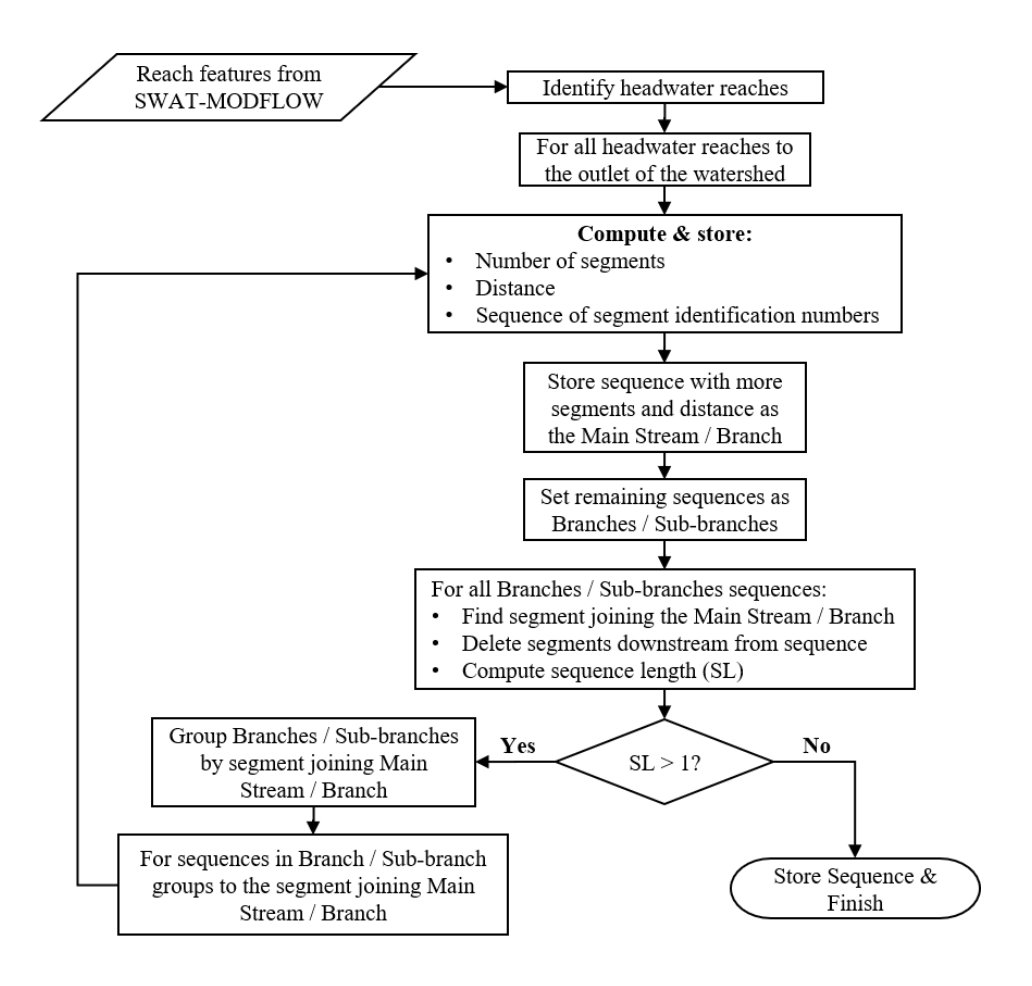


Figure 4. Flowchart describing WASP river network building.

Based on the results of this algorithm, dispersion coefficients were computed for all river segments using Fischer's equation (Equation 38) for average streamflow (Fischer et al., 1979):

$$E_{x} = \frac{0.011 * U^{2} * B^{2}}{D * u^{*}} \tag{38}$$

where, E_x is longitudinal dispersion coefficient (m²/s), U is average streamflow speed (m/s), B is channel width (m), D is hydraulic radius (m²), and u is longitudinal speed (m/s) (Ramos-Ramírez et al., 2020). Segment lengths and simulation time steps were then approximated for each subbasin based on these coefficients and computational stability and accuracy criteria (Noorishad et al., 1992). Using these lengths and timesteps, the one-dimensional stream network was then

configured in WASP employing kinematic wave and ponded weir equations to simulate river segments and reservoirs (Ambrose and Wool, 2017). An additional water balance element was connected to each segment, allowing rivers to receive surface runoff and sediments, and to exchange flow and chemicals with aquifers. Next, river inflows for each sub-catchment were obtained from SWAT-MODFLOW-RT3D and incorporated into WASP. The complete river network and the location of reservoirs, WWTP point sources, and PFAS observation points can be seen in Figure 5. Subbasins where hydrographs of the two models were compared are also highlighted in Figure 5.

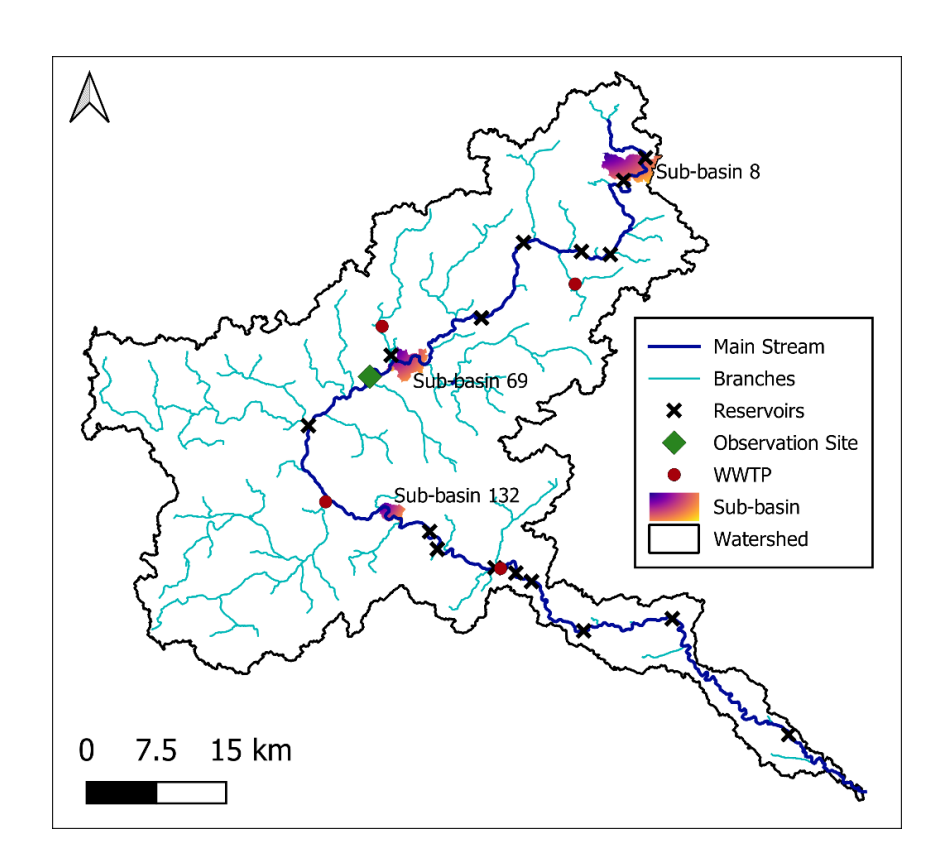


Figure 5. Stream network for WASP simulation, wastewater treatment plants, and PFAS observation sites.

Once water transport was configured, fate and transport of PFOA and PFOS was simulated. In absence of measured sediment concentrations in the catchment, loads from SWAT-MODFLOW-RT3D were imported through the water balance elements. This allowed a first

estimate of the portions of PFOA and PFOS moving in water both as a solute and adsorbed to solid particles. It was assumed that adsorption is only driven by partition coefficients in steady equilibrium conditions. Accordingly, the simulation included advection, dispersion, adsorption, and settling as main transport mechanisms (Ahrens and Bundschuh, 2014; Kwok et al., 2013; Winchell et al., 2022), while decay, volatilization, atmospheric deposition and diffusive exchange with sediments were not considered. This because of the persistence and low volatilization rates of the species of interest (Lampic and Parnis, 2020), and the absence of regional concentrations in air and sediments. According to these assumptions, Equation 39 shows the general transport equation considered for the simulation:

$$\frac{\partial C}{\partial t} = -u_x \frac{\partial C}{\partial x} + D \frac{\partial^2 C}{\partial x^2} - \frac{v_s}{H} F_p C + S \tag{39}$$

Where C is the concentration of PFOA or PFOS at a given stream segment, u_x is the velocity of water in the x-direction (L/T), D is the dispersion coefficient (L²/T), v_s is the sediment settling velocity (L/T), H is the water depth (L), F_p is the particulate fraction, and S are the external contaminant sources (M/L³/T).

5.2.9 PFAS monitoring within the Huron River watershed

Although PFAS have been observed in air, soil, and water, within the Huron River catchment, surface water has been the main area of monitoring (EGLE, 2019a). To date, PFAS emissions in air have not been sampled, nor monitored for deposition (MPART, 2021b). Surface water has been sampled the most, since it was the goal of EGLE to use surface water monitoring data to identify sources (Figure A1) (EGLE, 2019b). Groundwater has been sampled, but only in select areas (Figure A1) over a short period of time (Table A1). These select areas can give insight into the movement of the contaminant plume within the monitoring areas, but do not show the

distribution of PFAS contamination within the groundwater within the watershed leaving the non-point source distribution largely unknown. Unless on a contaminated site from industrial PFAS use or biosolid application from the Wixom WWTP, soil has also not been widely sampled within the Huron River catchment (Figure A2) (EGLE, 2020). Stormwater is similar with only select industrial sites being sampled (Figure A3). Drinking water intake from the Huron River at Barton dam and outflow from the Ann Arbor Drinking water plant have been sampled for PFAS on a biweekly basis (City of Ann Arbor, 2021). Finally, suspended sediment has not been tested within stormwater nor surface water for PFAS within the Huron River catchment.

In summary, 30 surface water locations, 20 fish tissue locations, 17 groundwater locations, 14 stormwater locations, and 6 soil locations have been sampled (EGLE, 2019b). All materials were sampled for PFAS by Test America or Eurofins laboratory, which follows the US EPA method 537 for quantifying 24 different PFAS (Eurofins, 2021). Groundwater has been sampled in 4 locations, although only one location was temporally sufficient (Table S1). Groundwater monitoring has been performed in areas with known PFAS contamination and suspected sources (MPART, 2020). Even though multiple sites have had detectable PFAS concentrations, they do not capture seasonal variation without regular monitoring within wet and dry periods. Soil sampling for PFOA, PFOS, and other PFAS occurred on six agricultural sites in the northeast corner of the Huron River catchment (Bogdan, 2021). In addition to the soil, biosolids were tested for both PFOA and PFOS. Although biosolids were reported to be used as a soil amendment on four of the field sites from 2010 to 2015 and the other two from 1995 to 2001, all soil locations were only tested once in 2018 (Bogdan, 2021). Unfortunately, monitoring data from one point in time only shows a snapshot in time rather than retention and mobility of PFAS within the environment.

As forementioned, surface water and stormwater have been sampled the most, but of the 26 monitoring locations, only 18 have been sampled more than once and 7 have been sampled more than 4 times (Table S2). For water quality modeling, it is suggested to have at least 12 sampling times for each location spanning over a wet period and dry period in areas with seasons, such as Michigan (Runkel et al., 2004). In addition to temporal data, it is important to sample a variety of spatial locations, including headwater, outlet, riffles, pools, and reservoirs, to ensure all steam habitats are considered (Olden et al., 2012). Therefore, even though there are two locations with enough temporal data, they are both point sources and do not eliminate the concentration differential within the river network. In terms of stormwater data, out of the 14 locations, two have been sampled more than once, but the two sampling locations with temporal data did not capture a wet and dry period.

Bluegill, rainbow trout and other game fish have been tested for PFAS along the Huron River, especially within highly contaminated areas, and have been found to have elevated PFAS levels. Deer have also been tested for PFAS in high-risk areas, such as around the Willow Run airport, but have been observed to have low concentrations to no detect. PFAS awareness and regulations have motivated increased sampling and monitoring of water, aquatic organisms, and animals within the Huron River watershed. Fish tissue is similar to surface water with a large spatial distribution of samples without any replication, therefore the temporal requirements of using this monitoring data for modeling have not been met. To ensure monitoring data can be used for modeling and predictability purposes, a plan should be organized to capture all environmental media, special variation, and temporal variability (i.e., seasonality and wet and dry periods).

5.2.10 The integrated model calibration

The general criteria for the model calibration/validation on a monthly basis include the Nash–Sutcliffe model efficiency coefficient (NSE) above 0.5, percent bias (PBIAS) below ±25%, and the ratio of the root mean square error to the standard deviation of measured data (RSR) less than or equal to 0.7 (Moriasi et al., 2007). The SWAT-MODFLOW model was calibrated for daily streamflow and baseflow for a five-year period (2015-2020) at two stations. The USGS 04173500 station located in Mill Creek represented flow through agricultural portions of the watershed (USGS, 2021b), while USGS 04172000 station located on the main Huron River segment in Hamburg, Michigan was used to calibrate the rest of the watershed (USGS, 2021c). A combined version of mean squared error (MSE) and NSE were used as performance criteria. These error functions were also used in the objective function of our calibration algorithm. We carried out the automatic parameter calibration using the Multi-Memory Particle Swarm Optimization (Rafiei et al., 2022).

Unfortunately, no streamflow data was available closer to the river outlet for the timeperiod due to the number of reservoirs on the middle and lower portion of the Huron River. The
results from flood modeling performed by Zajac et al. (2017) suggests that there is an increase in
uncertainty of flow magnitude with closer proximity to reservoirs in hydrodynamic models.
Therefore, the USGS station 04174500, which was the furthest downstream, was disregarded.
Though flow was calibrated and validated against observed values, insufficient water quality data
prevented calibration and validation of sediment and nutrient loads. It was assumed that the
sediment load transport estimated by the modified universal soil loss equation (MUSLE) generated
a realistic estimate through the use of current land use and soil data (Neitsch et al., 2011). It should

be noted that there was no daily groundwater head elevation recording for the catchment so that we could include it in the model calibration.

We used different parameters to calibrate the integrated model. For the groundwater model, we included Horizontal Hydraulic Conductivity (HK), Vertical Hydraulic Conductivity (VK), Horizontal Anisotropy ratio (HAN), Specific Storage (SS), Specific Yield (SY), River Conductance (RC), and Riverbed (RB). We also included the following SWAT parameters for surface water: surface lag time (SURLAG), snow melting coefficient (TIMP), CN Coefficient (CNOEF), Manning's Roughness in main and tributary channels (n). Regarding the 16 major reservoirs in the catchment, we included the following parameters for SWAT reservoir storage and discharge: reservoir weir discharge coefficient (weirk), maximum reservoir volume at the emergency pool (ResMaxVolume), the reservoir volume at the normal pool (RES_PVOL), reservoir groundwater conductance (RES_CON), and reservoir bottom percolation (RES_BOTE). For WASP, physicochemical properties, such as molecular weight, solubility, and partition coefficients to sediments, were obtained from related literature to parameterize transport equations for both PFOS and PFOA (Lampic and Parnis, 2020; Sima and Jaffé, 2021; Zhan et al., 2010; Zhou et al., 2021). Note that partition coefficients were specifically computed from the Freundlich adsorption isotherms developed with experimental data for both species (Zhou et al., 2021).

Figure A4 shows the result of 3000 model evaluations (the vertical axis shows the objective function value and the horizontal axis is the range of parameters). The NSE criteria for monthly and daily baseflow for both stations are above 0.68 (Figure 6 and A5). For streamflow, NSE criteria for monthly is above 0.84 for both stations (Figure A6). For daily streamflow, the NSE is above 0.69 (Figure 7). In a similar study with the SWAT model in the Huron River catchment, Xu et al. (2019) achieved an NSE of less than 0.60 for these stations for daily performance and less than

0.72 monthly performance. In addition, PBIAS and RSR values also met the Moriasi et al. (2007) model performance criteria. Therefore, based on the performance criteria and comparison with the previous study, we consider the model calibrated for reproducing streamflow and baseflow. The simulated annual groundwater water table was in reasonable agreement with the sparse head record that we had (Figure A7). However, further monitoring at daily steps are necessary to improve the groundwater head calibration.

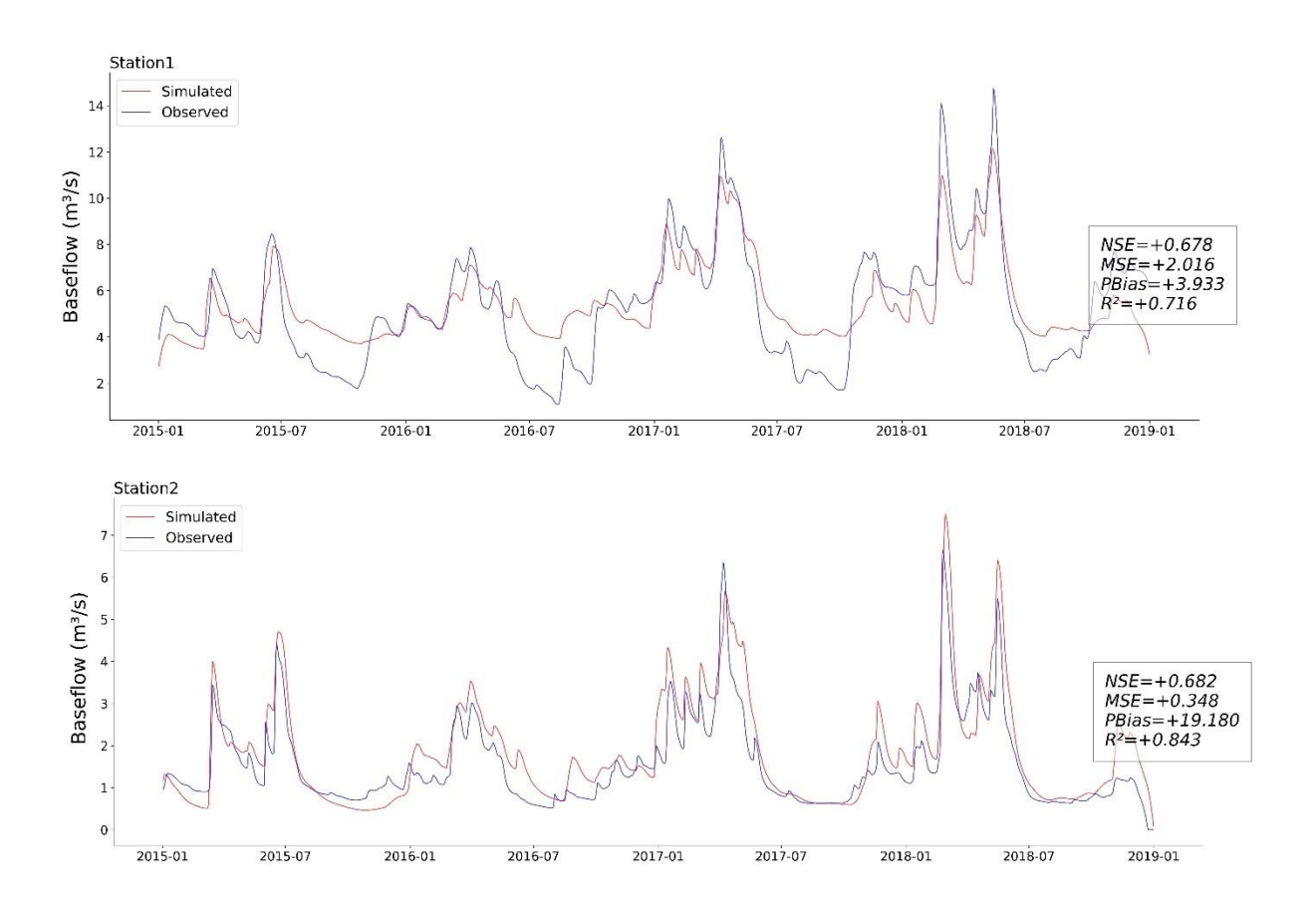


Figure 6. Daily baseflow rate simulated vs. observed.

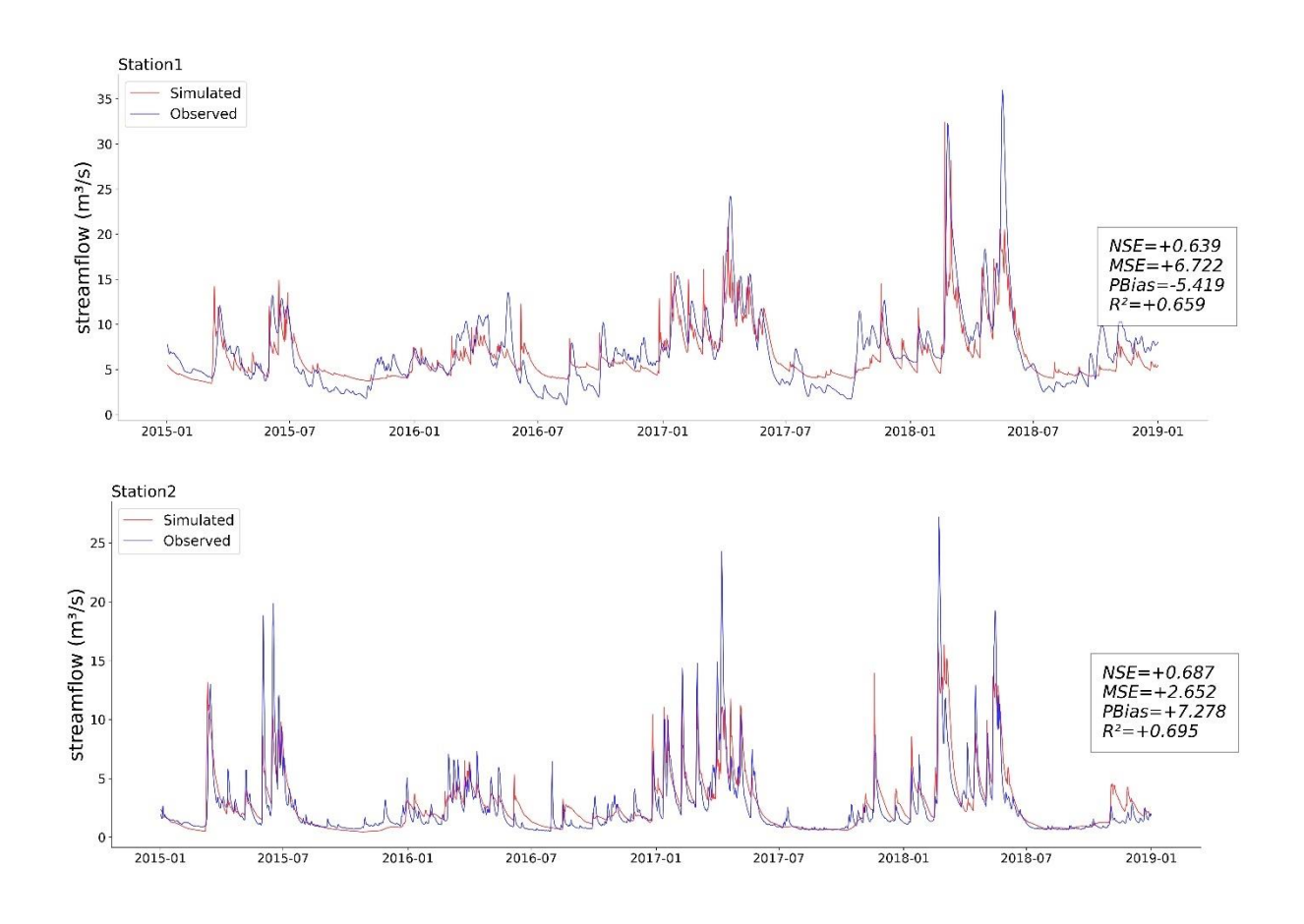


Figure 7. Daily streamflow calibrated vs. observed.

Noting these limitations and strengths of the calibration, it was possible to reproduce the hydrographs from SWAT-MODFLOW-RT3D in WASP as shown in Figure 8. It is worth mentioning that the magnitude of water exchanged from the main river to the aquifer was reduced in some segments to avoid the stream to dry out and stop the simulation. This was done manually to retain the relationship between the riverbed and underlying aquifer as closely as possible. Despite this additional process, results show that the streamflow computed in WASP followed the magnitudes from SWAT-MODFLOW-RT3D well. Specifically, an NSE of 0.85 or above was obtained in the three subbasins highlighted in Figure 4, representing the headwater, middle, and lower Huron River. In addition, an acceptable average NSE of 0.79 was obtained for all subbasins

in the main river, although performance decreases towards the outlet due to propagation of error and to the high number of reservoirs in this area.

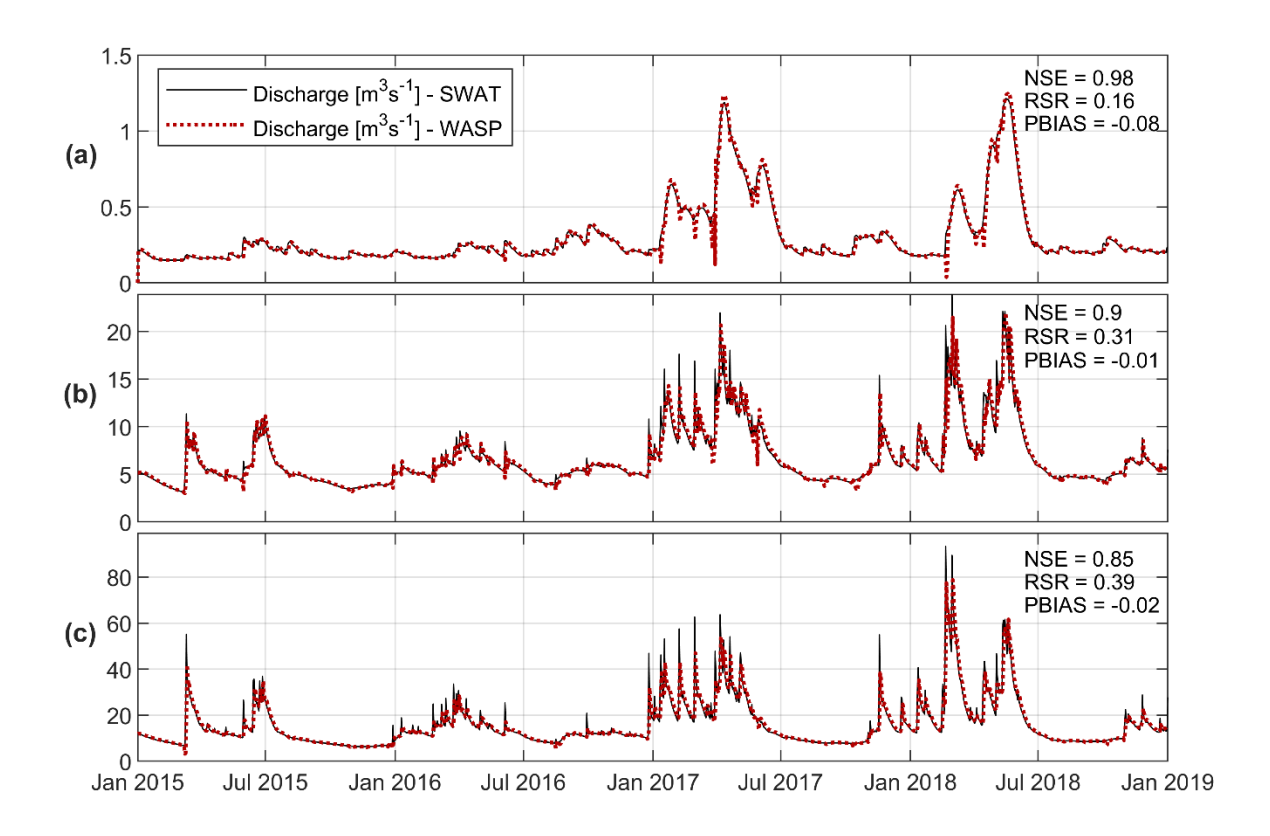


Figure 8. Comparison of hydrographs in SWAT and WASP: a) Headwaters (subbasin 8); b) Middle river (subbasin 69); c) Lower river (subbasin 132).

Finally, PFOS and PFOA were incorporated into the model along with the previously imported sediment loads, noting that these PFAS species adsorb to solids and are the two most tested in the Huron River. For sediment transport, particle diameter and settling velocity were the two parameters included. In absence of detailed sediment information in the region, the first was set to 0.025 mm and the second to 28 m/day. Regarding PFAS transport, molecular weights and partition coefficients to sediments were the two parameters considered. Values of these parameters were 500.13 g/mol and 900 L/Kg for PFOS, and 414.07 g/mol and 200 L/Kg for PFOA (Lampic and Parnis, 2020; Zhou et al., 2021). Although further research and calibration of some of these

values is required to validate their actual regional magnitude, they allowed a first approach to simulate fate and transport of these two species in the Huron River Watershed.

5.3 Evaluation of the integrated model for PFAS fate and transport

As described earlier, the integrated model was calibrated and validated for groundwater and streamflow. However, the lack of PFAS monitoring data at a reasonable spatiotemporal resolution makes assessing model performance on PFAS concentrations impractical. Thus, we examined this performance at five monitoring sites qualitatively on the Huron River. These sites are shown in Figure 5, and more details on their available information are found in Table A2. Results for observed and modelled total concentration of PFOS and PFOA at all sites are presented in Figure A9, and more details on their concentration in water and sediments at the Strawberry Lake monitoring site are displayed in Figure 9. Being the only data available regionally, we considered the loads of PFOA and PFOS released by the four WWTPs shown in Figure 5 as the only sources of these contaminants during simulation.

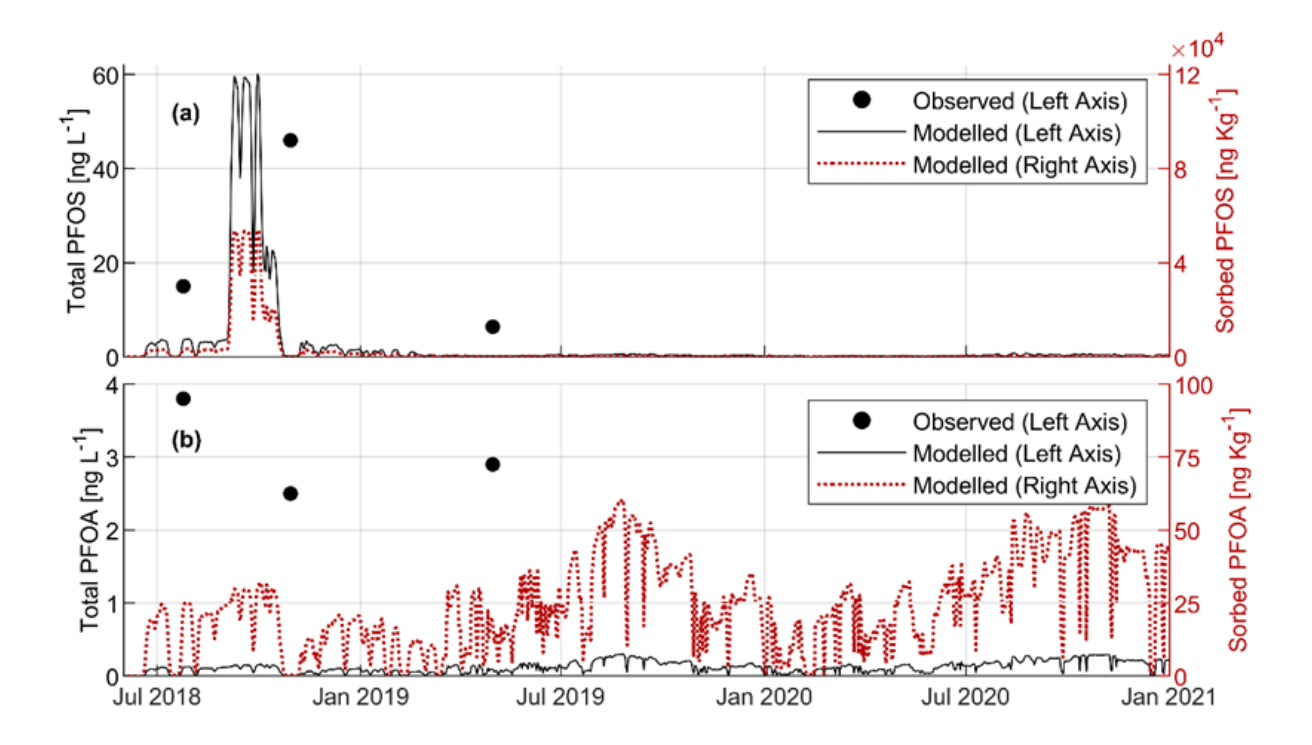


Figure 9. Comparison between the results from the integrated model and observed values at the Strawberry Lake monitoring site: a) PFOS; b) PFOA.

Results show that the integrated model was able to capture overall concentration trends from Strawberry Lake. Additional comparisons can be viewed in Figure A9, from Wixom to the Regan Drain Downstream when observations were available. Total concentrations of PFOS and PFOA were generally underestimated at these four sites, especially for PFOA, and completely disregarded in the first site at Wixom Rd. This suggests the model is conceptually consistent to describe the spatiotemporal variations of these concentrations to some extent, but still unable to reach observed magnitudes. Although there is a lack of calibrated rates, constants, and sediments, results suggest it is not possible to reach observed concentrations only accounting for the loads released by WWTPs. This is especially evident in the first site, where the lack of these plants results in a modelled concentration of zero, but observations suggest otherwise. Thus, additional PFAS sources must be considered to achieve a closer representation of reality. These sources include additional point discharges, diffuse sources, and potential exchanges with air, soil, and

sediments, and their legacy. This is apparent given the possible deposition of volatile species that could turn into PFOS and PFOA, the long half-life of these compounds, and the presence of multiple dams. These dams could release PFAS under circumstances promoting resuspension and diffusion, as they tend to accumulate sediments and the simulation suggests significant concentrations of PFAS species adsorbed to suspended solids.

5.4 Technical gaps in simulating PFAS

There are several critical processes for simulating PFAS that SWAT-MODFLOW-RT3D and WASP can carry out (Table 3). Several major knowledge and technical gaps for modeling PFAS fate and transport have been identified and discussed based on findings presented in Table 3.

Table 3. List of processes available in SWAT, MODFLOW-RT3D, SWAT-MODFLOW-RT3D, and WASP for simulating PFAS. – means that the model cannot simulate the process. √ means that the model can potentially simulate the process but need further model development.

Processes	SWAT	MODFLOW-RT3D	SWAT-MODFLOW-	WASP
			RT3D	
Air				
Drift	_	_	_	_
Deposition	_	_	_	_
Plant				
Plant root uptake	$\sqrt{}$	_	\checkmark	-
Soil (saturated)				
Runoff	$\sqrt{}$	_	\checkmark	_
Lateral flow	$\sqrt{}$	_	\checkmark	_

Table 3 (cont'd).

Infiltration	\checkmark	_	\checkmark	_
Percolation	\checkmark	_	\checkmark	_
Volatilization	$\sqrt{}$	_	$\sqrt{}$	_
Degradation	$\sqrt{}$	_	$\sqrt{}$	_
Sorption	$\sqrt{}$	_	$\sqrt{}$	_
Erosion	$\sqrt{}$	_	$\sqrt{}$	_
Aquifer				
Advection	_	\checkmark	Θ	_
Adsorption	_	\checkmark	Θ	_
Degradation	_	\checkmark	θ	_
4 'C D'		-1	0	_
Aquifer-River	_	$\sqrt{}$	Θ	_
load exchange	_	V	Ð	
	_	V	0	
load exchange		_	√	√
load exchange River	_ √ √	- -	√	√ √
load exchange River Deposition		- - -	√ √ √	√ √ √
load exchange River Deposition Resuspension	$\sqrt{}$	- - -	√ √ √ √ √ √ √ √	√ √ √
load exchange River Deposition Resuspension Volatilization	√ √	- - - -	√ √ √	√ √ √ √
load exchange River Deposition Resuspension Volatilization Degradation	√ √ √	- - - - -	√ √ √	√ √ √ √ √
load exchange River Deposition Resuspension Volatilization Degradation Advection	√ √ √		√ √ √ √	√ √ √ √ √
load exchange River Deposition Resuspension Volatilization Degradation Advection Dispersion	√ √ √ −		√ √ √ √ ⊕	√ √ √ √ √ √

Table 3 (cont'd).

_	_	Θ	$\sqrt{}$
-	_	Θ	$\sqrt{}$
$\sqrt{}$	$\sqrt{}$	Θ	$\sqrt{}$
$\sqrt{}$	$\sqrt{}$	Θ	$\sqrt{}$
$\sqrt{}$	$\sqrt{}$	Θ	$\sqrt{}$
$\sqrt{}$	$\sqrt{}$	Θ	$\sqrt{}$
$\sqrt{}$	$\sqrt{}$	Θ	$\sqrt{}$
_	_	Θ	$\sqrt{}$
$\sqrt{}$	_	Θ	$\sqrt{}$
_	_	Θ	$\sqrt{}$
_	_	Θ	$\sqrt{}$
_	_	θ	$\sqrt{}$
_	_	Θ	$\sqrt{}$
	√ √ √ √ √ −		$\begin{array}{cccccccccccccccccccccccccccccccccccc$

1. SWAT can only simulate one type of pesticide/chemical at one time: This simplification results in the wrong estimation of PFAS transport via water and sediment due to multiple PFAS competing for sorption sites when coexisting together in the environment (Sima and Jaffé, 2020, Kah et al., 2021). Therefore, the model should be modified to consider several major PFAS compounds since simulating all PFAS is not practical. Further studies should be undertaken to better understand the interaction among PFAS compounds and the impact of coexistence on PFAS sorption.

2. Simulating PFAS sorption in soil environment using the SWAT model: Among the 455 PFAS discovered between 2009 and 2017, 45% were anions, 29% were zwitterions, 17% were cations,

and 8% were neutrals (Xiao et al., 2017). In geosorbents (soils/sediments/aquifer solids), the sorption isotherms of anionic PFAS and a few neutral PFAS have frequently been found to be linear or nearly linear. However, experimental evidence indicates that cationic and zwitterionic PFAS sorption in natural soils is highly nonlinear (Xiao et al., 2019). As a result, the Freundlich isotherm, Equation 40(, is commonly used to represent the nonlinear sorption coefficient:

$$K_F = \frac{S_e}{C_w^N} \tag{40}$$

where, K_F (mg/kg)/(mg/L) and N are the Freundlich constants, which vary significantly with the specific PFAS and the characteristics of the sorbent (Sima and Jaffé, 2020). Thus, the SWAT model should be amended to incorporate a similar nonlinear equation. However, the Freundlich equation is purely empirical and the K_F and N should be determined for each specific compound with respect to different geosorbents. Therefore, a more physically based approach to consider critical environmental factors such as the soil organic matter content, soil PH, and other physicochemical properties is required for accurate estimates of PFAS sorption in the soil.

3. PFAS translocation: Because pesticides are applied as a nonpoint source via spraying on crops, SWAT assumes that plants intercept sprayed pesticides via their foliage. The pesticide interception is a function of the Leaf Area Index at the growing stage. In comparison, the nonpoint source of PFAS to the soil is via biosolids or irrigation. Thus, additional modifications to the SWAT source code are required to remove the foliage interception and consider PFAS application via biosolids or irrigation rather than spraying. Additionally, the current version of SWAT does not simulate plant uptake of pesticides from the soil environment. As a result, additional developments in the SWAT source code are required to simulate PFAS uptake by plants based on their type and biomass.

- 4. PFAS leaching to aquifer: in SWAT, the percolated pesticide from the previous year's spraying is lost from the system. This means that SWAT does not have an internal mechanism to track the percolated PFAS to groundwater. Additionally, return flow from polluted groundwater has been observed to contain PFAS, which should be considered in the model. Therefore, further modifications to the SWAT source code are required to simulate the exchange of PFAS between surface water and groundwater. This part can be implemented with a similar approach to the coupling of nitrate transport from SWAT with MODFLOW-RT3D.
- 5. PFAS simulation in the interaction between surface water and groundwater: The SWAT model simulates pesticides in wetlands and ponds; however, similar to the land phase processes, the model is not able to simulate the interaction between groundwater and wetlands/ponds/reservoirs. Therefore, the pesticides leaving the waterbodies via percolation/seepage are considered a loss for the system. Further modifications to the source code are required to link SWAT reservoir/wetlands components with MODFLOW. This part cannot be easily performed since reservoirs and wetlands are not represented spatially in the SWAT model. Therefore, further modification is required to define a shared boundary condition for SWAT and MODFLOW to exchange flow and chemicals in wetlands/reservoirs.
- 6. Replacing RT3D with MT3D: The RT3D generally has been recommended for simulating the fate and transport of biochemical particles such as nitrate and phosphorous, which does not require sophisticated sorption equations. RT3D can simulate mobile particles (i.e., nitrate) and immobile particles (i.e., phosphorous). However, MT3D can provide a detailed chemical mass balance equation with more details for simulating transport mechanisms, such as dual domain sorption. Therefore, replacing RT3D with MT3D would be more helpful for simulating PFAS fate and

transport in groundwater. This conversion can be easily performed as almost all of the RT3D module and MT3D module inputs are the same.

- 7- Air drift and deposition: The SWAT model cannot simulate the fate of pesticide drifted by air and deposited to other parts of the catchment. However, SWAT has been recently coupled with AgDRIFT to simulate drift and deposition (Zhang et al., 2018). Through the coupled SWAT-AgDRIFT model, the wind speed and direction can be used to simulate the amounts of pesticide moving offsite for each drift event and deposited as a point source to the receiving waters.
- 8. Chemical interactions: The diversity of PFAS compounds and their chemical structures makes their reactions and transport mechanisms complex. Evidence has shown that PFAS can be present in deposited sediment (Mussabek et al., 2019b), yet records on how PFAS species diffuse back to the water column under a concentration gradient is still limited. In addition, the PFAS release rate from foams to water is unknown and should be further studied. For the WASP model to improve PFAS transport simulations, reactions between different PFAS compounds should be considered. Additionally, competition for sorption sites on sediment particles should also be simulated, given the number of PFAS which have a high affinity for sediment.
- 9. Technical gaps in linking WASP with SWAT-MODFLOW-RT3D: The connection between the coupled SWAT-MODFLOW-RT3D model and WASP has not been well established. There are limitations for transferring balances of water, sediments, hydraulic features, and PFAS contaminants from SWAT-MODFLOW-RT3D to the stream network. Additionally, sediment and PFAS loads from surface runoff, subsurface flow, soil, and groundwater aquifers cannot be easily linked with the WASP river network but rather need to be manually entered. To build an accurate water quality model, a direct link between the coupled SWAT model and WASP should

be established. Some possible solutions include adding the necessary equations to SWAT-MODFLOW-RT3D coupled model to replace WASP altogether or designing procedures for the coupled model to interact with WASP through the hydrodynamic linkage module.

5.5 Conclusion

The aim of this study was to summarize potential opportunities and challenges of modeling PFAS within an integrated system at a large scale. To address this goal, three categories were established and assessed, namely PFAS sources, models, and monitoring for surface water, groundwater, and the vadose zone. For each category, suggested improvements and observations from the comprehensive literature review and case study were compiled.

Sources: Point sources and nonpoint sources have been identified as polluting PFAS. Even though identification of major polluters in an area of interest area can be straightforward, the rate at which PFAS is released into the environment has not been tracked for all polluters. For many PFAS users or manufacturing locations and municipalities, the rate and concentration of PFAS within discharge and emissions have not been regularly measured. To better predict PFAS exposure sites, sampling needs to be conducted on soil, streams, vadose zone, groundwater, sediment, and runoff. The sediment trapped behind reservoirs can act as PFAS sources within the right conditions, with diffusion driving the PFAS into the water from the sediment or resuspension of contaminated sediment from turbulent flow. Groundwater is especially important since it is the main source of drinking water and irrigation for rural areas and can retain high concentrations of PFAS when contaminated. Additionally, air emissions must be monitored for better source load prediction.

Modeling: Although there are many models which have been developed for simulating contaminant transport through the vadose zone, groundwater, and surface water, none of them are suited for simulating different compounds of PFAS transport. The unique characteristics of PFAS

allow them to travel through all media via a plethora of transport mechanisms. For this integrated model, sediment transport, advection, dispersion, adsorption, and settling were simulated and were all found to significantly influence PFAS transport within the Huron River. Unfortunately, not many existing models include all avenues of transport, especially from one environmental media (e.g., surface water) to the next (e.g., groundwater). Therefore, existing models must be improved to account for PFAS transport within and in between different media. This is especially important in areas with a large industrial presence and strong surface water-groundwater connections.

Monitoring: The results from the literature review and the case study of the Huron River watershed showed that contaminated environmental media had not been monitored on a regular basis to provide temporal trends of PFAS movement over time. Currently, many of the monitoring sites have had a single observation, providing a snapshot in time and space. These observations can be useful for identifying areas of concern for follow-up monitoring but are not as useful for understanding PFAS fate and transport. To paint a better picture of PFAS movement in the environment, monitoring studies must be organized to cover both spatial and temporal variation. Surface water should be monitored to cover different flow regimes and periods (i.e., high flow and low flow). Sediment concentrations of PFAS must also be monitored, especially during intense storms and seasonal melting, to understand the connection between the overland and surface water environment and the impact of sediment resuspension and redistribution on dissolved PFAS concentration. Groundwater monitoring should capture the direction and magnitude of PFAS concentration and movement throughout a year, with more monitoring wells at plumes and less in lower impacted areas. Finally, soil should be monitored to capture the movement patterns between the stratified layers. Without these observations, dispersed non-point sources cannot be identified and PFAS models cannot be calibrated or validated, preventing them from being used as a prediction tool. To fill gaps, the algorithm for population-based emissions can be used to estimate the magnitude of PFAS contamination within the watershed and identify high risk areas which should be more heavily monitored.

Despite the fact that many studies have been done to better understand and control PFAS in our environment, our level of knowledge of PFAS compounds fate and transport are limited. Therefore, future work should include improved source detection and monitoring, characterization of PFAS fate and transport mechanisms in models, environmental media integration, and goal-oriented monitoring.

6 Overall Conclusion

PFAS are an emerging contaminant with a global footprint having been found in all environmental media. To better understand the fate and transport of PFAS within the environment, sampling and modeling strategies must be developed in order to generate effective mitigation strategies. The aim of this work was to summarize the potential opportunities and challenges of modeling PFAS on a large-scale. This requires that all modes of transport within different environmental mediums (e.g., vadose zone, groundwater, streamflow) be simultaneously considered within the area of interest. Through literature review and a case study, many opportunities and challenges for large scale PFAS fate and transport modeling were identified that are summarized here:

Sources

- Discharge concentrations and rates from WWTPs, industry and residential areas are
 grossly unknown. In addition, many studies only provide individual snapshots in time
 or space at limited scales that are not appropriate for understanding the overall load
 situations within an area of interest.
- To better predict PFAS exposure sites, sampling needs to be conducted on air, soil, surface water, groundwater, sediment, and runoff. Groundwater is especially important since it is the main source of drinking water and irrigation for rural areas and can retain high concentrations of PFAS when contaminated.
- PFAS concentrations within air emissions from industry or incineration plants must be monitored to incorporate air deposition during dry and wet periods as a pollution source.

Modeling

- Many models have been developed for simulating contaminant transport through the
 vadose zone, groundwater, and surface water, but none of them are ready to account
 for all forms of PFAS fate and transport. This can be accomplished by considering the
 unique characteristics of PFAS that allow them to travel through all media via a
 plethora of transport mechanisms.
- The seamless integration of environmental models is challenging as different models
 require different inputs data while they come in varieties of special and temporal
 resolutions.

Monitoring

- Contaminated environmental media have not been monitored on a regular basis to provide temporal trends of PFAS movement over time.
- To date, many of the monitoring sites have limited observations that are useful for identifying the point of concern. However, if it is not impossible, it is very difficult to draw conclusions or understand a large-scale system behavior from point observations.
 In addition, these data types are not helpful in environmental modeling as they do not provide minimal information for the model calibration/validation.
- Monitoring studies must be organized to cover both spatial and temporal variation to generate a complete overview of PFAS fate and transport. Surface water should be monitored to understand PFAS concentrations and loads for different flow regimes and periods (e.g., high flow and low flow). This effort should also measure PFAS concentrations in contaminated sediment under suspension and deposition conditions. In addition, groundwater monitoring should capture the direction and magnitude of groundwater movement during wet and dry periods, and soil should be monitored to

capture the PFAS movement patterns between the stratified layers. Without these observations, PFAS models cannot be calibrated or validated, preventing them from being used as prediction tools.

7 Future Research Recommendations

This work highlighted major knowledge gaps within the current research on modeling PFAS fate and transport through the environment. In general, future research should address three major issues with PFAS studies that include source identification, models integration and parametrization, and model calibration through goal-oriented monitoring. Regarding PFAS source data identifications, it is suggested that PFAS producers and consumers are required to report their production and consumption to regulatory agencies.

To effectively understand PFAS transport within the environment, more effort needs to be put into identification and monitoring of sources, model development, and monitoring of environmental media. Although many PFAS sources have been identified, the rate and history of PFAS contamination remains unknown preventing accurate predictions of high-risk areas. Additionally, the PFAS fate and transport modeling research has mainly been represented within one environmental media rather than accounting for others through an integrated system. Plus, the most widely used models have limited contaminant transport capabilities, as related to the PFAS compounds. Finally, current monitoring data tends not to be sufficient for model calibration or validation given the low number of data points at a certain location or not accounting for seasonal variation. To bridge these gaps, sampling improvements and modeling improvements are required with our suggestions summarized below into sources, modeling, and monitoring.

Sources:

- Sample PFAS within the different environmental media, such as surface water, groundwater, soil, sediment, and runoff.
- Identify source rate of PFAS emissions or discharge and seasonal variability.

 Compute average source emission rates for well-known PFAS sources, such as WWTP, specific industry, and military grounds.

Models:

- Modify existing widely used models to include PFAS fate and transport mechanisms.
- Establish the average and range of values for different parameters that have been used to study PFAS fate and transport in various environmental media through research synthesis.

Monitoring:

- Organize sampling studies for long-term site investigation covering different media and seasonal variability.
- Provide complete sampling data (i.e., spatial and temporal information) to modelers under a memorandum of understanding if necessary.

APPENDIX

Table A1. Groundwater sampling locations and frequency of PFAS within the Huron River Watershed.

Location	PFOS	PFOA	ΣΡΓΑS	Date Range
Proud Lake Rec Area	9	9	0	4/2019 - 10/2019
Former Chrysler Scio Facility	65	65	520	5/2018 - 8/2020
Willow Run Airport	12	12	324	9/2020 - 11/2020
Glengary Elementary/WLS	3	3	66	4/2019 - 9/2019

Table A2. Surface water sampling locations and frequency of PFAS within the Huron River watershed.

Location	PFOS	PFOA	ΣPFAS	Date Range
Ann Arbor WWTP	15	15	0	11/2/2018 - 4/14/2021
Brighton WWTP	9	9	0	3/20/2019 - 2/23/2021
Dexter WWTP	6	6	0	8/14/2018 - 11/19/2020
Wixom WWTP	37	37	0	6/14/2018 - 4/6/2021
Argo Pond	2	2	48	9/28/2018 - 6/4/2020
Base Line Lake	1	1	28	8/13/2020
Behind Edgelake Drive	1	1	22	4/30/2019
Chrysler SCIO	1	1	28	8/4/2020
Regan Drain downstream	2	2	53	10/14/2020
Flat Rock Impoundment	2	2	56	8/4/2020 - 8/25/2020
HR at Burns Rd	6	6	139	7/24/2018 - 8/3/2020
HR at Central Rd	1	1	22	7/24/2018
HR at Delhi Rd	1	1	22	7/24/2018
HR at E Huron River Dr	3	3	73	7/24/2018 - 8/4/2020
HR at GM Road	2	2	44	8/30/2018 - 10/30/2018
HR at McCabe Rd.	1	1	22	10/30/2018
HR at N Territorial Rd	2	2	44	7/24/2018
HR at Rawsonville Rd	1	1	22	7/24/2018
HR at Stark Strasse	1	1	22	7/24/2018
HR at White Lake Rd	1	1	22	7/24/2018
HR at Wixom Rd	6	6	139	7/24/2018 - 8/3/2020
HR Barton Pond	2	2	42	7/24/2018 - 9/28/2018
HR DS Base Line and Portage Lakes	4	4	100	7/24/2018 - 8/4/2020
HR US Strawberry Lake	3	3	67	7/24/2018 - 4/30/2019
Hubbell Pond	1	1	22	10/2/2018
Huron River at Benstein Rd.	1	1	22	8/30/2018
Kent Lake	2	2	48	10/29/2018 - 6/14/2020
Kent Lake at W. Buno Rd	1	1	22	10/30/2018
Regan Drain upstream	3	3	81	8/25/2020 - 10/14/2020
Zeeb Rd	2	2	56	8/4/2020

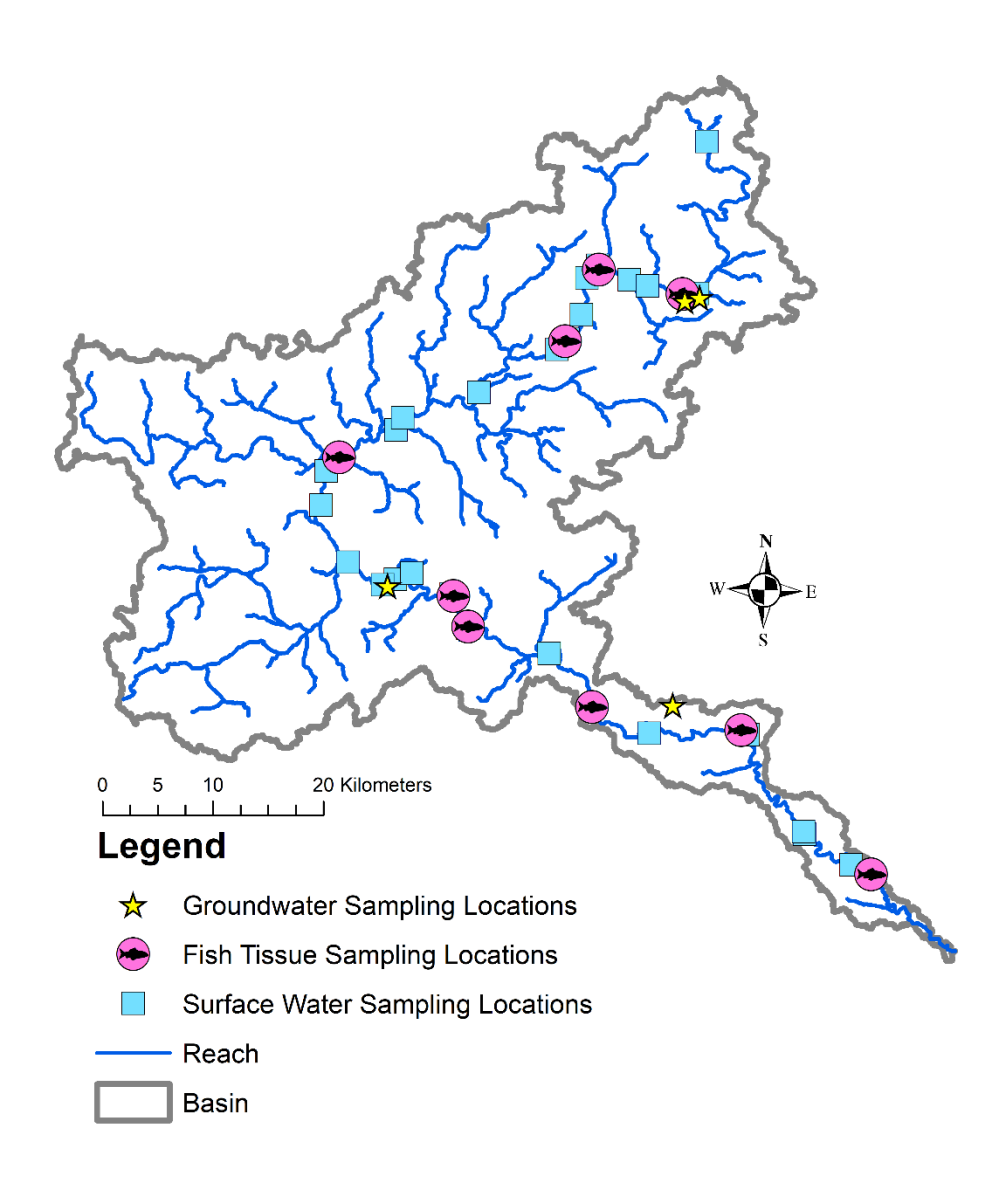


Figure A1. Groundwater, fish, and surface water PFAS sampling sites in the Huron River watershed.

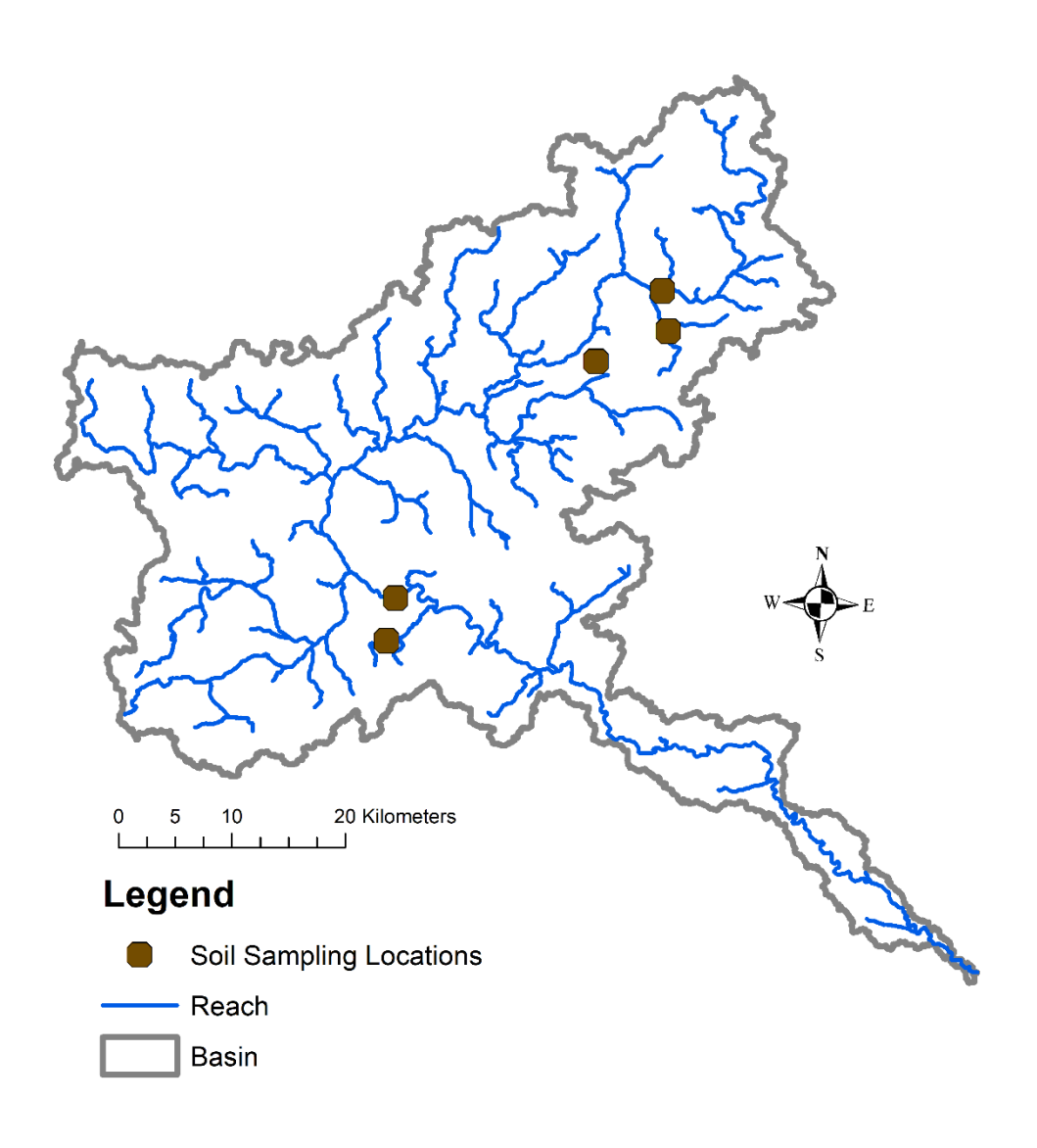


Figure A2. Soil sampling locations of PFAS within the Huron River watershed.

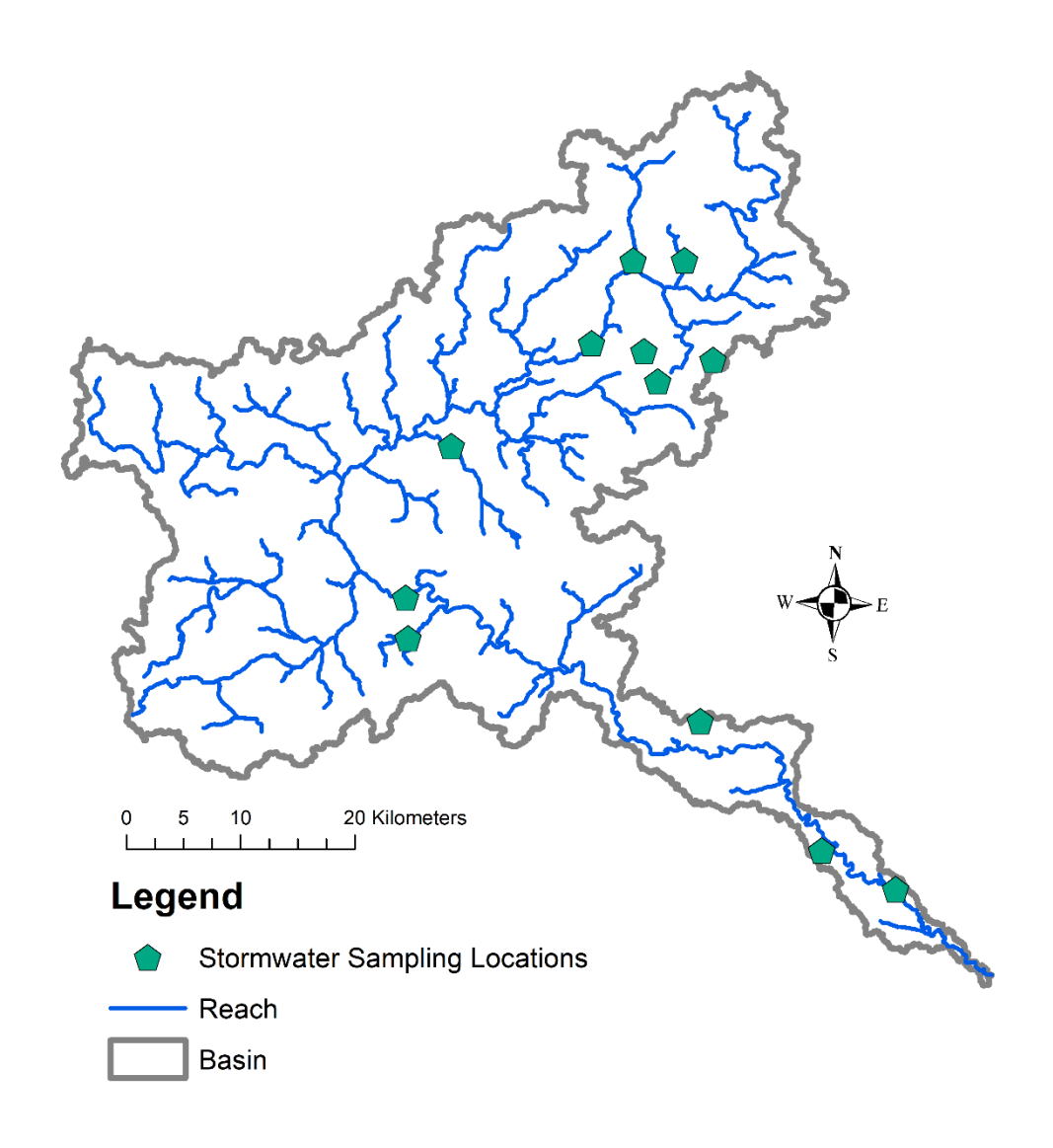


Figure A3. Stormwater PFAS sampling locations within the Huron River watershed.

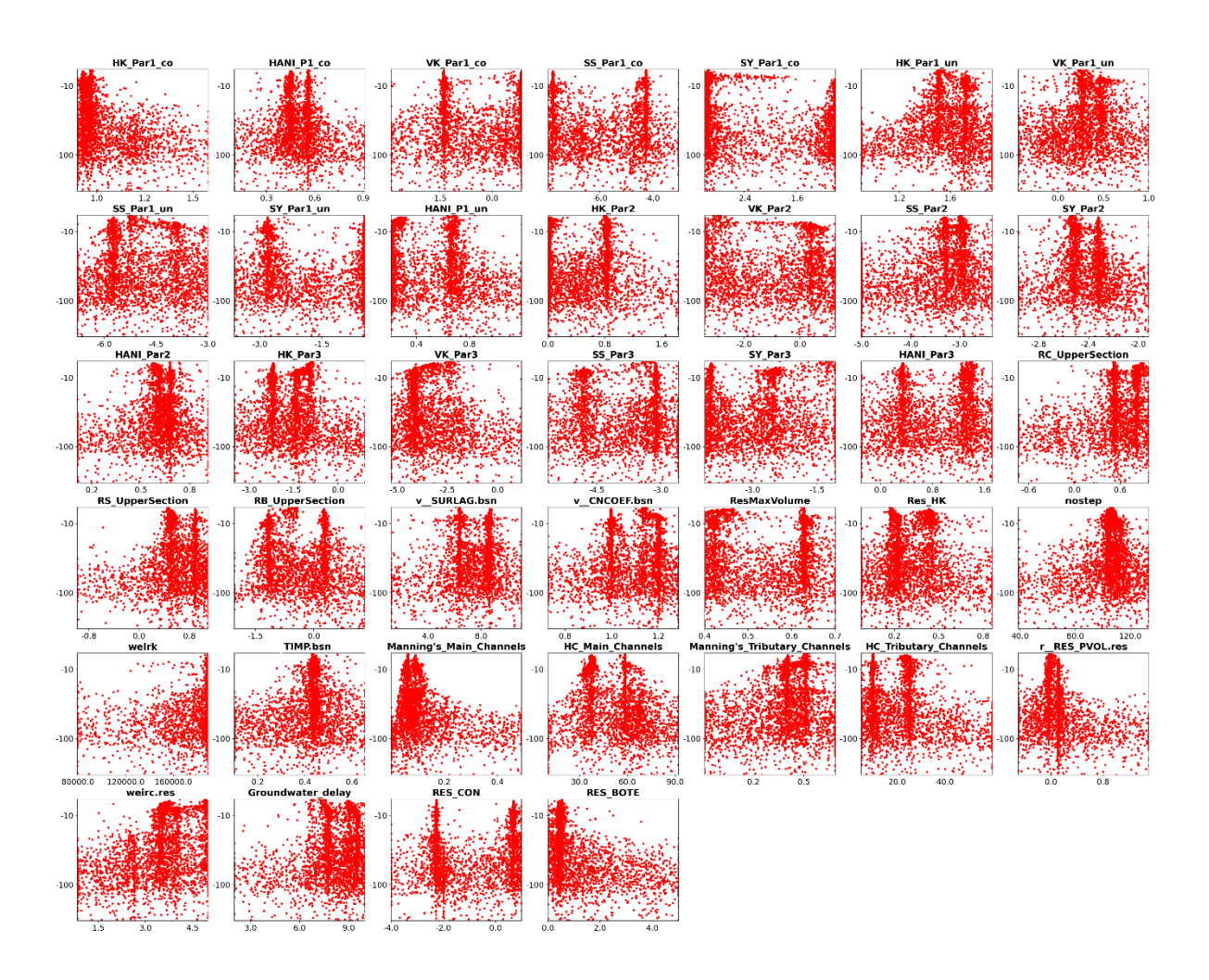


Figure A4. Parameters value vs. objective function. The parameter value with index r_ shows relative change to the original value. The values in the horizontal axes for HK, VK, SS, and SY are the exponent of 10. Co stands for confined aquifer in the first layer; Un stands for the unconfined aquifer. Par1, Par2, Par3 stand for the layers of the groundwater.

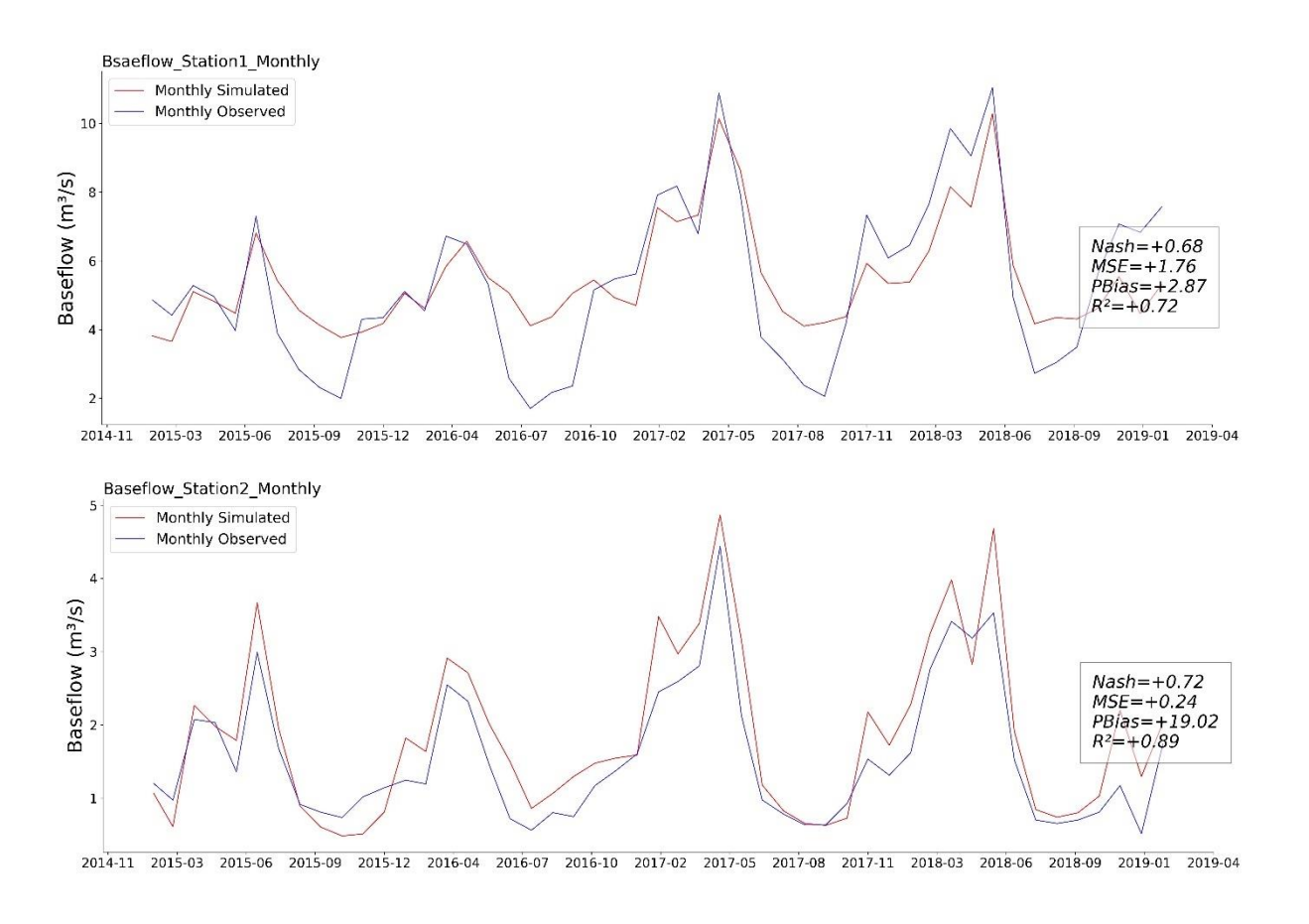


Figure A5. Monthly simulated vs. observed baseflow.

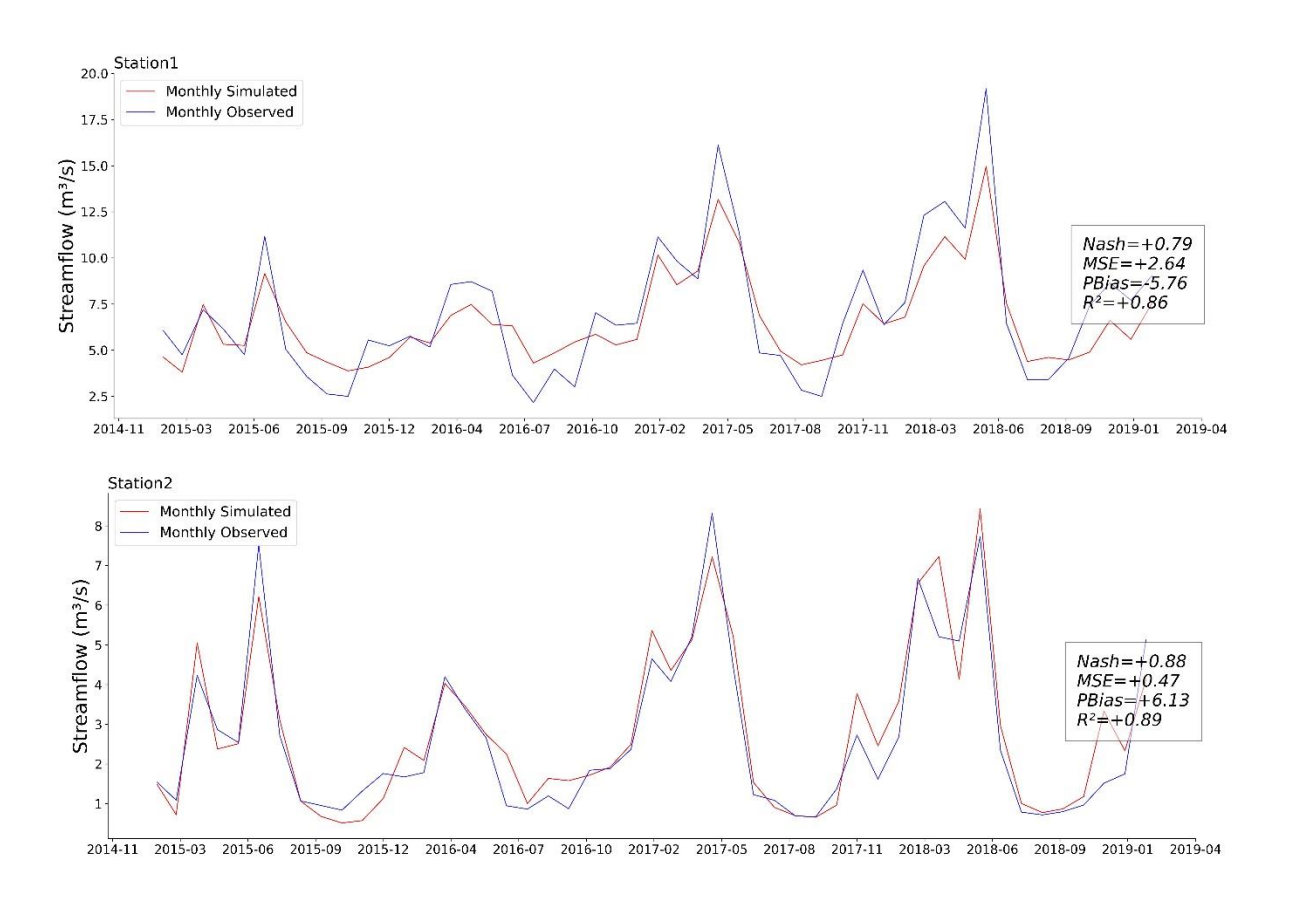


Figure A6. Monthly streamflow simulated vs. observed.

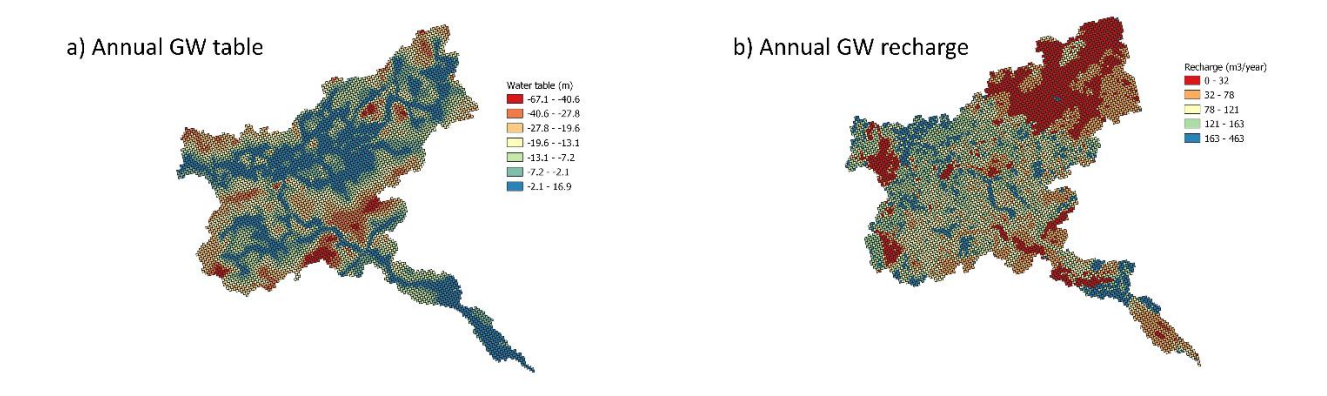


Figure A7. Simulated a) annual cell-by-cell groundwater water table and b) annual cell-by-cell recharge.

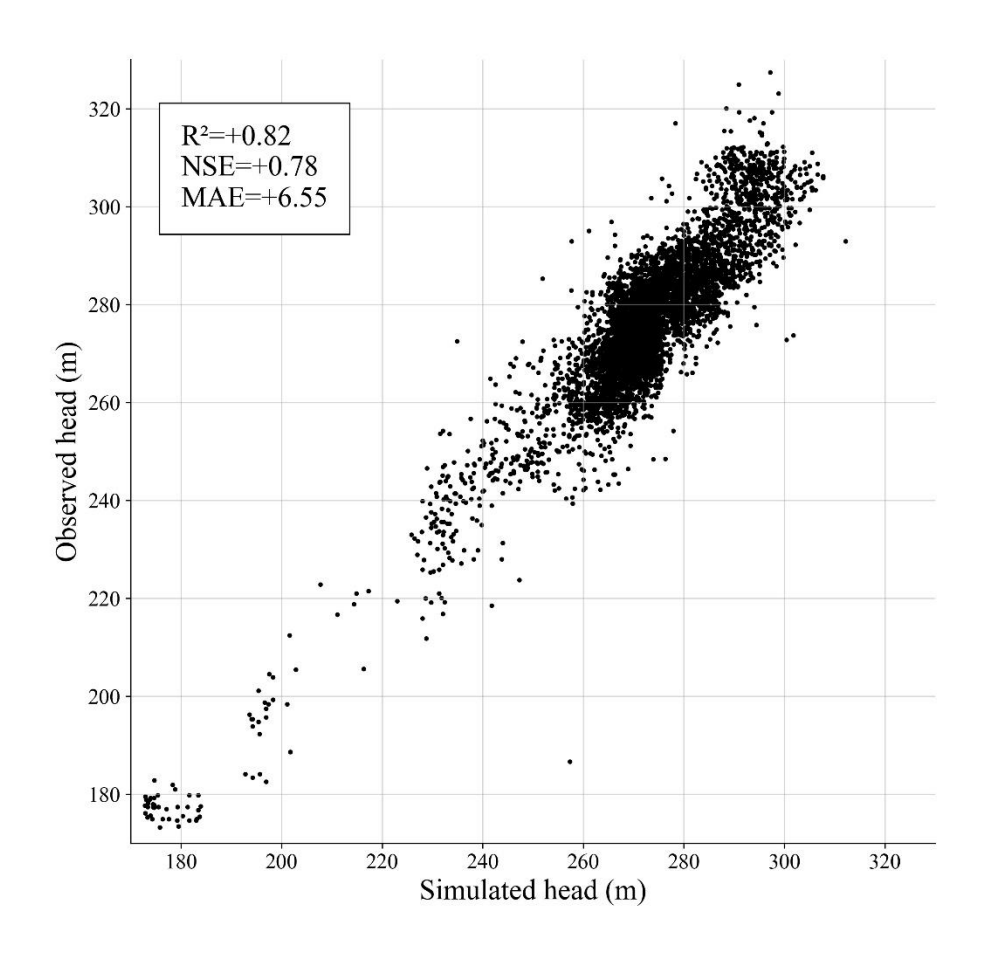


Figure A8. Model samples in relation to observations from groundwater wells within the study area.

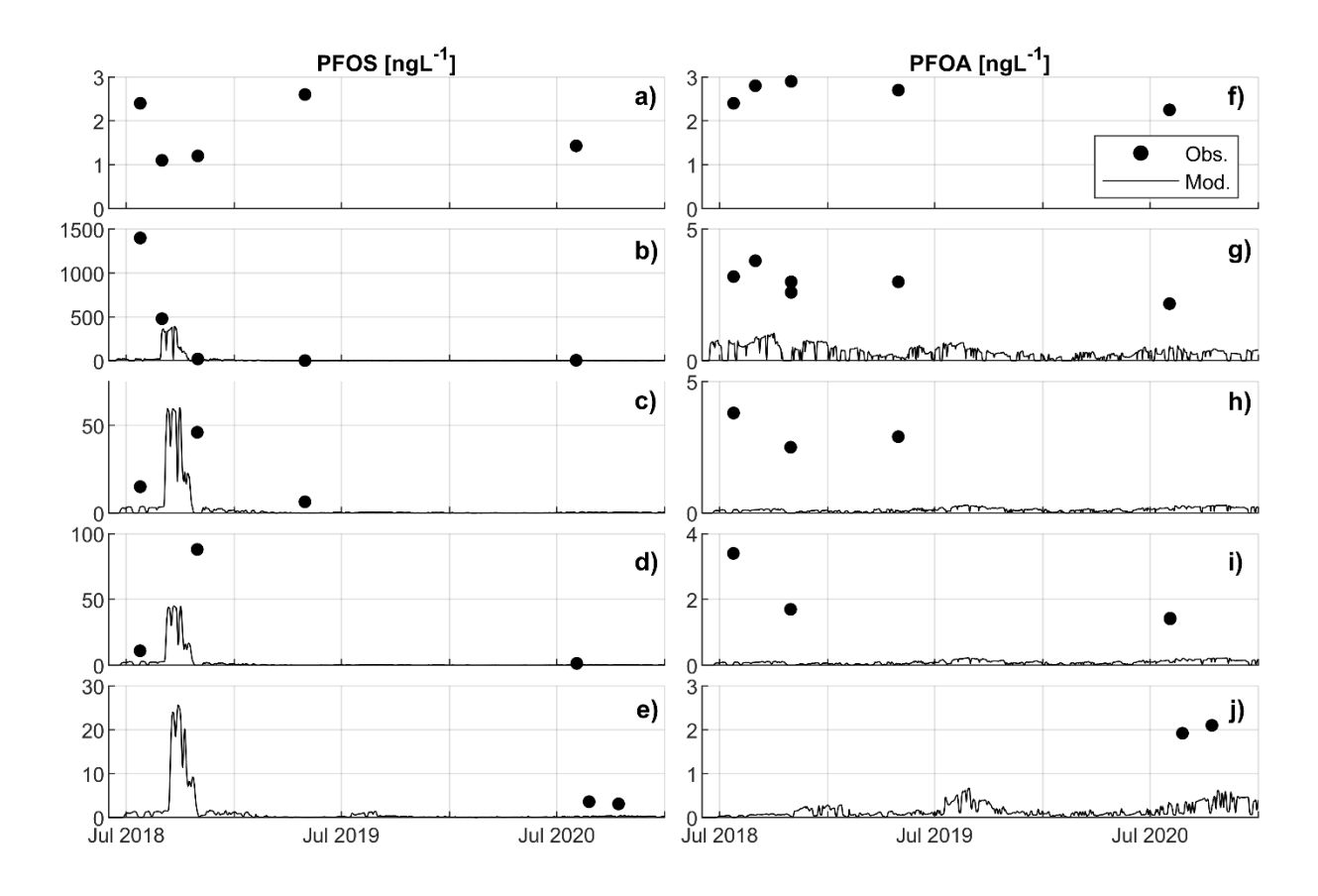


Figure A9. Huron River observations and model results for PFOS and PFOA at a) Wixom Rd, b) Burns Rd, c) Strawberry Lake, d) Base Line and Portage Lakes, and e) Regan Drain Downstream.

BIBLIOGRAPHY

BIBLIOGRAPHY

- Abouali, M., Nejadhashemi, A. P., Daneshvar, F., & Woznicki, S. A. (2016). Two-phase approach to improve stream health modeling. *Ecological Informatics*, *34*, 13–21. https://doi.org/10.1016/j.ecoinf.2016.04.009
- Abu Hasan, H., Muhammad, M. H., & Ismail, N. I. (2020). A review of biological drinking water treatment technologies for contaminants removal from polluted water resources. In *Journal of Water Process Engineering* (Vol. 33). Elsevier Ltd. https://doi.org/10.1016/j.jwpe.2019.101035
- Ahrens, L., & Bundschuh, M. (2014). Fate and effects of poly- and perfluoroalkyl substances in the aquatic environment: A review. *Environmental Toxicology and Chemistry*, *33*(9), 1921–1929. https://doi.org/10.1002/etc.2663
- Åkerblom, S., Negm, N., Wu, P., Bishop, K., & Ahrens, L. (2017). Variation and accumulation patterns of poly- and perfluoroalkyl substances (PFAS) in European perch (Perca fluviatilis) across a gradient of pristine Swedish lakes. *Science of The Total Environment*, *599–600*, 1685–1692. https://doi.org/10.1016/J.SCITOTENV.2017.05.032
- Al-Ansari, A. M., Saleem, A., Kimpe, L. E., Sherry, J. P., McMaster, M. E., Trudeau, V. L., & Blais, J. M. (2010). Bioaccumulation of the pharmaceutical 17α-ethinylestradiol in shorthead redhorse suckers (Moxostoma macrolepidotum) from the St. Clair River, Canada. *Environmental Pollution*, 158(8), 2566–2571. https://doi.org/10.1016/j.envpol.2010.05.020
- Al-Fifi, Z., Abada, E., Al-Rajab, A. J., Mahdhi, M., & Sharma, M. (2019). Molecular identification of biological contaminants in different drinking water resources of the Jazan region, Saudi Arabia. *Journal of Water and Health*, *17*(4), 622–632. https://doi.org/10.2166/wh.2019.019
- Alley, W. M. (2009). Ground Water. *Encyclopedia of Inland Waters*, 684–690. https://doi.org/10.1016/B978-012370626-3.00015-6
- Aly, N. A., Luo, Y. S., Liu, Y., Casillas, G., McDonald, T. J., Kaihatu, J. M., Jun, M., Ellis, N., Gossett, S., Dodds, J. N., Baker, E. S., Bhandari, S., Chiu, W. A., & Rusyn, I. (2020). Temporal and spatial analysis of per and polyfluoroalkyl substances in surface waters of Houston ship channel following a large-scale industrial fire incident. *Environmental Pollution*, 265, 115009. https://doi.org/10.1016/J.ENVPOL.2020.115009
- Ambrose, B., Avant, B., Han, Y., Knightes, C., & Wool, T. (2017). Water Quality Assessment Simulation Program (WASP8): Upgrades to the Advanced Toxicant Module for Simulating Dissolved Chemicals, Nanomaterials, and Solids (Issue September).
- Ambrose, R. B., & Wool, T. (2017). WASP8 Stream Transport Model Theory and User's Guide.
- Aminov, R. I. (2010a). A brief history of the antibiotic era: Lessons learned and challenges for the future. *Frontiers in Microbiology*, *1*(DEC). https://doi.org/10.3389/fmicb.2010.00134

- Aminov, R. I. (2010b). A brief history of the antibiotic era: Lessons learned and challenges for the future. *Frontiers in Microbiology*, *I*(DEC). https://doi.org/10.3389/fmicb.2010.00134
- Anderson, M. P., Woessner, W. W., & Hunt, R. J. (2015). *Applied Groundwater Modeling: Simulation of Flow and Advective Transport*. Academic Press. https://books.google.com/books?id=jcOcBAAAQBAJ&pg=PA70&dq=governing+equation+for+groundwater+modeling&hl=de&sa=X&ved=0ahUKEwjOhZjFvuPpAhXidc0KHeM4DeAQ6AEIPzAC#v=onepage&q=governing equation for groundwater modeling&f=false
- Ankley, G. T., Bennett, R. S., Erickson, R. J., Hoff, D. J., Hornung, M. W., Johnson, R. D., Mount, D. R., Nichols, J. W., Russom, C. L., Schmieder, P. K., Serrrano, J. A., Tietge, J. E., & Villeneuve, D. L. (2010). Adverse outcome pathways: A conceptual framework to support ecotoxicology research and risk assessment. *Environmental Toxicology and Chemistry*, 29(3), 730–741. https://doi.org/10.1002/etc.34
- Arcadis. (2020). REVIEW OF MODELS FOR EVALUATING PER- AND POLYFLUOROALKYL SUBSTANCES IN LAND APPLIED RESIDUALS AND BIOSOLIDS (Issue June).
- Armitage, J. M., Macleod, M., & Cousins, I. T. (2009). Comparative assessment of the global fate and transport pathways of long-chain perfluorocarboxylic acids (PFCAs) and perfluorocarboxylates (PFCs) emitted from direct sources. *Environmental Science and Technology*, 43(15), 5830–5836. https://doi.org/10.1021/es900753y
- Arnold, J. G., Srinivasan, R., Muttiah, R. S., & Williams, J. R. (1998). Large area hydrologic modeling and assessment part I: Model development. *Journal of the American Water Resources Association*, *34*(1), 73–89. https://doi.org/10.1111/j.1752-1688.1998.tb05961.x
- Auer, M. T., Tomlinson, L. M., Higgins, S. N., Malkin, S. Y., Howell, E. T., & Bootsma, H. A. (2010). Great Lakes Cladophora in the 21st century: same algae—different ecosystem. *Journal of Great Lakes Research*, 36(2), 248–255. https://doi.org/https://doi.org/10.1016/j.jglr.2010.03.001
- Awad, Y. M., Kim, S. C., Abd El-Azeem, S. A. M., Kim, K. H., Kim, K. R., Kim, K., Jeon, C., Lee, S. S., & Ok, Y. S. (2014). Veterinary antibiotics contamination in water, sediment, and soil near a swine manure composting facility. *Environmental Earth Sciences*, 71(3), 1433–1440. https://doi.org/10.1007/s12665-013-2548-z
- Barr. (2017). DRAFT Conceptual Modeling of PFOA Fate and Transport: North Bennington, Vermont.
- Baynes, R. E., Dix, K. J., & Riviere, J. E. (2012). Distribution and Pharmacokinetics Models. In *Pesticide Biotransformation and Disposition* (pp. 117–147). https://doi.org/10.1016/B978-0-12-385481-0.00006-X
- Beck, H., Eckart, K., W., M., & Wittkowski, R. (1989). Per a a mon Press plc PCDD AND PCDF BODY BURDEN FROM FOOD INTAKE IN THE FEDERAL REPUILIC OF GERMANY. *Chemosphere*, 18(1–6), 417–424.

- Bedekar, V., Morway, E. D., Langevin, C. D., & Tonkin, M. J. (2016). MT3D-USGS Version 1: A U.S. Geological Survey Release of MT3DMS Updated with New and Expanded Transport Capabilities for Use with MODFLOW. *U.S. Geological Survey Techniques and Methods 6-A53*, 69.
- Begnudelli, L., & Sanders, B. F. (2006). Unstructured Grid Finite-Volume Algorithm for Shallow-Water Flow and Scalar Transport with Wetting and Drying. *Journal of Hydraulic Engineering*, 132(4), 371–384. https://doi.org/10.1061/ASCE0733-94292006132:4371
- Behr, A. C., Plinsch, C., Braeuning, A., & Buhrke, T. (2020). Activation of human nuclear receptors by perfluoroalkylated substances (PFAS). *Toxicology in Vitro*, 62. https://doi.org/10.1016/j.tiv.2019.104700
- Berger, U., Glynn, A., Holmström, K. E., Berglund, M., Ankarberg, E. H., & Törnkvist, A. (2009). Fish consumption as a source of human exposure to perfluorinated alkyl substances in Sweden Analysis of edible fish from Lake Vättern and the Baltic Sea. *Chemosphere*, 76, 799–804. https://doi.org/10.1016/j.chemosphere.2009.04.044
- Bhavsar, S. P., Zhang, X., Guo, R., Braekevelt, E., Petro, S., Gandhi, N., Reiner, E. J., Lee, H., Bronson, R., & Tittlemier, S. A. (2014). Cooking fish is not effective in reducing exposure to perfluoroalkyl and polyfluoroalkyl substances. *Environment International*, *66*, 107–114. https://doi.org/10.1016/j.envint.2014.01.024
- Boards, L. (2006). Local Board of Health Guide to On-Site Wastewater Treatment Systems ©2006. *East*.
- Boisvert, G., Sonne, C., Rigét, F. F., Dietz, R., & Letcher, R. J. (2019). Bioaccumulation and biomagnification of perfluoroalkyl acids and precursors in East Greenland polar bears and their ringed seal prey. *Environmental Pollution*, 252, 1335–1343. https://doi.org/10.1016/j.envpol.2019.06.035
- Borthakur, A., Wang, M., He, M., Ascencio, K., Blotevogel, J., Adamson, D. T., Mahendra, S., & Mohanty, S. K. (2021). Perfluoroalkyl acids on suspended particles: Significant transport pathways in surface runoff, surface waters, and subsurface soils. *Journal of Hazardous Materials*, 417, 126159. https://doi.org/10.1016/J.JHAZMAT.2021.126159
- Brand, C. J. (1945). SOME FERTILIZER HISTORY CONNECTED WITH WORLD WAR I. *Agricultural History*, 19(2), 104.
- Browne, M. A., Crump, P., Niven, S. J., Teuten, E., Tonkin, A., Galloway, T., & Thompson, R. (2011). Accumulation of microplastic on shorelines woldwide: Sources and sinks. *Environmental Science and Technology*, 45(21), 9175–9179. https://doi.org/10.1021/es201811s
- Brusseau, M. L. (2018). Assessing the potential contributions of additional retention processes to PFAS retardation in the subsurface. *Science of The Total Environment*, 613–614, 176–185. https://doi.org/https://doi.org/10.1016/j.scitotenv.2017.09.065

- Brusseau, M. L. (2020). Simulating PFAS transport influenced by rate-limited multi-process retention. *Water Research*, *168*, 115179. https://doi.org/10.1016/j.watres.2019.115179
- Brusseau, M. L., Anderson, R. H., & Guo, B. (2020). PFAS concentrations in soils: Background levels versus contaminated sites. *Science of the Total Environment*, 740, 140017. https://doi.org/10.1016/j.scitotenv.2020.140017
- Brusseau, M. L., & Chorover, J. (2019). Chemical Processes Affecting Contaminant Transport and Fate. In *Environmental and Pollution Science* (Third, pp. 113–130). Academic Press. https://doi.org/10.1016/B978-0-12-814719-1.00008-2
- Brusseau, M. L., & Van Glubt, S. (2019). The influence of surfactant and solution composition on PFAS adsorption at fluid-fluid interfaces. *Water Research*, *161*, 17–26. https://doi.org/10.1016/j.watres.2019.05.095
- Brusseau, M. L., Yan, N., Van Glubt, S., Wang, Y., Chen, W., Lyu, Y., Dungan, B., Carroll, K. C., & Holguin, F. O. (2019). Comprehensive retention model for PFAS transport in subsurface systems. *Water Research*, *148*, 41–50. https://doi.org/10.1016/j.watres.2018.10.035
- Caldwell, D. J., Mastrocco, F., Nowak, E., Johnston, J., Yekel, H., Pfeiffer, D., Hoyt, M., DuPlessie, B. M., & Anderson, P. D. (2010). An assessment of potential exposure and risk from estrogens in drinking water. *Environ. Health. Pers.*, *118*(3), 338–344. https://doi.org/10.1289/ehp.0900654.S1
- Carsel, R. F., Mulkey, L. A., Lorber, M. N., & Baskin, L. B. (1985). The Pesticide Root Zone Model (PRZM): A procedure for evaluating pesticide leaching threats to groundwater. *Ecological Modelling*, 30(1–2), 49–69. https://doi.org/10.1016/0304-3800(85)90036-5
- Centner, T. J., & Feitshans, T. A. (2006). Regulating manure application discharges from concentrated animal feeding operations in the United States. *Environmental Pollution*, 141(3), 571–573. https://doi.org/10.1016/j.envpol.2005.09.003
- Chang, H.-J., Lin, T.-F., Whang, L.-M., & Wu, Y.-J. (2016). Congener profiles of polychlorinated dibenzo-p-dioxins and polychlorinated dibenzofurans (PCDD/Fs) in sediment, water, and fish at a soil contamination site in Taiwan. *Journal of Environmental Science and Health, Part A*, 51(3), 251–261. https://doi.org/10.1080/10934529.2015.1094346
- Chanpiwat, P., Sthiannopkao, S., Widmer, K., Himeno, S., Miyataka, H., Vu, N. U., Tran, V. V., & Pham, T. T. N. (2016). Assessment of metal and bacterial contamination in cultivated fish and impact on human health for residents living in the Mekong Delta. *Chemosphere*, *163*, 342–350. https://doi.org/10.1016/j.chemosphere.2016.08.003
- Chen, H. L., Lee, C. C., Liao, P. C., Guo, Y. L., Chen, C. H., & Su, H. J. (2003). Associations between dietary intake and serum polychlorinated dibenzo-p-dioxin and dibenzofuran (PCDD/F) levels in Taiwanese. *Environmental Research*, *91*(3), 172–178. https://doi.org/10.1016/S0013-9351(02)00058-0

- Chen, J., Tang, L., Chen, W.-Q., Peaslee, G. F., & Jiang, D. (2020). The Flows, Stock, and Emissions of Poly-and Perfluoroalkyl Substances (PFAS) in California Carpet in 2000-2030 under Different Scenarios. https://doi.org/10.1021/acs.est.9b06956
- Clara, M., Gans, O., Weiss, S., Sanz-Escribano, D., Scharf, S., & Scheffknecht, C. (2009). Perfluorinated alkylated substances in the aquatic environment: An Austrian case study. *Water Research*, 43(18), 4760–4768. https://doi.org/10.1016/j.watres.2009.08.004
- Codling, G., Yuan, H., Jones, P. D., Giesy, J. P., & Hecker, M. (2020). Metals and PFAS in stormwater and surface runoff in a semi-arid Canadian city subject to large variations in temperature among seasons. *Environmental Science and Pollution Research* 2020 27:15, 27(15), 18232–18241. https://doi.org/10.1007/S11356-020-08070-2
- Conder, J. M., Hoke, R. A., De Wolf, W., Russell, M. H., & Buck, R. C. (2008). Are PFCAs bioaccumulative? A critical review and comparison with regulatory criteria and persistent lipophilic compounds. *Environmental Science and Technology*, 42(4), 995–1003. https://doi.org/10.1021/es070895g
- Costello, M. C. S., & Lee, L. S. (2020). Sources, Fate, and Plant Uptake in Agricultural Systems of Per- and Polyfluoroalkyl Substances. *Current Pollution Reports*, 1–21. https://doi.org/10.1007/S40726-020-00168-Y/TABLES/2
- Crane, J. L. (1996). Carcinogenic human health risks associated with consuming contaminated fish from five Great Lakes Areas of Concern. *Journal of Great Lakes Research*, 22(3), 653–668. https://doi.org/10.1016/S0380-1330(96)70987-5
- Cui, Y., Lv, S., Liu, J., Nie, S., Chen, J., Dong, Q., Huang, C., & Yang, D. (2017). Chronic perfluorooctanesulfonic acid exposure disrupts lipid metabolism in zebrafish. *Human & Experimental Toxicology*, *36*(3), 207–217. https://doi.org/10.1177/0960327116646615
- Das, K. P., Wood, C. R., Lin, M. J., Starkov, A. A., Lau, C., Wallace, K. B., Corton, J. C., & Abbott, B. D. (2017). Perfluoroalkyl acids-induced liver steatosis: Effects on genes controlling lipid homeostasis. *Toxicology*, *378*, 37–52. https://doi.org/10.1016/j.tox.2016.12.007
- Dauchy, X., Boiteux, V., Colin, A., Bach, C., Rosin, C., & Munoz, J. F. (2019). Poly- and Perfluoroalkyl Substances in Runoff Water and Wastewater Sampled at a Firefighter Training Area. *Archives of Environmental Contamination and Toxicology*, 76(2), 206–215. https://doi.org/10.1007/s00244-018-0585-z
- Deltares. (2021). Delft3D 3D/2D modelling suite for integral water solutions.
- Derraik, J. G. B. (2002). The pollution of the marine environment by plastic debris: A review. In *Marine Pollution Bulletin* (Vol. 44, Issue 9, pp. 842–852). https://doi.org/10.1016/S0025-326X(02)00220-5
- DHI. (2017). MIKE SHE (Vol. 2).

- Diaz, R. J., & Rosenberg, R. (2008). Spreading dead zones and consequences for marine ecosystems. In *Science* (Vol. 321, Issue 5891, pp. 926–929). https://doi.org/10.1126/science.1156401
- Doney, S. C., Balch, W. M., Fabry, V. J., & Feely, R. A. (2009). Ocean acidification: A critical emerging problem for the ocean sciences. *Oceanography*, 22(SPL.ISS. 4), 16–25. https://doi.org/10.5670/oceanog.2009.93
- Dufour, A., Bartram, J., Bos, R., & Gannon, V. (2012). Summary Statement 1.
- EGLE. (2019a). Investigation of the Occurrence and Source(s) of PFAS in the Huron River Watershed July 2018 Dec 2019 (Issue February).
- EGLE. (2019b). Investigation of the Occurrence and Source(s) of PFAS in the Huron River Watershed July 2018 Dec 2019.
- EGLE. (2020). *PFAS Response PFAS and Biosolids*. https://www.michigan.gov/pfasresponse/0,9038,7-365-86704_89705---,00.html
- Entertainment Close-up. (2011). Research and Markets Offers Report: US Animal Production Industry (Issue December 5).
- EPA. (2021). *CompTox Chemicals Dashboard | PFASMASTER Chemicals*. https://comptox.epa.gov/dashboard/chemical_lists/pfasmaster
- Erisman, J. W., Sutton, M. A., Galloway, J., Klimont, Z., & Winiwarter, W. (2008). How a century of ammonia synthesis changed the world. *Nature Geoscience*, *1*(10), 636–639. https://doi.org/10.1038/ngeo325
- Evans, S., Andrews, D., Stoiber, T., & Naidenko, O. (2020, January 22). PFAS Contamination of Drinking Water Far More Prevalent Than Previously Reported. *EWG*.
- Fent, K. (1996). Organotin compounds in municipal wastewater and sewage sludge: Contamination, fate in treatment process and ecotoxicological consequences. *Science of the Total Environment*, 185(1–3), 151–159. https://doi.org/10.1016/0048-9697(95)05048-5
- Fischer, H. B., List, E. J., Koh, R. C., Imberger, J., & Brooks, N. H. (1979). Mixing in Inland and Coastal Waters. *Elsevier*. https://doi.org/https://doi.org/10.1016/C2009-0-22051-4
- Fisk, A. T., Hobson, K. A., & Norstrom, R. J. (2001). Influence of Chemical and Biological Factors on Trophic Transfer of Persistent Organic Pollutants in the Northwater Polynya Marine Food Web. *Environemental Science and Technology*, 35(4), 732–738. https://doi.org/10.1021/es001459w
- Fleisher, J. M., Fleming, L. E., Solo-Gabriele, H. M., Kish, J. K., Sinigalliano, C. D., Plano, L., Elmir, S. M., Wang, J. D., Withum, K., Shibata, T., Gidley, M. L., Abdelzaher, A., He, G., Ortega, C., Zhu, X., Wright, M., Hollenbeck, J., & Backer, L. C. (2010). The BEACHES study: Health effects and exposures from non-point source microbial contaminants in

- subtropical recreational marine waters. *International Journal of Epidemiology*, 39(5), 1291–1298. https://doi.org/10.1093/ije/dyq084
- Frisbee, S. J., Brooks, A. P., Maher, A., Flensborg, P., Arnold, S., Fletcher, T., Steenland, K., Shankar, A., Knox, S. S., Pollard, C., Halverson, J. A., Vieira, V. M., Jin, C., Leyden, K. M., & Ducatman, A. M. (2009). The C8 health project: Design, methods, and participants. *Environmental Health Perspectives*, 117(12), 1873–1882. https://doi.org/10.1289/ehp.0800379
- Gallo, V., Leonardi, G., Genser, B., Lopez-Espinosa, M. J., Frisbee, S. J., Karlsson, L., Ducatman, A. M., & Fletcher, T. (2012). Serum perfluorooctanoate (PFOA) and perfluorooctane sulfonate (PFOS) concentrations and liver function biomarkers in a population with elevated PFOA exposure. *Environmental Health Perspectives*, 120(5), 655–660. https://doi.org/10.1289/ehp.1104436
- Gao, P., Ding, Y., Li, H., & Xagoraraki, I. (2012). Occurrence of pharmaceuticals in a municipal wastewater treatment plant: Mass balance and removal processes. *Chemosphere*, 88(1), 17–24. https://doi.org/10.1016/j.chemosphere.2012.02.017
- Gassmann, M., Weidemann, E., & Stahl, T. (2020). Combined leaching and plant uptake simulations of PFOA and PFOS under field conditions. *Environmental Science and Pollution Research*, 28(2), 2097–2107. https://doi.org/10.1007/S11356-020-10594-6
- Ge, J., Wang, C., Nie, X., Yang, J., Lu, H., Song, X., Su, K., Li, T., Han, J., Zhang, Y., Mao, J., Gu, Y., Zhao, J., Jiang, S., & Wu, Q. (2016). ROS-mediated apoptosis of HAPI microglia through p53 signaling following PFOS exposure. *Environmental Toxicology and Pharmacology*, 46, 9–16. https://doi.org/10.1016/j.etap.2016.06.025
- GeoStudio. (2021). *Vadose Zone Hydrology*. http://www.geoslope.com/solutions/vadose-zone-hydrology
- Ghiold, J. (2019). CHEMOURS FAYETTEVILLE WORKS CAPE FEAR RIVER PFAS MASS LOADING MODEL SCOPE OF WORK.
- Glaser, D., Lamoureux, E., Opdyke, D., LaRoe, S., Reidy, D., & Connolly, J. (2021). The impact of precursors on aquatic exposure assessment for PFAS: Insights from bioaccumulation modeling. *Integrated Environmental Assessment and Management*, 17(4), 705–715. https://doi.org/10.1002/IEAM.4414
- Glibert, P. M. (2017). Eutrophication, harmful algae and biodiversity Challenging paradigms in a world of complex nutrient changes. *Marine Pollution Bulletin*, 124(2), 591–606. https://doi.org/10.1016/j.marpolbul.2017.04.027
- Glibert, P. M., Maranger, R., Sobota, D. J., & Bouwman, L. (2014). The Haber Bosch-harmful algal bloom (HB-HAB) link. *Environmental Research Letters*, 9(10). https://doi.org/10.1088/1748-9326/9/10/105001

- Goode, D. J., & Senior, L. A. (2020). Groundwater Withdrawals and Regional Flow Paths at and near Willow Grove and Warminster, Pennsylvania—Data Compilation and Preliminary Simulations for Conditions in 1999, 2010, 2013, 2016, and 2017.
- Gore, A. C., Chappell, V. A., Fenton, S. E., Flaws, J. A., Nadal, A., Prins, G. S., Toppari, J., & Zoeller, R. T. (2015). EDC-2: The Endocrine Society's Second Scientific Statement on Endocrine-Disrupting Chemicals. In *Endocrine Reviews* (Vol. 36, Issue 6, pp. 1–150). Endocrine Society. https://doi.org/10.1210/er.2015-1010
- Green, B. C., & Johnson, C. L. E. (2019). Characterisation of microplastic contamination in sediment of England's inshore waters. *Marine Pollution Bulletin*, 110788. https://doi.org/10.1016/j.marpolbul.2019.110788
- Gregory, M. R. (1991). The hazards of persistent marine pollution: Drift plastics and conservation islands. *Journal of the Royal Society of New Zealand*, 21(2), 83–100. https://doi.org/10.1080/03036758.1991.10431398
- Gremmel, C., Frömel, T., & Knepper, T. P. (2016). Systematic determination of perfluoroalkyl and polyfluoroalkyl substances (PFASs) in outdoor jackets. *Chemosphere*, *160*, 173–180. https://doi.org/10.1016/j.chemosphere.2016.06.043
- Groffen, T., Nkuba, B., Wepener, V., & Bervoets, L. (2021). Risks posed by per- and polyfluoroalkyl substances (PFAS) on the African continent, emphasizing aquatic ecosystems. *Integrated Environmental Assessment and Management*, 17(4), 726–732. https://doi.org/10.1002/IEAM.4404
- Guelfo, J. L., & Adamson, D. T. (2018). Evaluation of a national data set for insights into sources, composition, and concentrations of per- and polyfluoroalkyl substances (PFASs) in U.S. drinking water. *Environmental Pollution*, 236, 513. https://doi.org/10.1016/J.ENVPOL.2018.01.066
- Guelfo, J. L., Wunsch, A., McCray, J., Stults, J. F., & Higgins, C. P. (2020). Subsurface transport potential of perfluoroalkyl acids (PFAAs): Column experiments and modeling. *Journal of Contaminant Hydrology*, 233, 103661. https://doi.org/10.1016/J.JCONHYD.2020.103661
- Guo, B., Zeng, J., & Brusseau, M. L. (2020). A Mathematical Model for the Release, Transport, and Retention of Per- and Polyfluoroalkyl Substances (PFAS) in the Vadose Zone. *Water Resources Research*, *56*(2), 1–21. https://doi.org/10.1029/2019WR026667
- Hameri, K., Aalto, P., Kulmala, M., Sammaljlrvi, E., Spring, E., & Pihkala, P. (1996). TECHNICAL NOTE FORMATION OF RESPIRABLE PARTICLES DURING SKI WAXING. In *I. Aerosol Sci* (Vol. 27, Issue 2).
- Harbaugh, A. W. (2005). MODFLOW-2005, The U.S. Geological Survey Modular Ground-Water Model-the Ground-Water Flow Process. In USGS (Ed.), *Book 6. Modeling techniques, Section A. Ground Water*.

- Haukås, M., Berger, U., Hop, H., Gulliksen, B., & Gabrielsen, G. W. (2007). Bioaccumulation of per- and polyfluorinated alkyl substances (PFAS) in selected species from the Barents Sea food web. *Environmental Pollution*, *148*(1), 360–371. https://doi.org/10.1016/j.envpol.2006.09.021
- Henderson, J., Gloy, B., & Boehlje, M. (2011). Agriculture's Boom-Bust Cycles: Is This Time Different? *Economic Review* (01612387), p83.
- Heng, B. C. P., Sander, G. C., & Scott, C. F. (2009). Modeling overland flow and soil erosion on nonuniform hillslopes: A finite volume scheme. *Water Resources Research*, 45(5). https://doi.org/10.1029/2008WR007502
- Hodgkins, L. M., Mulligan, R. P., McCallum, J. M., & Weber, K. P. (2019). Modelling the transport of shipborne per- and polyfluoroalkyl substances (PFAS) in the coastal environment. *Science of the Total Environment*, 658, 602–613. https://doi.org/10.1016/j.scitotenv.2018.12.230
- Hogue, C. (2019, July 1). 3M admits to unlawful release of PFAS. *C&EN*, 16. https://doi.org/10.1021/acs.est.5b05058
- Hopmans, J. W., & van Genuchten, M. T. (2005). VADOSE ZONE | Hydrologic Processes. *Encyclopedia of Soils in the Environment*, 4, 209–216. https://doi.org/10.1016/B0-12-348530-4/00434-3
- Houde, M., Czub, G., Small, J. M., Backus, S., Wang, X., Alaee, M., & Muir, D. C. G. (2008). Fractionation and bioaccumulation of perfluorooctane sulfonate (PFOS) isomers in a lake ontario food web. *Environmental Science and Technology*, 42(24), 9397–9403. https://doi.org/10.1021/es800906r
- HRWC. (2021a). Dams and Impoundments. https://www.hrwc.org/our-watershed/threats/dams/
- HRWC. (2021b). History of the Huron River. https://www.hrwc.org/about/history/
- Hu, X. C., Andrews, D. Q., Lindstrom, A. B., Bruton, T. A., Schaider, L. A., Grandjean, P., Lohmann, R., Carignan, C. C., Blum, A., Balan, S. A., Higgins, C. P., & Sunderland, E. M. (2016). Detection of Poly- and Perfluoroalkyl Substances (PFASs) in U.S. Drinking Water Linked to Industrial Sites, Military Fire Training Areas, and Wastewater Treatment Plants. *Environmental Science and Technology Letters*, 3(10), 344–350. https://doi.org/10.1021/acs.estlett.6b00260
- Hu, X. C., Ge, B., Ruyle, B. J., Sun, J., & Sunderland, E. M. (2021). A Statistical Approach for Identifying Private Wells Susceptible to Perfluoroalkyl Substances (PFAS) Contamination. *Environmental Science and Technology Letters*, 8, 596–602. https://doi.org/10.1021/acs.estlett.1c00264
- Huang, D., Xiao, R., Du, L., Zhang, G., Yin, L. S., Deng, R., & Wang, G. (2021). Phytoremediation of poly- and perfluoroalkyl substances: A review on aquatic plants, influencing factors, and

- phytotoxicity. *Journal of Hazardous Materials*, 418, 126314. https://doi.org/10.1016/J.JHAZMAT.2021.126314
- Huo, X., Chen, D., He, Y., Zhu, W., Zhou, W., & Zhang, J. (2015). Bisphenol-a and female infertility: A possible role of gene-environment interactions. In *International Journal of Environmental Research and Public Health* (Vol. 12, Issue 9, pp. 11101–11116). MDPI AG. https://doi.org/10.3390/ijerph120911101
- ITRC. (2018). Aqueous Film-Forming Foam (AFFF).
- ITRC. (2020). PFAS Releases to the Environment. In *PFAS Technical and Regulatory Guidance Document and Fact Sheets PFAS-1*.
- Ivleva, N. P., Wiesheu, A. C., & Niessner, R. (2017). Microplastic in Aquatic Ecosystems. *Angewandte Chemie - International Edition*, 56(7), 1720–1739. https://doi.org/10.1002/anie.201606957
- Jantzen, C. E., Annunziato, K. A., Bugel, S. M., & Cooper, K. R. (2016). PFOS, PFNA, and PFOA sub-lethal exposure to embryonic zebrafish have different toxicity profiles in terms of morphometrics, behavior and gene expression. *Aquatic Toxicology*, *175*, 160–170. https://doi.org/10.1016/j.aquatox.2016.03.026
- Jarvis, N., & Larsson, M. (2001). Modeling Macropore Flow in Soils: Field Validation and Use for Management Purposes. In *Conceptual Models of Flow and Transport in the Fractured Vadose Zone* (pp. 189–210). National Academies Press. https://doi.org/10.17226/10102
- Jayasundara, S., Wagner-Riddle, C., Parkin, G., Von Bertoldi, P., Warland, J., Kay, B., & Voroney, P. (2007). Minimizing nitrogen losses from a corn-soybean-winter wheat rotation with best management practices. *Nutrient Cycling in Agroecosystems*, 79(2), 141–159. https://doi.org/10.1007/s10705-007-9103-9
- Jones, P. D., Hu, W., De Coen, W., Newsted, J. L., & Giesy, J. P. (2003). Binding of perfluorinated fatty acids to serum proteins. *Environmental Toxicology and Chemistry*, 22(11), 2639–2649. https://doi.org/10.1897/02-553
- Kanter, D. R., Zhang, X., Mauzerall, D. L., Malyshev, S., & Shevliakova, E. (2016). The importance of climate change and nitrogen use efficiency for future nitrous oxide emissions from agriculture. *Environmental Research Letters*, 11(9). https://doi.org/10.1088/1748-9326/11/9/094003
- Kasorndorkbua, C., Opriessnig, T., Huang, F. F., Guenette, D. K., Thomas, P. J., Meng, X. J., & Halbur, P. G. (2005). Infectious swine hepatitis E virus is present in pig manure storage facilities on United States farms, but evidence of water contamination is lacking. *Applied and Environmental Microbiology*, 71(12), 7831–7837. https://doi.org/10.1128/AEM.71.12.7831-7837.2005
- Keiter, S., Baumann, L., Färber, H., Holbech, H., Skutlarek, D., Engwall, M., & Braunbeck, T. (2012). Aquatic Toxicology Long-term effects of a binary mixture of perfluorooctane

- sulfonate (PFOS) and bisphenol A (BPA) in zebrafish (Danio rerio). *Aquatic Toxicology*, 116–129. https://doi.org/10.1016/j.aquatox.2012.04.003
- Kidd, K. A., Burkhard, L. P., Babut, M., Borgå, K., Muir, D. C. G., Perceval, O., Ruedel, H., Woodburn, K., & Embry, M. R. (2019). Practical advice for selecting or determining trophic magnification factors for application under the European Union Water Framework Directive. Integrated Environmental Assessment and Management, 15(2), 266–277. https://doi.org/10.1002/ieam.4102
- Kim, S. C., & Carlson, K. (2006). Occurrence of ionophore antibiotics in water and sediments of a mixed-landscape watershed. *Water Research*, 40(13), 2549–2560. https://doi.org/10.1016/j.watres.2006.04.036
- Kim, Y., Jung, J., Kim, M., Park, J., Boxall, A. B. A., & Choi, K. (2008). Prioritizing veterinary pharmaceuticals for aquatic environment in Korea. *Environmental Toxicology and Pharmacology*, 26, 167–176. https://doi.org/10.1016/j.etap.2008.03.006
- Klein, M., Müller, M., Dust, M., Görlitz, G., Gottesbüren, B., Hassink, J., Kloskowski, R., Kubiak, R., Resseler, H., Schäfer, H., Stein, B., & Vereecken, H. (1997). Validation of the pesticide leaching model PELMO using lysimeter studies performed for registration. *Chemosphere*, 35(11), 2563–2587. https://doi.org/10.1016/S0045-6535(97)00325-1
- Knobeloch, L., Salna, B., Hogan, A., Postle, J., & Anderson, H. (2000). Blue babies and nitrate-contaminated well water. *Environmental Health Perspectives*, 108(7), 675–678. https://doi.org/10.1289/ehp.00108675
- Koba, O., Grabicova, K., Cerveny, D., Turek, J., Kolarova, J., Randak, T., Zlabek, V., & Grabic, R. (2018). Transport of pharmaceuticals and their metabolites between water and sediments as a further potential exposure for aquatic organisms. *Journal of Hazardous Materials*, *342*, 401–407. https://doi.org/10.1016/j.jhazmat.2017.08.039
- Kolpin, D. W., Furlong, E. T., Meyer, M. T., Thurman, E. M., Zaugg, S. D., Barber, L. B., & Buxton, H. T. (2002a). Pharmaceuticals, hormones, and other organic wastewater contaminants in U.S. streams, 1999-2000: A national reconnaissance. *Environmental Science and Technology*, 36(6), 1202–1211. https://doi.org/10.1021/es011055j
- Kolpin, D. W., Furlong, E. T., Meyer, M. T., Thurman, E. M., Zaugg, S. D., Barber, L. B., & Buxton, H. T. (2002b). Pharmaceuticals, hormones, and other organic wastewater contaminants in U.S. streams, 1999-2000: A national reconnaissance. *Environmental Science and Technology*, 36(6), 1202–1211. https://doi.org/10.1021/es011055j
- Kotthoff, M., Müller, J., Jürling, H., Schlummer, M., & Fiedler, D. (2015). Perfluoroalkyl and polyfluoroalkyl substances in consumer products. *Environmental Science and Pollution Research*, 22(19), 14546–14559. https://doi.org/10.1007/s11356-015-4202-7
- Kulkarni, P. S., Crespo, J. G., & Afonso, C. A. M. (2008). Dioxins sources and current remediation technologies A review. In *Environment International* (Vol. 34, Issue 1, pp. 139–153). Elsevier Ltd. https://doi.org/10.1016/j.envint.2007.07.009

- Kümmer, K. (2010). Pharmaceuticals in the environment. *Annual Review of Environmental Resources*, *35*, 57–75. https://doi.org/10.1146/annurev-environ-052809-161223
- Labadie, P., & Budzinski, H. (2006). Alteration of steroid hormone balance in juvenile turbot (Psetta maxima) exposed to nonylphenol, bisphenol A, tetrabromodiphenyl ether 47, diallylphthalate, oil, and oil spiked with alkylphenols. *Archives of Environmental Contamination and Toxicology*, 50(4), 552–561. https://doi.org/10.1007/s00244-005-1043-2
- Larcher, S., & Yargeau, V. (2012). Biodegradation of sulfamethoxazole: Current knowledge and perspectives. In *Applied Microbiology and Biotechnology* (Vol. 96, Issue 2, pp. 309–318). https://doi.org/10.1007/s00253-012-4326-3
- Lassaletta, L., Billen, G., Grizzetti, B., Anglade, J., & Garnier, J. (2014). 50 year trends in nitrogen use efficiency of world cropping systems: The relationship between yield and nitrogen input to cropland. *Environmental Research Letters*, *9*(10). https://doi.org/10.1088/1748-9326/9/10/105011
- Lathers, C. M. (2001). Role of veterinary medicine in public health: Antibiotic use in food animals and humans and the effect on evolution of antibacterial resistance. *Journal of Clinical Pharmacology*, *41*(6), 595–599. https://doi.org/10.1177/00912700122010474
- Law, K. L. (2017). Plastics in the Marine Environment. *Annual Review of Marine Science*, 9(1), 205–229. https://doi.org/10.1146/annurev-marine-010816-060409
- Li, Q., Wang, T., Zhu, Z., Meng, J., Wang, P., Suriyanarayanan, S., Zhang, Y., Zhou, Y., Song, S., Lu, Y., & Yvette, B. (2017). Using hydrodynamic model to predict PFOS and PFOA transport in the Daling River and its tributary, a heavily polluted river into the Bohai Sea, China. *Chemosphere*, 167, 344–352. https://doi.org/https://doi.org/10.1016/j.chemosphere.2016.09.119
- Lindim, C., Cousins, I. T., & Vangils, J. (2015). Estimating emissions of PFOS and PFOA to the Danube River catchment and evaluating them using a catchment-scale chemical transport and fate model. *Environmental Pollution*, 207, 97–106. https://doi.org/10.1016/J.ENVPOL.2015.08.050
- Lindim, C., van Gils, J., & Cousins, I. T. (2016). A large-scale model for simulating the fate & transport of organic contaminants in river basins. *Chemosphere*, 144, 803–810. https://doi.org/10.1016/j.chemosphere.2015.09.051
- Lindstrom, A. B., Strynar, M. J., & Libelo, E. L. (2011). Polyfluorinated Compounds: Past, Present, and Future. *Environ. Sci. Technol*, 45, 7954–7961. https://doi.org/10.1021/es2011622
- Liu, C., & Gin, K. Y. H. (2018). Immunotoxicity in green mussels under perfluoroalkyl substance (PFAS) exposure: Reversible response and response model development. *Environmental Toxicology and Chemistry*, 37(4), 1138–1145. https://doi.org/10.1002/etc.4060

- Liu, J., You, L., Amini, M., Obersteiner, M., Herrero, M., Zehnder, A. J. B., & Yang, H. (2010). A high-resolution assessment on global nitrogen flows in cropland. *Proceedings of the National Academy of Sciences of the United States of America*, 107(17), 8035–8040. https://doi.org/10.1073/pnas.0913658107
- Liu, T., Bruins, R. J. F., & Heberling, M. T. (2018). Factors influencing farmers' adoption of best management practices: A review and synthesis. In *Sustainability (Switzerland)* (Vol. 10, Issue 2, p. 432). MDPI AG. https://doi.org/10.3390/su10020432
- Lyu, Y., Brusseau, M. L., Chen, W., Yan, N., Fu, X., & Lin, X. (2018). Adsorption of PFOA at the Air-Water Interface during Transport in Unsaturated Porous Media. *Environmental Science & Technology*, 52, 7745–7753. https://doi.org/10.1021/ACS.EST.8B02348
- Maclean, R. C., & Millan, A. S. (2019). The evolution of antibiotic resistance Clinically relevant evolution studies are needed to help fight the spread of antibiotic resistance. https://doi.org/10.1126/science.aax3879
- Mahinroosta, R., Senevirathna, L., Li, M., & KrishnaPillai, K. (2021). A methodology for transport modelling of a contaminated site with perfluorooctane sulfonate due to climate interaction. *Process Safety and Environmental Protection*, 147, 642–653. https://doi.org/10.1016/J.PSEP.2020.12.034
- Marin, C. M., Guvanasen, V., & Saleem, Z. A. (2010). The 3MRA Risk Assessment Framework-A Flexible Approach for Performing Multimedia, Multipathway, and Multireceptor Risk Assessments Under Uncertainty. *Human and Ecological Risk Assessment*, *9*(7), 1655–1677. https://doi.org/10.1080/714044790
- Martin, J. W., Mabury, S. A., Solomon, K. R., & Muir, D. C. G. (2003). Bioconcentration and Tissue Distribution of Perfluorinated Acids in Rainbow Trout (Oncorhynchus Mykiss). *Environmental Toxicology and Chemistry*, 22(1), 196. https://doi.org/10.1897/1551-5028(2003)022<0196:batdop>2.0.co;2
- Matheny, K. (2019, May 12). 3M kept PFAS dangers a secret for decades, internal documents show. *Detroit Free Press, May*, 1–8.
- Matuszczak, E., Komarowska, M. D., Debek, W., & Hermanowicz, A. (2019). The Impact of Bisphenol A on Fertility, Reproductive System, and Development: A Review of the Literature. *International Journal of Endocrinology*, 2019. https://doi.org/10.1155/2019/4068717
- McCrystal, L. (2019, August 29). Before DuPont and 3M hearing in Congress, activists highlight companies 'history with PFAS. *Philidelphia Inquirer*.
- McLachlan, M. S., Felizeter, S., Klein, M., Kotthoff, M., & De Voogt, P. (2019). Fate of a perfluoroalkyl acid mixture in an agricultural soil studied in lysimeters. *Chemosphere*, 223, 180–187. https://doi.org/10.1016/J.CHEMOSPHERE.2019.02.012

- Mclellan, S. L., & Salmore, A. K. (2003). Evidence for localized bacterial loading as the cause of chronic beach closings in a freshwater marina. *Water Research*, *37*, 2700–2708. https://doi.org/10.1016/S0043-1354(03)00068-X
- Mei, W., Sun, H., Song, M., Jiang, L., Li, Y., Lu, W., Ying, G. G., Luo, C., & Zhang, G. (2021). Per- and polyfluoroalkyl substances (PFASs) in the soil–plant system: Sorption, root uptake, and translocation. *Environment International*, 156, 106642. https://doi.org/10.1016/J.ENVINT.2021.106642
- Metheny, M. a. (2004). Evaluation of Groundwater Flow and Contaminant Transport.
- Michigan briefs. (2018). Crain's Detroit Business, 34(2).
- Mitch, W. A., Sharp, J. O., Trussell, R. R., Valentine, R. L., Alvarez-Cohen, L., & Sedlak, D. L. (2003). N-nitrosodimethylamine (NDMA) as a drinking water contaminant: A review. *Environmental Engineering Science*, 20(5), 389–404. https://doi.org/10.1089/109287503768335896
- Mitrou, P. I., Dimitriadis, G., & Raptis, S. A. (2001). Toxic effects of 2,3,7,8-tetrachlorodibenzo-p-dioxin and related compounds. In *European Journal of Internal Medicine*. https://doi.org/10.1016/S0953-6205(01)00146-7
- Möller, A., Ahrens, L., Surm, R., Westerveld, J., Van Der Wielen, F., Ebinghaus, R., & De Voogt, P. (2010). Distribution and sources of polyfluoroalkyl substances (PFAS) in the River Rhine watershed. *Environmental Pollution*, 158(10), 3243–3250. https://doi.org/10.1016/j.envpol.2010.07.019
- Moody, C. A., Hebert, G. N., Strauss, S. H., & Field, J. A. (2003). Occurrence and persistence of perfluorooctanesulfonate and other perfluorinated surfactants in groundwater at a fire-training area at Wurtsmith Air Force Base, Michigan, USA. *Journal of Environmental Monitoring*, 5(2), 341–345. https://doi.org/10.1039/b212497a
- Mortensen, A. S., Letcher, R. J., Cangialosi, M. V, Chu, S., & Arukwe, A. (2011). Tissue bioaccumulation patterns, xenobiotic biotransformation and steroid hormone levels in Atlantic salmon (Salmo salar) fed a diet containing perfluoroactane sulfonic or perfluoroactane carboxylic acids. *Chemosphere*, 83(8), 1035–1044. https://doi.org/10.1016/j.chemosphere.2011.01.067
- MPART. (2021). *PFAS Response Huron River: 2018 Present*. https://www.michigan.gov/pfasresponse/0,9038,7-365-86511_95792_95795-509572--.00.html
- Mussabek, D., Ahrens, L., Persson, K. M., & Berndtsson, R. (2019a). Temporal trends and sediment—water partitioning of per- and polyfluoroalkyl substances (PFAS)in lake sediment. *Chemosphere*, 227, 624–629. https://doi.org/10.1016/j.chemosphere.2019.04.074

- Mussabek, D., Ahrens, L., Persson, K. M., & Berndtsson, R. (2019b). Temporal trends and sediment—water partitioning of per- and polyfluoroalkyl substances (PFAS)in lake sediment. *Chemosphere*, 227, 624–629. https://doi.org/10.1016/j.chemosphere.2019.04.074
- Myers, S. S., Gaffikin, L., Golden, C. D., Ostfeld, R. S., Redford, K. H., Ricketts, T. H., Turner, W. R., & Osofsky, S. A. (2013). Human health impacts of ecosystem alteration. In *Proceedings of the National Academy of Sciences of the United States of America* (Vol. 110, Issue 47, pp. 18753–18760). https://doi.org/10.1073/pnas.1218656110
- Nguyen, T. V., Reinhard, M., Chen, H., & Gin, K. Y. H. (2016). Fate and transport of perfluoro-and polyfluoroalkyl substances including perfluorooctane sulfonamides in a managed urban water body. *Environmental Science and Pollution Research*, 23(11), 10382–10392. https://doi.org/10.1007/s11356-016-6788-9
- Nigam, S. K., Bush, K. T., Martovetsky, G., Ahn, S. Y., Liu, H. C., Richard, E., Bhatnagar, V., & Wu, W. (2015). The organic anion transporter (OAT) family: A systems biology perspective. *Physiological Reviews*, *95*(1), 83–123. https://doi.org/10.1152/physrev.00025.2013
- Nilsson, H., Kärrman, A., Rotander, A., Van Bavel, B., Lindström, G., & Westberg, H. (2013). Professional ski waxers' exposure to PFAS and aerosol concentrations in gas phase and different particle size fractions. *Environmental Sciences: Processes and Impacts*, *15*(4), 814–822. https://doi.org/10.1039/c3em30739e
- Noorishad, J., Tsang, C. F., Perrochet, P., & Musy, A. (1992). A perspective on the numerical solution of convection-dominated transport problems: A price to pay for the easy way out. *Water Resources Research*, 28(2), 551–561.
- Norris, D., & Hobbs, S. (2006). The HPA Axis and Functions of Corticosteroids in Fishes. In *Fish Endocrinology* (2 *Vols.*) (pp. 721–765). https://doi.org/10.1201/b10745-31
- Nygård, T., Sandercock, B. K., Reinsborg, Tore, & Einvik, Kjell. (2019). Population recovery of peregrine falcons in central Norway in the 4 decades since the DDT-ban. *Ecotoxicology*, 28, 1160–1168. https://doi.org/10.1007/s10646-019-02111-4
- O'Driscoll, K., Mayer, B., Ilyina, T., & Pohlmann, T. (2013). Modelling the cycling of persistent organic pollutants (POPs) in the North Sea system: Fluxes, loading, seasonality, trends. *Journal of Marine Systems*, 111–112, 69–82. https://doi.org/10.1016/j.jmarsys.2012.09.011
- OECD. (2002). Perfluorooctane Sulfonate (PFOS) and related chemical products.
- Report to Congressional Requesters, Chemical Regulation (2007). https://doi.org/10.1089/blr.2006.9996
- Ord, J., Fazeli, A., & Watt, P. J. (2017). Long-term effects of the periconception period on embryo epigenetic profile and phenotype: The role of stress and how this effect is mediated. In *Advances in Experimental Medicine and Biology* (Vol. 1014, pp. 117–135). Springer New York LLC. https://doi.org/10.1007/978-3-319-62414-3_7

- Pajević, S., Borišev, M., Rončević, S., Vukov, D., & Igić, R. (2008). Heavy metal accumulation of Danube river aquatic plants Indication of chemical contamination. *Central European Journal of Biology*, *3*(3), 285–294. https://doi.org/10.2478/s11535-008-0017-6
- Park, M., Wu, S., Lopez, I. J., Chang, J. Y., Karanfil, T., & Snyder, S. A. (2020). Adsorption of perfluoroalkyl substances (PFAS) in groundwater by granular activated carbons: Roles of hydrophobicity of PFAS and carbon characteristics. *Water Research*, *170*. https://doi.org/10.1016/j.watres.2019.115364
- Park, R. A., & Clough, J. S. (2014). Aquatox (Release 3.1 plus) Modeling Environmental Fate and Ecological Effects in Aquatic Ecosystems.
- Patil, S. B., & Chore, H. S. (2014). Contaminant transport through porous media: An overview of experimental and numerical studies. *Advances in Environmental Research*, 3(1), 45–69.
- Patlewicz, G., Richard, A. M., Williams, A. J., Grulke, C. M., Sams, R., Lambert, J., Noyes, P. D., DeVito, M. J., Hines, R. N., Strynar, M., Guiseppi-Elie, A., & Thomas, R. S. (2019). A chemical category-based prioritization approach for selecting 75 per- and polyfluoroalkyl substances (PFAS) for tiered toxicity and toxicokinetic testing. *Environmental Health Perspectives*, 127(1). https://doi.org/10.1289/EHP4555
- Penland, T. N., Cope, W. G., Kwak, T. J., Strynar, M. J., Grieshaber, C. A., Heise, R. J., & Sessions, F. W. (2020). Trophodynamics of Per-and Polyfluoroalkyl Substances in the Food Web of a Large Atlantic Slope River. *Environmental Science and Technology*, *54*(11), 6800–6811. https://doi.org/10.1021/acs.est.9b05007
- Persson, J., & Andersson, N. (2016). *Modeling groundwater flow and PFOS transport*. KTH Royal Institute of Technology.
- Pettersson, K. (2020). Groundwater Movement and PFAS Transportation in the Vreta-Bålsta Esker. Uppsala University.
- Plassmann, M. M., & Berger, U. (2013). Perfluoroalkyl carboxylic acids with up to 22 carbon atoms in snow and soil samples from a ski area. *Chemosphere*, 91(6), 832–837. https://doi.org/10.1016/j.chemosphere.2013.01.066
- Popovic, M., Zaja, R., Fent, K., & Smital, T. (2013). Molecular characterization of zebrafish Oatp1d1 (Slco1d1), a novel organic anion-transporting polypeptide. *Journal of Biological Chemistry*, 288(47), 33894–33911. https://doi.org/10.1074/jbc.M113.518506
- Popovic, M., Zaja, R., Fent, K., & Smital, T. (2014). Interaction of environmental contaminants with zebrafish organic anion transporting polypeptide, Oatp1d1 (Slco1d1). *Toxicology and Applied Pharmacology*, 280(1), 149–158. https://doi.org/10.1016/j.taap.2014.07.015
- Prevedouros, K., Cousins, I. T., Buck, R. C., & Korzeniowski, S. H. (2006). Sources, Fate and Transport of Perfluorocarboxylates. *Environmental Science & Technology*, 40(1). https://doi.org/10.1021/es0512475

- Rabalais, N. N., Turner, R. E., Díaz, R. J., & Justić, D. (2009). Global change and eutrophication of coastal waters. *ICES Journal of Marine Science*, 66(7), 1528–1537. https://doi.org/10.1093/icesjms/fsp047
- Rahman, M. F., Peldszus, S., & Anderson, W. B. (2014). Behaviour and fate of perfluoroalkyl and polyfluoroalkyl substances (PFASs) in drinking water treatment: A review. *Water Research*, 50, 318–340. https://doi.org/10.1016/j.watres.2013.10.045
- Redmon, J. H., Womack, D., Lillys, T., Truesdale, R., & Knappe, D. (2019). A Hydrogeological Modeling Approach to Understand the Fate and Transport of PFAS in the Cape Fear Watershed.
- Richards, L. A. (1931). Capillary conduction of liquids through porous mediums. *Journal of Applied Physics*, 1(5), 318–333. https://doi.org/10.1063/1.1745010
- Rodriguez-Moza, S., & Weinberg, H. S. (2010a). Meeting report: Pharmaceuticals in water-an interdisciplinary approach to a public health challenge. *Environmental Health Perspectives*, *118*(7), 1016–1020. https://doi.org/10.1289/ehp.0901532
- Rodriguez-Moza, S., & Weinberg, H. S. (2010b). Meeting report: Pharmaceuticals in water-an interdisciplinary approach to a public health challenge. *Environmental Health Perspectives*, 118(7), 1016–1020. https://doi.org/10.1289/ehp.0901532
- Rodriguez-Moza, S., & Weinberg, H. S. (2010c). Meeting report: Pharmaceuticals in water-an interdisciplinary approach to a public health challenge. *Environmental Health Perspectives*, 118(7), 1016–1020. https://doi.org/10.1289/ehp.0901532
- Rosenmai, A. K., Taxvig, C., Svingen, T., Trier, X., van Vugt-Lussenburg, B. M. A., Pedersen, M., Lesné, L., Jégou, B., & Vinggaard, A. M. (2016). Fluorinated alkyl substances and technical mixtures used in food paper-packaging exhibit endocrine-related activity in vitro. *Andrology*, *4*(4), 662–672. https://doi.org/10.1111/andr.12190
- Runnalls, T. J., Margiotta-Casaluci, L., Kugathas, S., & Sumpter, J. P. (2010). Pharmaceuticals in the Aquatic Environment: Steroids and Anti-Steroids as High Priorities for Research. *Human and Ecological Risk Assessment: An International Journal*, *16*(6), 1318–1338. https://doi.org/10.1080/10807039.2010.526503
- Sainju, U. M., Lenssen, A. W., Caesar-TonThat, T., Jabro, J. D., Lartey, R. T., Evans, R. G., & Allen, B. L. (2012). Dryland soil nitrogen cycling influenced by tillage, crop rotation, and cultural practice. *Nutrient Cycling in Agroecosystems*, 93(3), 309–322. https://doi.org/10.1007/s10705-012-9518-9
- Sajid, M., & Ilyas, M. (2017). PTFE-coated non-stick cookware and toxicity concerns: a perspective. *Environmental Science and Pollution Research*, 24(30), 23436–23440. https://doi.org/10.1007/s11356-017-0095-y
- Salgado-Freiría, R., López-Doval, S., & Lafuente, A. (2018). Perfluorooctane sulfonate (PFOS) can alter the hypothalamic–pituitary–adrenal (HPA) axis activity by modifying CRF1 and

- glucocorticoid receptors. *Toxicology Letters*, 295, 1–9. https://doi.org/10.1016/j.toxlet.2018.05.025
- Salice, C. J., Anderson, T. A., Anderson, R. H., & Olson, A. D. (2018). Ecological risk assessment of perfluooroctane sulfonate to aquatic fauna from a bayou adjacent to former fire training areas at a US Air Force installation. *Environmental Toxicology and Chemistry*, *37*(8), 2198–2209. https://doi.org/10.1002/etc.4162
- Sans, P., & Combris, P. (2015). World meat consumption patterns: An overview of the last fifty years (1961-2011). *Meat Science*, 109, 106–111. https://doi.org/10.1016/j.meatsci.2015.05.012
- Santos, L. H. M. L. M., Araújo, A. N., Fachini, A., Pena, A., Delerue-Matos, C., & Montenegro, M. C. B. S. M. (2010). Ecotoxicological aspects related to the presence of pharmaceuticals in the aquatic environment. In *Journal of Hazardous Materials* (Vol. 175, Issues 1–3, pp. 45–95). Elsevier. https://doi.org/10.1016/j.jhazmat.2009.10.100
- Schaefer, C. E., Culina, V., Nguyen, D., & Field, J. (2019). Uptake of Poly-and Perfluoroalkyl Substances at the Air–Water Interface. *Environ. Sci. Technol*, 53, 56. https://doi.org/10.1021/acs.est.9b04008
- Scippo, M.-L. (2011). Bisphenol A in our food: same toxicological studies but different risk assessment and risk management decisions around the world. *Food Science & Law*, 5, 5–9.
- SETAC. (2019). Environmental Risk Assessment of Per- and Polyfluoroalkyl Substances (PFAS). SETAC.
- Sharma, B. M., Bharat, G., Tayal, S., Becanova, J., Larssen, T., Butter, D., & Nizzetto, L. (2015). Perfluoroalkyl substances (PFAS) in river and ground / drinking water of the Ganges River basin: Emissions and implications for human exposure. *Environmental Pollution*, *November*, 1–10. https://doi.org/10.1016/j.envpol.2015.10.050
- Shin, H. M., Vieira, V. M., Ryan, P. B., Detwiler, R., Sanders, B., Steenland, K., & Bartell, S. M. (2011). Environmental fate and transport modeling for perfluorooctanoic acid emitted from the Washington works facility in West Virginia. *Environmental Science and Technology*, 45(4), 1435–1442. https://doi.org/10.1021/es102769t
- Sidebottom, M. A., Junk, C. P., Salerno, H. L. S., Burch, H. E., Blackman, G. S., & Krick, B. A. (2018). Wear-Induced Microstructural and Chemical Changes in Poly[tetrafluoroethylene-co-(perfluoroalkyl vinyl ether)] (PFA). *Macromolecules*, 51(23), 9700–9709. https://doi.org/10.1021/acs.macromol.8b01564
- Sigler, M. (2014). The_effects_of_plastic_polluti.PDF. In *Water Air Soil Pollut* (Vol. 225, Issue 2184, pp. 1–9).
- Silva, J. A. K., Šimůnek, J., & McCray, J. E. (2020). A modified hydrus model for simulating pfas transport in the vadose zone. *Water (Switzerland)*, *12*(10). https://doi.org/10.3390/w12102758

- Sima, M. W., & Jaffé, P. R. (2021). A critical review of modeling Poly- and Perfluoroalkyl Substances (PFAS) in the soil-water environment. *Science of the Total Environment*, 757, 143793. https://doi.org/10.1016/j.scitotenv.2020.143793
- Simmonet-Laprade, C., Budzinski, H., Babut, M., Le Menach, K., Munoz, G., Lauzent, M., Ferrari, B. J. D., & Labadie, P. (2019). Investigation of the spatial variability of poly- and perfluoroalkyl substance trophic magnification in selected riverine ecosystems. *Science of the Total Environment*, 686, 393–401. https://doi.org/10.1016/j.scitotenv.2019.05.461
- Simon, J. A. (2019). The unprecedented rate of developments concerning PFAS issues. In *Remediation* (Vol. 29, Issue 2, pp. 3–5). John Wiley and Sons Inc. https://doi.org/10.1002/rem.21594
- Simon, J. A., Abrams, S., Bradburne, T., Bryant, D., Burns, M., Cassidy, D., Cherry, J., Chiang, S. Y., Cox, D., Crimi, M., Denly, E., DiGuiseppi, B., Fenstermacher, J., Fiorenza, S., Guarnaccia, J., Hagelin, N., Hall, L., Hesemann, J., Houtz, E., ... Wice, R. (2019). PFAS Experts Symposium: Statements on regulatory policy, chemistry and analtyics, toxicology, transport/fate, and remediation for per- and polyfluoroalkyl substances (PFAS) contamination issues. *Remediation*, 29(4), 31–48. https://doi.org/10.1002/rem.21624
- Šimůnek, J., & Bradford, S. A. (2008). Vadose Zone Modeling: Introduction and Importance. *Vadose Zone Journal*, 7(2), 581–586. https://doi.org/10.2136/VZJ2008.0012
- Šimůnek, J., Van Genuchten, M. T., & Šejna, M. (2011). HYDRUS Technical Manual Version 2.0.
- Šimůnek, J., Van Genuchten, M. T., Šejna, M., Šimůnek, J., & Zone, V. (2016). Recent Developments and Applications of the HYDRUS Computer Software Packages Review and Analysis. *Vadose Zone Journal*. https://doi.org/10.2136/vzj2016.04.0033
- Skiba, U. M., & Rees, R. M. (2014). Nitrous oxide, climate change and agriculture. In *CAB Reviews: Perspectives in Agriculture, Veterinary Science, Nutrition and Natural Resources* (Vol. 9). https://doi.org/10.1079/PAVSNNR20149010
- Stahl, T., Riebe, R. A., Falk, S., Failing, K., & Brunn, H. (2013). Long-term lysimeter experiment to investigate the leaching of perfluoroalkyl substances (PFASs) and the carry-over from soil to plants: Results of a pilot study. *Journal of Agricultural and Food Chemistry*, 61(8), 1784–1793. https://doi.org/10.1021/jf305003h
- Steenland, K., Fletcher, T., & Savitz, D. A. (2010). Epidemiologic evidence on the health effects of perfluorooctanoic acid (PFOA). In *Environmental Health Perspectives* (Vol. 118, Issue 8, pp. 1100–1108). National Institute of Environmental Health Sciences. https://doi.org/10.1289/ehp.0901827
- Templeton, M. R., Graham, N., & Voulvoulis, N. (2009). Emerging chemical contaminants in water and wastewater. In *Philosophical Transactions of the Royal Society A: Mathematical, Physical and Engineering Sciences* (Vol. 367, Issue 1904, pp. 3873–3875). Royal Society. https://doi.org/10.1098/rsta.2009.0144

- Ternes, T. A. (1998). Occurrence of drugs in German sewage treatment plants and rivers. *Water Research*, 32(11), 3245–3260. https://doi.org/10.1016/S0043-1354(98)00099-2
- Thiel, M., Hinojosa, I. A., Miranda, L., Pantoja, J. F., Rivadeneira, M. M., & Vásquez, N. (2013). Anthropogenic marine debris in the coastal environment: A multi-year comparison between coastal waters and local shores. *Marine Pollution Bulletin*, 71, 307–316. https://doi.org/10.1016/j.marpolbul.2013.01.005
- Torres-Olvera, M. J., Durán-Rodríguez, O. Y., Torres-García, U., Pineda-López, R., & Ramírez-Herrejón, J. P. (2018). Validation of an index of biological integrity based on aquatic macroinvertebrates assemblages in two subtropical basins of central Mexico. *Latin American Journal of Aquatic Research*, 46(5), 945–960. https://doi.org/10.3856/vol46-issue5-fulltext-8
- Tysklind, M., Fängmark, I., Marklund, S., Lindskog, A., Thaning, L., & Rappe, C. (1993). Atmospheric Transport and Transformation of Polychlorinated Dibenzo-p-dioxins and Dibenzofurans. *Environmental Science and Technology*, 27(10), 2190–2197. https://doi.org/10.1021/es00047a028
- Ullah, A., Pirzada, M., Jahan, S., Ullah, H., Shaheen, G., Rehman, H., Siddiqui, M. F., & Butt, M. A. (2018). Bisphenol A and its analogs bisphenol B, bisphenol F, and bisphenol S: Comparative in vitro and in vivo studies on the sperms and testicular tissues of rats. *Chemosphere*, 209, 508–516. https://doi.org/10.1016/j.chemosphere.2018.06.089
- United Nations Children Fund, & World health Organisation. (2017). Progress on Drinking Water, Sanitation and Hygiene Joint Monitoring Programme 2017 Update and SDG Baselines. In *Who*. https://doi.org/10.1111 / tmi.12329
- US Environmental Protection Agency. (2019). *National Priorities: Research on PFAS impacts in rural communities and agricultural operations*.
- US EPA. (2012). Recreational Water Quality Criteria. Office of Water 820-F-12-058.
- US EPA. (2016a). Health Effects Support Document for Perfluorooctane Sulfonate (PFOS).
- US EPA. (2016b). Drinking Water Health Advisory for Perfluorooctane Sulfonate (PFOS).
- US EPA. (2018a, November 19). *Ground Water*. Report on the Environment. https://www.epa.gov/report-environment/ground-water
- US EPA. (2018b, December 6). *Basic Information on PFAS*. PFOA, PFOS and Other PFASs. https://www.epa.gov/pfas/basic-information-pfas
- US EPA. (2021, August 5). *Basic Information about Biosolids* . Biosolids. https://www.epa.gov/biosolids/basic-information-about-biosolids
- USDA. (1986). Urban Hydrology for Small Watersheds (Issue Technical Release 55 (TR-55)).

- USEPA. (2017). Technical Fact Sheet Perfluorooctane Sulfonate (PFOS) and Perfluorooctanoic Acid (PFOA).
- USGS. (2021, August 30). *MODFLOW and Related Programs*. Water Resources. https://www.usgs.gov/mission-areas/water-resources/science/modflow-and-related-programs?qt-science_center_objects=0#qt-science_center_objects
- Vanden Heuvel, A., McDermott, C., Pillsbury, R., Sandrin, T., Kinzelman, J., Ferguson, J., Sadowsky, M., Byappanahalli, M., Whitman, R., & Kleinheinz, G. T. (2010). The Green Alga, Cladophora, Promotes Escherichia coli Growth and Contamination of Recreational Waters in Lake Michigan. *Journal of Environmental Quality*, 39(1), 333–344. https://doi.org/10.2134/jeq2009.0152
- Villeneuve, D. L., Coady, K., Escher, B. I., Mihaich, E., Murphy, C. A., Schlekat, T., & Garcia-Reyero, N. (2019). High-throughput screening and environmental risk assessment: State of the science and emerging applications. *Environmental Toxicology and Chemistry*, 38(1), 12–26. https://doi.org/10.1002/etc.4315
- Wang, T. T., Ying, G. G., He, L. Y., Liu, Y. S., & Zhao, J. L. (2020b). Uptake mechanism, subcellular distribution, and uptake process of perfluorooctanoic acid and perfluorooctane sulfonic acid by wetland plant Alisma orientale. *Science of The Total Environment*, 733, 139383. https://doi.org/10.1016/J.SCITOTENV.2020.139383
- Wang, W., Rhodes, G., Ge, J., Yu, X., & Li, H. (2020a). Uptake and accumulation of per- and polyfluoroalkyl substances in plants. *Chemosphere*, 261. https://doi.org/10.1016/J.CHEMOSPHERE.2020.127584
- Wang, Z., Cousins, I. T., Scheringer, M., Buck, R. C., & Hungerbühler, K. (2014). Global emission inventories for C4-C14 perfluoroalkyl carboxylic acid (PFCA) homologues from 1951 to 2030, Part I: Production and emissions from quantifiable sources. In *Environment International* (Vol. 70, pp. 62–75). https://doi.org/10.1016/j.envint.2014.04.013
- Washington, J. W., Rankin, K., Libelo, E. L., Lynch, D. G., & Cyterski, M. (2019). Determining global background soil PFAS loads and the fluorotelomer-based polymer degradation rates that can account for these loads. *Science of the Total Environment*, 651, 2444–2449. https://doi.org/10.1016/j.scitotenv.2018.10.071
- Wei, C., Wu, H., Kong, Q., Wei, J., Feng, C., Qiu, G., Wei, C., & Li, F. (2019). Residual chemical oxygen demand (COD) fractionation in bio-treated coking wastewater integrating solution property characterization. *Journal of Environmental Management*, 246, 324–333. https://doi.org/10.1016/j.jenvman.2019.06.001
- Weill, S., Mouche, E., & Patin, J. (2009). A generalized Richards equation for surface/subsurface flow modelling. *Journal of Hydrology*, *366*(1–4), 9–20. https://doi.org/10.1016/J.JHYDROL.2008.12.007

- Weinke, A. D., & Biddanda, B. A. (2018). From Bacteria to Fish: Ecological Consequences of Seasonal Hypoxia in a Great Lakes Estuary. *Ecosystems*, 21(3), 426–442. https://doi.org/10.1007/s10021-017-0160-x
- Wen, B., Li, L., Liu, Y., Zhang, H., Hu, X., Shan, X., & Zhang, S. (2013). Mechanistic studies of perfluorooctane sulfonate, perfluorooctanoic acid uptake by maize (Zea mays L. cv. TY2). *Plant and Soil 2013 370:1*, *370*(1), 345–354. https://doi.org/10.1007/S11104-013-1637-9
- Wetmore, B. A., Wambaugh, J. F., Allen, B., Ferguson, S. S., Sochaski, M. A., Setzer, R. W., Houck, K. A., Strope, C. L., Cantwell, K., Judson, R. S., LeCluyse, E., Clewell, H. J., Thomas, R. S., & Andersen, M. E. (2015). Incorporating High-Throughput Exposure Predictions With Dosimetry-Adjusted In Vitro Bioactivity to Inform Chemical Toxicity Testing. *Toxicological Sciences*, *148*(1), 121–136.
- WHO/SDE/WSH. (2016). Nitrate and Nitrite in Drinking-Water Background Document for Development of WHO Guidelines for drinking-Water Quality. *Guidelines for Drinking-Water Quality Fourth Edition*, 2, 41.
- Willi, R. A., & Fent, K. (2018). Interaction of environmental steroids with organic anion transporting polypeptide (Oatp1d1) in zebrafish (*Danio rerio*). *Environmental Toxicology and Chemistry*, 37(10), 2670–2676. https://doi.org/10.1002/etc.4231
- Winchell, M., & Propato, M. (2019). Demonstration of an Agricultural Chemical Fate and Transport Model to Determine Biosolids PFAS Screening Level Concentrations Required for Groundwater Protection.
- Wittersheim, R. (1993). The Huron River.
- Wool, T., Ambrose, R. B., Martin, J. L., & Comer, A. (2020). WASP 8: The next generation in the 50-year evolution of USEPA's water quality model. *Water*, *12*, 1–33. https://doi.org/10.3390/W12051398
- World Health Organisation. (2018). A global overview of national regulations and standards for drinking-water quality.
- World Health Organization. (2016). *WHO | Waterborne disease related to unsafe water and sanitation*. Who. https://www.who.int/sustainable-development/housing/health-risks/waterborne-disease/en/
- Xu, F. L., Li, Y. L., Wang, Y., He, W., Kong, X. Z., Qin, N., Liu, W. X., Wu, W. J., & Jorgensen, S. E. (2015). Key issues for the development and application of the species sensitivity distribution (SSD) model for ecological risk assessment. *Ecological Indicators*, *54*, 227–237. https://doi.org/10.1016/j.ecolind.2015.02.001
- Xu, J., Tian, Y. Z., Zhang, Y., Guo, C. S., Shi, G. L., Zhang, C. Y., & Feng, Y. C. (2013). Source apportionment of perfluorinated compounds (PFCs) in sediments: Using three multivariate factor analysis receptor models. *Journal of Hazardous Materials*, 260, 483–488. https://doi.org/10.1016/j.jhazmat.2013.06.001

- Yeh, G.-T., Cheng, H.-P., Cheng, J.-R., Lin, H.-C. J., & Martin, W. D. (1998). A Numerical Model Simulating Water Flow and Contaminant and Sediment Transport in WEterSHed Systems of 1-D Stream-River Network, 2-D Overland Regime, and 3-D Subsurface Media (WASH123D: Version 1.0).
- Zha, Y., Yang, J., Zeng, J., Tso, C.-H. M., Zeng, W., & Shi, L. (2019). Review of numerical solution of Richardson–Richards equation for variably saturated flow in soils. *Wiley Interdisciplinary Reviews: Water*, 6(5), e1364. https://doi.org/10.1002/WAT2.1364
- Zhan, X.-H., Ma, H.-L., Zhou, L.-X., Liang, J.-R., Jiang, T.-H., & Xu, G.-H. (2010). Accumulation of phenanthrene by roots of intact wheat (Triticum acstivnm L.) seedlings: passive or active uptake? *BMC Plant Biology*, 10(52).
- Zhang, H., & J., S. (2014). Animal Manure Production and Utilization in the US. In *Applied Manure and Nutrient Chemistry for Sustainable Agriculture and Environment*. Springer, Dordrecht. https://doi.org/https://doi.org/10.1007/978-94-017-8807-6_1
- Zhang, W., Zhang, D., Zagorevski, D. V., & Liang, Y. (2019). Exposure of Juncus effusus to seven perfluoroalkyl acids: Uptake, accumulation and phytotoxicity. *Chemosphere*, 233, 300–308. https://doi.org/10.1016/J.CHEMOSPHERE.2019.05.258
- Zhang, X., Luo, Y., & Goh, K. S. (2018). Modeling spray drift and runoff-related inputs of pesticides to receiving water. *Environmental Pollution*, 234, 48–58. https://doi.org/10.1016/J.ENVPOL.2017.11.032
- Zhao, Z., Xie, Z., Möller, A., Sturm, R., Tang, J., Zhang, G., & Ebinghaus, R. (2012). Distribution and long-range transport of polyfluoroalkyl substances in the Arctic, Atlantic Ocean and Antarctic coast. *Environmental Pollution*, 170, 71–77. https://doi.org/10.1016/j.envpol.2012.06.004
- Zheng, C., & Wang, P. P. (1999). MT3DMS A Modular Three-Dimensional Multispecies Transport Model. *Strategic Environmental Research and Development Program*, 1–40.
- Zhu, H., & Kannan, K. (2019). Distribution and partitioning of perfluoroalkyl carboxylic acids in surface soil, plants, and earthworms at a contaminated site. *Science of the Total Environment*, 647, 954–961. https://doi.org/10.1016/j.scitotenv.2018.08.051